Desalination 592 (2024) 118148

Contents lists available at ScienceDirect

Desalination

journal homepage: www.elsevier.com/locate/desal

Enhanced lithium separation from brines using nanofiltration (NF) technology: A review

Sajna M.S. [a], Tasneem Elmakki [a,b], Sifani Zavahir [a], Haseeb Tariq [c], Adil Abdulhameed [c], Hyunwoong Park [d], Ho Kyong Shon [e], Dong Suk Han [a,b,c,*]

[a] Center for Advanced Materials (CAM), Qatar University, PO Box 2713, Doha, Qatar
[b] Materials Science & Technology Master Program, College of Arts and Science, Qatar University, PO Box 2713, Doha, Qatar
[c] Department of Chemical Engineering, College of Engineering, Qatar University, PO Box 2713, Qatar
[d] School of Energy Engineering, Kyungpook National University, Daegu 41566, Republic of Korea
[e] Centre for Technology in Water and Wastewater (CTWW), School of Civil and Environmental Engineering, University of Technology Sydney (UTS), New South Wales, Australia

HIGHLIGHTS

- NF membranes enhance Li extraction from brines.
- Review covers diverse aqueous sources.
- Compares emerging and current Li recovery.
- Discusses Li-selective membrane challenges.
- Aims to boost targeted membrane research.

GRAPHICAL ABSTRACT

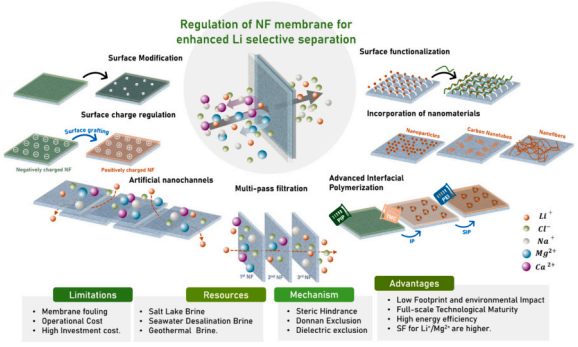

ARTICLE INFO

Keywords:
Resource recovery
Lithium
Nanofiltration (NF)
Brine
Selective separation

ABSTRACT

This study investigates the dynamics of the lithium (Li) market, focusing particularly on the use of nanofiltration (NF) membranes for Li extraction from various brines. It covers a range of aqueous resources, including brines from seawater desalination, oil- and gas-produced waters, salt lakes, and geothermal aquifers, emphasizing the value of repurposing leftover brines. The research compares current and emerging brine-based Li recovery methods, underlining their advantages over traditional sources. A critical aspect of the study is a comprehensive review of recent advancements in Li-selective NF membranes, exploring materials design principles and the development of membranes with enhanced Li^+ selectivity. The integration of NF systems in Li recovery, as supported by various studies, appears promising. This review also discusses the practical challenges and potential advancements in designing targeted Li^+ ion-selective membranes, aiming to spur continued research in this crucial area. Ultimately, the study provides an extensive analysis of Li extraction from various brine sources using NF technology, positioning it as an effective strategy in the field.

* Corresponding author at: Center for Advanced Materials (CAM), Qatar University, PO Box 2713, Doha, Qatar.
E-mail address: dhan@qu.edu.qa (D.S. Han).

https://doi.org/10.1016/j.desal.2024.118148
Received 3 May 2024; Received in revised form 21 September 2024; Accepted 21 September 2024
Available online 23 September 2024

1. Introduction

1.1. Lithium- a crucial element in modern technologies and energy transition

Lithium (Li), a crucial element for sustainable energy initiatives, is extensively utilized across various industries, including electronics, alloys, glass, ceramics, greases, and metallurgy [1]. It plays a key role in advancing renewable energy technologies, particularly through its application in lithium-ion batteries (LIBs). These batteries are essential for efficient energy storage solutions that facilitate the integration of solar and wind power into electrical grids and are crucial for extending the range and powering the drive trains of electric vehicles (EVs), contributing to a surge in Li demand [2–4]. The global Li market has experienced consistent growth, with an annual increase of 6 % from 2010 to 2016, and is projected to reach about 95,000 metric tons by 2025 [5]. Ambrose et al. predict a significant increase in Li production, estimating an output of 4.4 to 7.5 million metric tons of Li carbonate equivalent (LCE) per year by 2100 [6], highlighting the rising demand, trade activities, and prices of Li raw materials [7].

Current Li demand is surpassing supply, primarily due to its extensive use in electric and hybrid vehicles, as well as portable electronic devices [8]. Projections by Yang et al. [9] indicate a consistent increase in global Li consumption from 2015 to 2050, potentially reaching 5.11 million tons (Fig. 1a) — over one-third of the Earth's total Li reserves. At this consumption rate, terrestrial Li reserves are expected to be depleted by 2080 (Fig. 1b). In response, various countries are enhancing their Li production capabilities, exploring technological advancements such as direct Li extraction (DLE) and direct Li to product (DLP) to boost supply capacities [3]. Concurrently, research is advancing on LiBs to improve energy density, lifespan, and safety.

The 2023 Mineral Commodity Summaries from the U.S. Geological Survey (USGS) identified key countries rich in Li resources [10] (Fig. 1c), highlighting the importance of the Lithium Triangle —Argentina, Bolivia, and Chile — which contains roughly two-thirds of the global Li reserves [11]. This region is pivotal in the global Li market and plays a significant role in geopolitical strategies due to its substantial reserves [12]. Efforts to avoid foreign military interventions underscore the strategic importance of Li and its sensitivity in international relations [13]. Within the Lithium Triangle, each country has implemented distinct strategies to leverage its Li assets: Argentina is focusing on using its Li reserves to spur economic growth [14], while

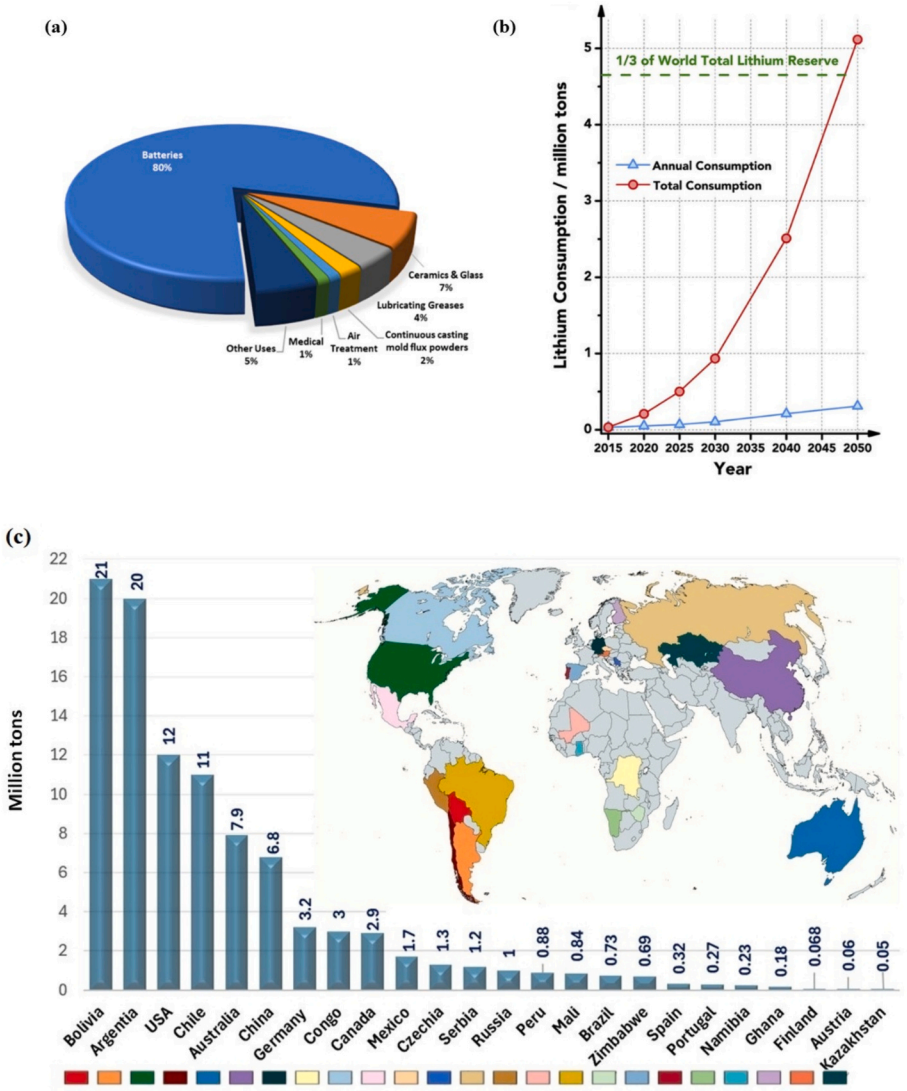

Fig. 1. Overview of Li usage and global distribution: (a) Global end-user distribution of Li across multiple applications, illustrating sector-specific utilization patterns. (b) Projection of Li consumption in millions of tons over the next decades, based on current and expected demands [9]. (c) Geographical distribution of global Li resources as reported by USGS in 2023, showing the reserves in million tons per country and highlighting regional variations in resource availability.

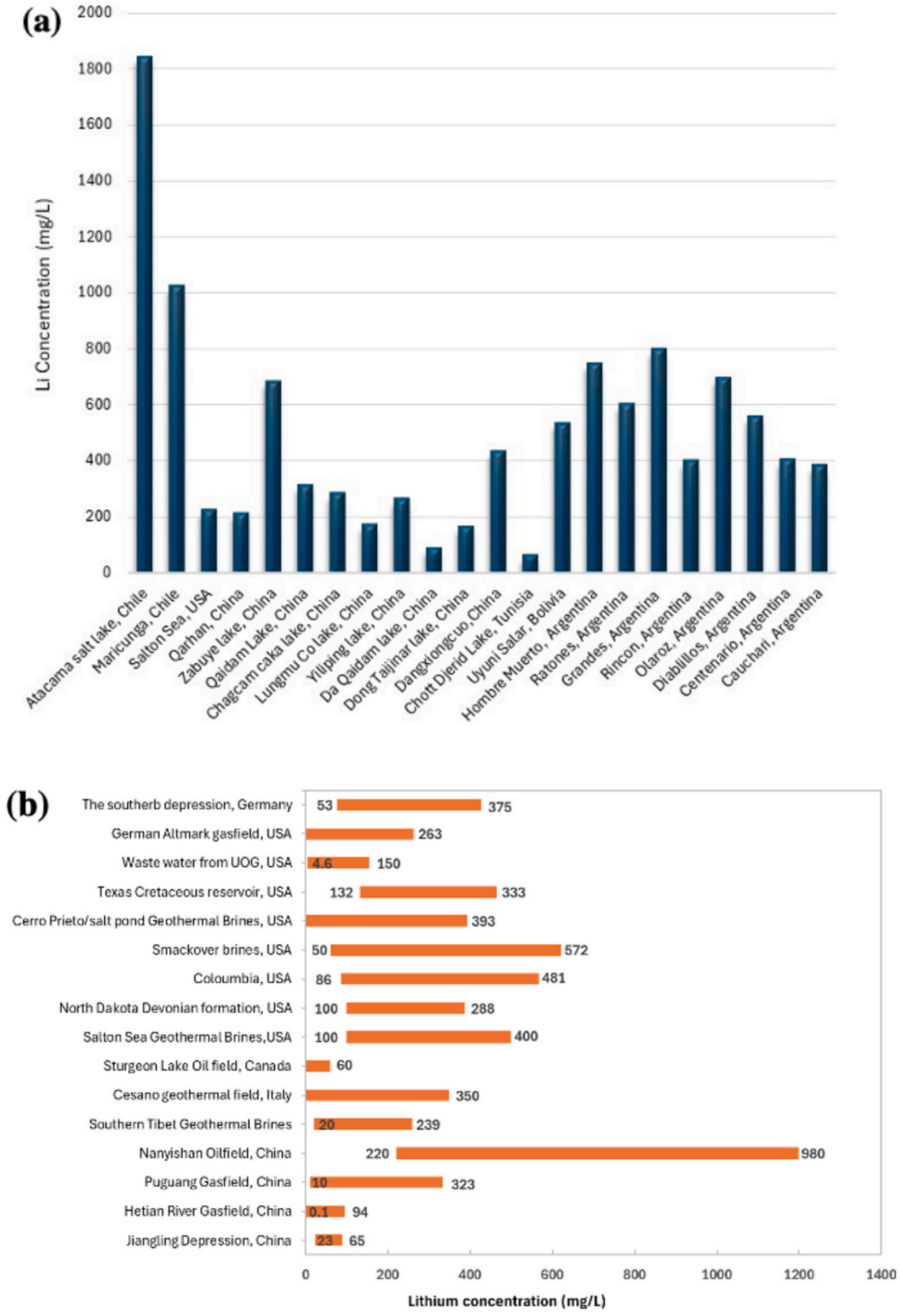

Fig. 2. Global distribution of Li sources: (a) Major Li-bearing salt lakes around the world, highlighting key locations where Li is extracted from saline environments. (b) Global distribution of unconventional oil and gas (UOG) fields with brines that contain appreciable concentrations of Li, indicating potential alternative sources for Li extraction.

Chile, with its established prominence, is exploring nationalization to strengthen its market position [15]. The term "White Gold" aptly reflects the economic and geopolitical significance of Li, emphasizing the critical role of the Lithium Triangle in shaping global energy policies [16].

Seawater presents a vast and largely untapped Li resource, with the potential to diversify and stabilize the global Li supply chain. Technological advancements in extraction could significantly transform the industry by providing a robust alternative to terrestrial brine sources, contributing to a more resilient and sustainable Li market. Such advancements could reduce dependence on geographically concentrated deposits, enhancing industry resilience and supporting the transition to clean energy. In regions without traditional Li mines, such as the Middle East, extracting Li from brine byproducts generated by seawater desalination or from produced water in oil and gas production facilities is particularly noteworthy. This method not only utilizes these resources as a Li source but also aligns with global efforts to expand Li production bases [17], thus reinforcing the Middle East's position in the clean energy landscape as terrestrial reserves diminish.

One of the recent reports by Zhai. et.al [18] investigates the potential of nanofiltration (NF) as a pretreatment technology for Li extraction

from geothermal brines, specifically those from the Salton Sea. The key findings reveal that NF membranes can achieve superior Li^+/Mg^{2+} selectivity under optimized conditions. The study also emphasizes the importance of integrating NF with calcium precipitation to manage high concentrations of divalent cations, such as calcium and magnesium, which pose significant challenges in the extraction process. In contrast, the current work broadens the scope of Li recovery, examining not only geothermal brines but also other resources, including seawater reverse osmosis (SWRO) brines, salt-lake brines, and oil and gas field brines. This study emphasizes the sustainable extraction of Li from waste brine resources using NF technologies. It also focuses on the regulatory implications and presents novel approaches to brine-based Li recovery, highlighting their advantages. The study reviews the selectivity mechanisms and recent technological advancements, identifying the optimal conditions for operating Li-selective NF membranes to maximize Li^+ ion recovery. Additionally, it evaluates the efficacy of various NF processes by assessing their technology readiness levels (TRL). The integration of NF systems into Li recovery workflows is examined, addressing practical implementation challenges and suggesting potential advancements in membrane design specifically tailored for Li-ion separation for commercial applications. Overall, this study provides a comprehensive analysis of NF technology as a viable method for Li separation from diverse brine sources.

1.2. Lithium extraction from brines: a sustainable alternative

Interest in Li extraction from natural water sources is increasing, as these sources contain around 70 % of global Li reserves and offer environmentally sound waste-to-value strategies. With traditional evaporative methods under scrutiny for their environmental impact, the industry is shifting towards more sustainable alternatives [19–25]. Li recovery from salt lake brines is now preferred over solid ore mining due to its cost-effectiveness and easier accessibility, attracting significant industrial attention [5].

The prevalent extraction method uses solar energy to evaporate brine in large open reservoirs, concentrating the Li. However, this process is slow and weather-dependent, typically achieving Li-ion concentrations of approximately 4200 to 4800 mg/L [26]. This method also results in a substantial water loss — 85-95 %, equating to 200–1400 m^3 per ton of Li extracted — which raises concerns about the impact on local water sources, including salt lakes, aquifers, and wetlands, particularly in arid regions like Chile's Atacama Salt Lake [27,28]. Additionally, the process generates significant waste, potentially damaging local ecosystems and creating conflicts with nearby communities [29]. The remote locations of many Li brine deposits further add logistical challenges and costs, such as transporting chemicals and providing energy, affecting the overall sustainability of these operations.

For effective recovery, brines should ideally have Li concentrations around 6000 ppm [27]. These brines contain other ions, such as calcium (Ca), sulfate (SO_4), magnesium (Mg), and potassium (K) [30]. Preliminary treatment and a series of operational phases are necessary to isolate Li from these minerals, including chemical treatments, filtration, and ion exchange processes [31]. Adjustments of pH levels and precipitation methods help to remove unwanted elements while keeping Li chloride in the solution [32]. This careful management of extraction processes is essential to minimize environmental impact and optimize Li recovery.

Several techniques are employed for the selective extraction of Li from brines. Adsorption methods using titanium- or manganese-based adsorbents are effective for extracting Li from petroleum brines, with adsorption capacity influenced by the brine's pH and potentially improved through specific pretreatments. Li-ion sieves, known for their high adsorption capacity and selectivity, are particularly effective for retrieving Li from highly saline brines with low Li content [30]. Direct Lithium Extraction (DLE) technologies offer sustainability advantages over traditional methods, with techniques including sorption, membranes, electrochemistry, and ion exchange gaining preference [33]. Aluminum-based adsorption in DLE systems is noted for its efficiency and minimal reagent usage, though it faces challenges such as high operational temperatures and water recycling complications. Ion exchange-based DLE is advantageous due to its high recovery rates and reduced water dependency, but stability remains a concern. Solvent extraction-DLE, while effective in achieving high Li concentration independent of climatic conditions, is associated with environmental risks and high costs.

Emerging technologies like Li-selective membranes shows promise due to their eco-friendliness and scalability, though they require further enhancements in stability and selectivity. Electrochemical methods support large-scale Li recovery with lower carbon footprints but still require advancements in membrane technologies. Direct carbonation processes offer simplicity and environmental benefits, though they typically have lower recovery rates and operational complexities. Certain DLE approaches also involve altering the brine's pH or heating to 80 °C to enhance Li recovery, which can increase energy and freshwater use [29]. Li brine concentration (LBC) methods aim to synergically enhance DLE processes, improving Li recovery efficiency and reducing water loss [28]. Effective extraction of Li from brines is crucial for the sustainable energy sector, especially given its critical role in rechargeable batteries and other industrial applications [30,34]

Extracting Li from salt-lake brines is a key strategy to address Li scarcity for commercial applications. Chile's Atacama salt lake, with an average Li concentration exceeding 1840 mg/L and estimated reserves of 6.3 Mt., stands out as a significant source. Bolivia's Uyuni salt lake, with substantial Li levels averaging 530 mg/L, also contributes to the global Li supply [35]. Fig. 2a provides an overview of the world's largest Li-containing salt lakes [36–38], emphasizing regions where Li is abundant, extraction costs are lower, and environmental impact is minimized [39]. The predominant cations in these brines include Li^+, Na^+, K^+, Ca^{2+}, Mg^{2+}, and B^{3+}, with anions such as Cl^-, SO_4^{2-}, CO_3^{2-}. However, the efficiency of Li extraction is often limited by low Li^+ concentration relative to other co-existing ions, particularly Mg^{2+}. Due to its similar ionic radius and chemical properties, Mg^{2+} often results in a high Mg-to-Li mass ratio [40,41]. This abundance of Mg^{2+} complicates both traditional and advanced extraction methods, as Mg^{2+} ions can interfere with Li^+ during the carbonate phase, hindering the crystallization of Li carbonate (Li_2CO_3) and increasing both the cost and energy consumption of the extraction process [42]. Research by Liu et al. highlights that varying the Mg/Li ratio affects the morphology, particle size, and purity of Li_2CO_3 crystals. Higher Mg^{2+} content leads to less efficient crystallization, reducing both the yield and purity of Li carbonate, necessitating additional processing steps to remove magnesium, thus increasing operational costs. Additionally, a study by Zeng et al. on Mg-Li alloys provides insights into the mechanical properties and microstructural changes related to varying Li concentrations in magnesium sheets, indirectly highlighting the extraction challenges posed by Mg. This requires precise control and optimization of the extraction process to achieve the desired properties, whether in alloy form or as a purified Li compound [43]. This detailed understanding aids in developing better strategies for Li resource utilization and enhancing the crystallization process in salt lakes. Therefore, research focuses on developing effective separation methods to improve the Li-to-Mg mass ratio in brines, crucial for enhancing Li enrichment from these sources.

Membrane technology can efficiently process low Li concentrations in oil and gas-produced water, provided that optimal temperature, pressure, and anti-fouling measures are maintained. Fig. 2b shows significant Li levels found in certain oilfield brines globally [37,44,45]. Although these wastewaters contain lower Li concentrations than other sources, they offer a dual benefit: they eliminate the need for drilling new wells and turn potential disposal costs into revenue through Li recovery. This creates a mutually beneficial scenario for both oil and gas producers and Li consumers.

Evaluating oil and gas wastewater as a Li source is important,

Table 1
Concentrations of Li and co-existing ions (mg/L) in various brine types. The table details the ionic composition of different brine sources, including seawater reverse osmosis (SWRO) brine, oil-and-gas-produced waters, industrially Li-containing wastewater, salt lakes, and geothermal aquifers, showcasing the variability in ion concentrations across these sources.

Brine type	Lithium (Li)	sodium (Na)	potassium (K)	Calcium (Ca)	Magnesium (Mg)	Strontium (Sr)	Rubidium (Rb)	Ref.
SWRO brine	0.39–0.41	23,100–24,800	790.2–810.1	789.3–804.2	2390.5–2524.1	15.42–16.11	0.19–0.23	[58]
Oil- and gas-produced waters	20	35,960	810	11,900	1120	370		[59]
Industrially Li-containing wastewater	1252.8	102.6	0.575	–	0.009	–	–	[60]
Salt lake	141	117,030	3793	434	5640	–	–	[40]
Geothermal aquifers	350	63,570	21,370	43	12	–	–	[61]

particularly for regions dependent on Li imports, due to its geopolitical implications. Using existing wells substantially reduces capital expenses for Li recovery, as evidenced by Daitch's techno-economic analysis of the Smackover Formation in the U.S. [46]. This approach to domestic sourcing helps reduce the risk of price monopolization by Li-rich countries and promotes energy independence. Companies like MGX have successfully extracted Li from oilfield wastewater [45,47]. In the U. S., the projected Li yield from conventional inland-produced waters, mainly from the Permian Basin and California oil fields, is estimated to reach 47,000 tons annually, with Li concentrations of 35 mg/L and 14 mg/L, respectively. This output is expected to surpass the country's annual Li demand [48–50]. In China's Nanyishan UOG field, Li concentrations can reach up to 980 mg/L, markedly higher than the typical 10–200 mg/L found in most salt lake brines, making Li extraction economically feasible and positioning it as a strategic resource. Effective Li recovery not only promotes sustainable practices but also enhances wastewater management and resource optimization [44].

Geothermal brines, a byproduct of geothermal energy production, contain Li in low yet economically viable concentrations (hundreds of ppm). The extraction process is complicated by their complex chemistry, high salinity, and temperatures exceeding 100 °C [51]. Nonetheless, the large volume of brines produced by geothermal plants renders makes even low-Li sources valuable. Paranthaman et al. highlights ongoing global projects focused on Li extraction from geothermal brine [52,53].

In parallel, the ocean, with its vast capacity and dilutive properties, is recognized as a sustainable resource for essential minerals. While direct extraction from seawater is limited by low Li concentrations (0.17 ppm) [54], the more concentrated brine byproduct from desalination plants offers a higher energy-efficient extraction option. The expansion of seawater desalination plants enhances the feasibility of extracting minerals like Li. Desalination brine, with its higher Li concentration, presents a viable method to reduce waste and recover valuable metals, offering environmental benefits [55]. The Li concentration in seawater reverse osmosis (SWRO) brines typically ranges from 0.27 to 0.4 ppm, depending on the specific conditions and technologies used [54]. The presence of co-existing ions (Table 1), such as Na and K, poses challenges to selective Li extraction from both seawater and SWRO brine [56]. However, recent technological advancements have made mineral recovery from desalination brine more cost-effective than traditional land-based mining [57]. Consequently, Li recovery from seawater desalination brine emerges as a technologically significant and environmentally sustainable solution, addressing resource scarcity and environmental concerns. Ongoing research explores the potential of NF and other innovative techniques to enhance Li recovery from various brine compositions.

Brine processing, particularly in desalination and oil/gas production, faces significant challenges related to scaling and economic feasibility. High salinity and potential scaling issues can cause the deposition of sparingly soluble salts, complicating operations and increasing expenses [62]. In oil and gas fields, inorganic scale deposits can severely impact production rates and profitability, especially in pre-salt oil fields. The inadequacy of laboratory testing to replicate field conditions often results in the prescription of unrealistically high doses of scale inhibitors, which are impractical at higher water cuts [63]. RO, the widely used technology for desalination, is not suitable for high-salinity water due to its inefficiency and susceptibility to membrane fouling and scaling. This fouling, primarily caused by inorganic ions like calcium and magnesium, can damage the membrane's functional layer and its porous structures, reducing its hydrophilicity and increasing electronegativity, which diminishes separation performance over time [64]. Additionally, halite scaling in high Total Dissolved Solids (TDS) environments presents another challenge, as accurately assessing solubility and Saturation Index (SI) is complex. While methods to simulate field conditions and assess halite scaling risk have been developed, they require careful optimization to be effective [65]. Geothermal systems also encounter scaling issues in heat exchangers, which can be mitigated by adjusting geothermal fluid to equilibrium conditions to prevent the precipitation of dissolved solids [66].

Economically, the conventional Li extraction practices from brines, such as evaporation, are characterized by inefficiency and unsustainability, requiring extensive land use, time, and chemical inputs, which generate large volumes of waste [67]. Although solvent extraction following NF treatment offers a more straightforward alternative, it still involves multiple steps and extensive chemical treatments, making it cost-prohibitive [68]. Emerging electrochemical methods present sustainable prospects but are limited by the need for large-area electrodes and high energy consumption, affecting their economic viability [67]. Overall, the economic feasibility of brine processing is constrained by the need for advanced technologies and meticulous control of scaling, which demands significant investment and precise optimization to ensure efficiency and cost-effectiveness. While NF represents a scalable and potentially cost-effective method for Li recovery, addressing these limitations is essential for its broader industrial application. Further research and development in membrane technology, process optimization, and economic modeling are necessary to enhance the efficiency and sustainability of Li extraction from various brine sources, supporting the growing demand in the sustainable energy sector.

2. NF-based pretreatment process for enhanced Li recovery

Conventional large-scale Li production methods, particularly solar evaporation, suffer from slow processing rates and a high risk of contamination, which introduces impurities that degrade product quality [5,69]. In response, membrane-based technologies have emerged as a sustainable option, designed to reduce water and energy consumption while decreasing waste, thereby enhancing the efficiency and purity of the Li extraction process. Park et al. developed a membrane-based Li recovery method that addresses the inefficiencies inherent in conventional evaporation techniques, with its relative effectiveness shown in Fig. 3a and b [70]. These methods are now preferred for their energy efficiency and sustainable approach to industrial extraction and separation [71–73].

Among the array of membrane technology—such as nanofiltration (NF) [74], reverse osmosis (RO) [75], ion-sieve membrane (ISM) [76], membrane distillation (MD), membrane distillation crystallization (MDC) [77–79], supported liquid membrane (SLM), and ion-imprinted membrane (IIM)—NF stands out [61,80]. NF membranes have proven effective in separating brines with high Mg^{2+}/Li^{+} ratios, which a

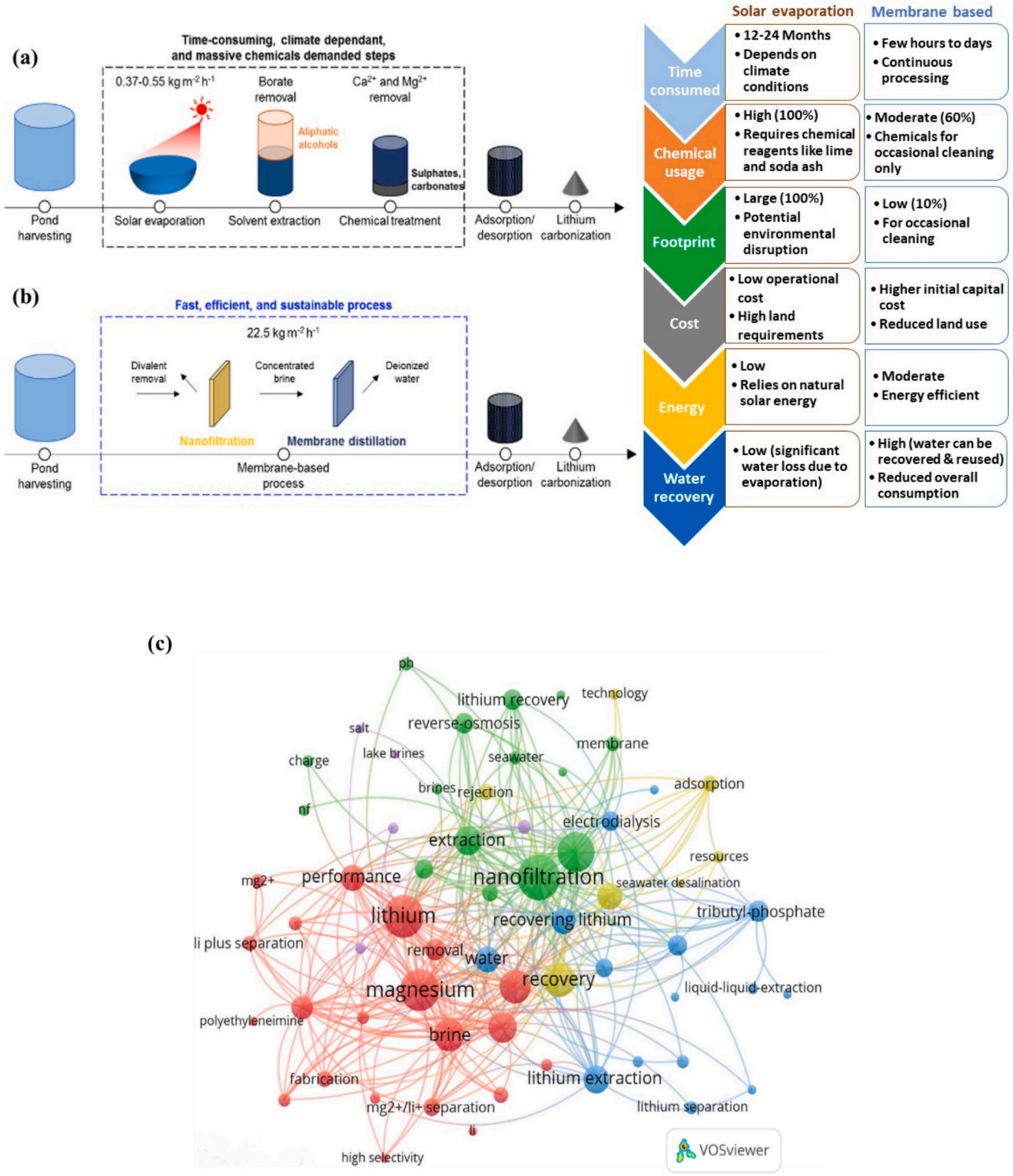

Fig. 3. Comparative schematic of Li production systems: (a) Conventional solar evaporation method depicting the process stages and its layout. (b) Advanced Li recovery utilizing membrane technologies, highlighting the integration of NF in the process chain. This figure compares the process durations for each method, adjusted for equivalent capital expenditures, and analyzes chemical usage and physical footprint reductions attributable to NF efficiency and process intensification [70]. (c) VOSviewer overlay map illustrating keyword co-occurrence based on the Web of Science database, with a focus on "Lithium", "Brine", and "Nanofiltration", emphasizing the thematic intersections relevant to Li recovery technologies.

common challenge in the extraction process [40,81–83]. Despite the complexity introduced by the coexistence of Mg and Ca, NF demonstrates substantial energy efficiency and the capability for continuous operation in Li recovery from salt lake brine [56]. The process uses mechanical pressure to drive brine through NF membranes, which efficiently retain multivalent ions [29]. Pressure plays a crucial role in the separation efficiency of Li and Mg, especially in membrane-based processes. Operating at significantly lower pressures than RO—typically between 35 and 100 bar—NF membranes exhibit a reduced propensity for fouling, a significant advantage over other membrane technologies [84]. Under an electric field with an applied pressure of 4 bar, Li et al. reported the ultrahigh separation efficiency of Mg^{2+}/Li^{+}

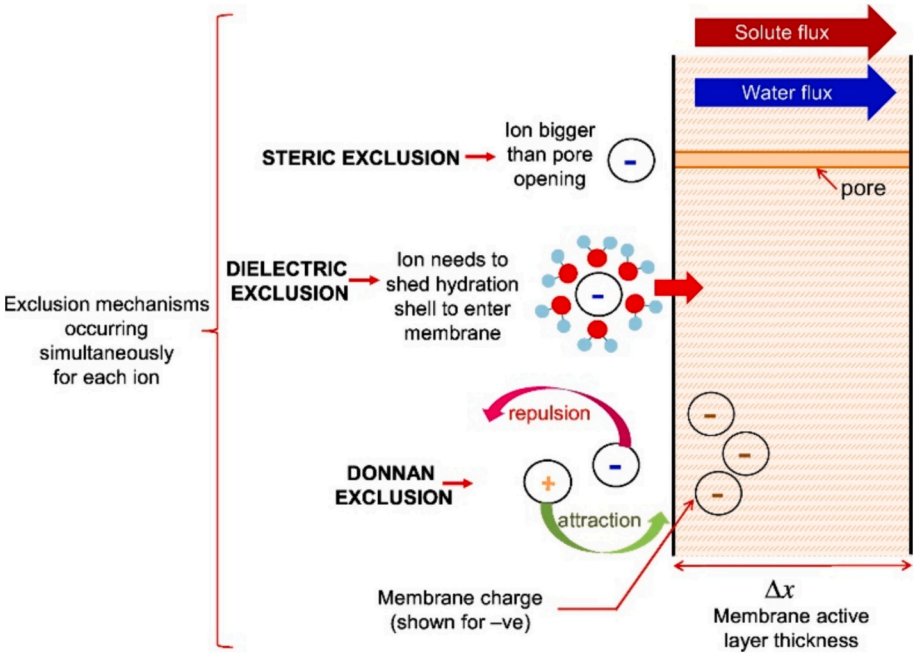

Fig. 4. Illustration of mechanisms of solute exclusion in NF according to the Donnan steric pore model with dielectric exclusion (DSPM–DE) [106].

(over 99 %) using an in-situ reconstructed positively charged NF membrane [85]. Research by Sun et al. also confirms that separation efficiency for Mg^{2+} and Li^{+} is highly dependent on operating pressure, alongside other factors such as inflow water temperature, pH, and the Mg^{2+}/Li^{+} ratio [40]. Their findings indicate that increased pressure tends to enhance permeate flux, thus improving the overall separation efficiency and effectiveness of the NF system in Li recovery.

The operational pressure required for Li recovery using NF membranes depends on variables such as feed concentration, desired separation efficiency, brine composition, membrane type, and the membrane's performance under high salinity conditions. A lab-scale NF system effectively reduced TDS and total hardness (TH) in brine discharge, operating at pressures between 4 and 7 bar [86]. Additionally, a tubular ceramic TiO_2 NF membrane demonstrated significant ion rejection rates in brackish water treatment at a relatively low pressure of 2 bar [87]. However, higher pressures are often necessary for more concentrated brines. Research by Foo et al. [36] shows that Li^{+}/Mg^{2+} selectivity decreases by about 43 % when feed salinities rise from 10 to 250 g/L, suggesting the need for higher pressures to sustain effective separation in high salinity scenarios. Despite these challenges, commercially available NF membranes, as demonstrated in Wang et al.'s multi-pass NF process, have shown resilience and the ability to maintain good Li/Mg selectivity even with brine recirculation [74]. Further studies indicate the efficacy of specific membranes under varied conditions. For example, the DK NF membrane achieved an 83 % Li yield from salt lake brine with a high Mg-to-Li mass ratio, though long-term use led to membrane fouling and reduced performance [64]. Conversely, novel polyamide NF membranes developed by Jin et al. exhibited exceptional performance, achieving an Mg^{2+} rejection rate of 99.96 % and a Li^{+}/Mg^{2+} selectivity exceeding 4000 under optimal pressure conditions [88].

Moreover, the Li-MFCDI process reported by Saif et al. maintained stable performance and high selectivity for Li over other monovalent cations, even in the presence of high Na^{+}/Li^{+} mass ratios, supporting the commercial viability of these membranes for handling high-salinity brines [89]. The Filmtec NF90-2540 membrane has also proven effective in managing high salinity feeds, with performance influenced by feed temperature and TDS levels [90]. Furthermore, Nafion membranes, typically used in energy applications, were effective in managing high salinity gradients, although the presence of divalent cations like magnesium reduced the power density [91]. These findings emphasize the viability and robustness of NF membranes in Li recovery applications, indicating that appropriate operational parameters and commercially available membranes like those from Filmtec and Nafion can be suitably deployed in high-salinity environments.

NF employs membranes such as DK and NF90, and their modified forms, including EDTA-modified NF membrane and the modified polyamide membrane with carbon nanotubes (MPMC), which is a high-flux, positively charged NF membrane. These membranes operate between RO and UF, featuring pore sizes ranging from 0.5 to 2 nm and molecular weight cut-offs (MWCO) from 200 to 1000 Da. This configuration is optimized for intercepting multivalent inorganic salts and small organic molecules [92], making them highly effective for Li selectivity from various brine sources. A comparative study by Somrani et al. [83] demonstrated the NF90 membrane's capacity to fully retain Mg^{2+} while allowing 15 % permeability for Li^{+} at lower operational pressures. This study used a transmembrane pressure range of 0–15 bars, observing maximum selectivity at 8 bars and a notable difference in Li and Na rejection of 40 %. The permeate flux for the NF90 membrane with diluted brine was measured at 0.7 L/h m^{-2} bar^{-1}, indicating its potential for scalability in full-scale experiments, although fouling mechanisms require further investigation.

The design of NF membranes with specialized pore size ensures efficient separation, especially beneficial for Li extraction from brine. The industry is actively enhancing NF processes to deliver high flow rates and precise extraction, focusing on Li^{+} selectivity over competing ions such as Mg^{2+}, Na^{+}, and K^{+}, NF membranes from manufacturers like Dow FilmTec and Osmonic Desal's DL/DK series have been successful in Li^{+}/Mg^{2+} separation, showing improved performance in less saline brines [81,93].

To gain insight into the landscape of Li recovery through NF, a comprehensive analysis was conducted via the Web of Science using the keywords "Lithium," "Brine," and "Nanofiltration" for the period from 2013 to 2023. This search identified 707 keywords. For clarity in network visualization, only keywords appearing a minimum of five times were included, resulting in 64 keywords meeting this criterion. These keywords were mapped using VOSviewer to create a bibliometric network, as illustrated in Fig. 3c. In this visualization, the size of each

Table 2
Characteristics of coexisting ions in Salt-Lake brine. It presents key physico-chemical properties of various ions, including their hydrated radius, Stokes radius, diffusion coefficient, and hydration-free energy, as derived from studies referenced in [83,107].

Ions	Li^+	Mg^{2+}	Na^+	K^+	H^+	Ca^{2+}	Cl^-
Hydrated radius (nm)	0.382	0.428	0.358	0.331	0.28	0.412	0.332
Stokes radius (nm)	0.238	0.348	0.184	0.125	–	0.347	0.121
Diffusion coefficient ($10^9.m^2S^{-1}$)	1.03	0.72	1.33	1.957	9.31	0.792	2.03
Hydration-free energy kJ/mol	−515	−1828	−365	−295		−1504	−340

cluster represents the frequency of the term, while the proximity of terms indicates their interrelation within the research field.

2.1. Properties of NF membrane and separation mechanisms

NF membranes are fabricated from various materials, including polymers, ceramics, or a combination thereof, each offering distinct separation properties [94]. The performance of an NF membrane hinges on several critical parameters, such as pore radius, surface charge density, and membrane thickness [95]. Pore size is a key characteristic and is typically evaluated by the rejection of neutral solutes; a 90 % rejection rate corresponds to the membrane's MWCO [19], which acts as an indicator of effective pore size [40]. The Stokes-Einstein equation is also used to calculate the radii of organic molecules [96], providing further insight into membrane selectivity. A membrane's hydrophilicity, influ-

Table 3
Summary of Literature on NF operating conditions for Li recovery, detailing NF membrane types, operational parameters (such as temperature, pressure, and pH), and outcomes (including Li molar flux and recovery percentages) across different brine sources.

Source and concentration (mg/L or ppm)	Membrane materials/process	Temperature (°C)	Pressure (Mpa)	pH	Lithium molar flux (LMH)	Remarks	Ref.
• Geothermal Brine • Li = 350 • Mg = 12 • TDS = 85,345	• NF2, made up of polyamide (PA) material produced by Rising Sun Membrane Technology, China	2–45	1.5	10	42	• Li recovery reaching >75 %.	[61]
• Artificial brine • Li = 204 • Mg = 5, 800 • TDS = 59,250	• Spiral wound membrane apparatus (0.44 nm pore size) • Laboratory scale	20–40	1.5–3.5	–	5–30	• % yield Li = 50–99 % at Mg/Li concentration ratio of 1.5–4 with 7–20 separation factor (SF)	[81]
• Salt lake brines (East Taijiner brine) • Mg^{2+}/Li^+ ratio was <20 • Li = 132 • Mg = 5640 • TDS = 126,038	• DL-2540 • Available membrane area 2.51 m^2	–	0.48–2.76	2–11	5.24	• Average rejection of $MgSO_4$ = 96 % • Water yield = 3.18 m^3 d^{-1}	[40]
• Synthetic brine • Li = 100 • Mg = 2400 • TDS = 2500	• EDTA modified • PA- NF membrane (0.2 nm pore size) • Laboratory scale	25	1	–	–	• % Rejection of Li = 68.1 % with a 24 (SF) and Mg/Li = 24 ionic solution	[82]
• Salt lake brine • Li = 159 ppm • Mg = 3400 ppm • TDS = 21,584	• NF90 membrane	21	>1.5	6.7	–	• NF of Tunisian salt lake brine diluted ten times, a 100 % rejection of Mg^{2+} and only 15 % for Li^+, with a separation of 85 % under low pressure (15 bars).	[83]
• High Mg^{2+}/Li^+ ratio brine. • Li = 10.9–21.7 • TDS = 60,000	• The NF element was a spiral-wound DK-1812model	20 ± 0.5	0.8	–	–	• The rejection of magnesium (R(Mg^{2+})) and the separation factor (SF) were 0.96 and 42, respectively. • The Mg^{2+}/Li^+ ratio in permeate could be reduced to 0.9, and Li^+ recovery ratio was 85 %	[108]
• Salt lake brine • Li = 159 • Mg = 3400 • TDS =21,584	• PA film Pilot scale	35	1.5	–	–	• % Recovery of Mg = 100 % • % Recovery of Li = 15 % • Mg/Li ratio = 3.3333	[83]
• Artificial brine • Li = 204 • Mg = 5, 800 • TDS = 59,250	• Concentrate flux = 120 L/h	39.85	3.5	4 ± 0.2	50	• Yield of Li =23 %;	[81]
• Artificial brine • Li = 10.9–21.7 • TDS = 60,000	• Spiral wound membrane apparatus (0.238 nm pore size) • Laboratory scale	20	0.5		–	• Mg/Li ratio = 0.96 • % Recovery of Li = 85 % up to 40 (SF)/ionic solution	[108]
• Synthetic brine • Li = 1000 • Mg = 1000 • TDS = 2000	• Polyacrylonitrile (PAN) UF hollow fiber membranes (1.66 nm pore size) • Laboratory scale	–	0.3	–	7.5	• % Rejection of Li = 40.7 %/ionic solution	[19]

enced by its surface roughness and composition, plays a crucial role in enhancing its rejection rates, flux performance, and resistance to fouling. The water contact angle is commonly employed as a measure of a membrane's hydrophilicity and overall filtration efficiency. The charge of membrane charge, which varies depending on the materials and manufacturing techniques used, is critical for its application specificity. For example, positively charged membranes are particularly effective for extracting Li^+ from brines with high Mg^{2+}-to-Li^+ ratios, due to their ability to repel similarly charged solutes [20,97].

The NF process, driven by applied pressure, excels in the efficient extraction of Li^+ ions, utilizing mechanisms such as Donnan exclusion, steric hindrance, and dielectric exclusion [5,98,99]. Donnan exclusion promotes separation through electrostatic interactions between the charged membrane surface and multivalent ions. Steric hindrance, or physical sieving, occurs when molecules of varying sizes pass through the membrane's pores. Dielectric exclusion leverages the polarized charges of ions and their interactions with the membrane's dielectric properties. The integrated Donnan steric pore model with dielectric exclusion (DSPM-DE) help elucidate the interactions at the membrane-feed interface, as depicted in Fig. 4, providing a rationale for the preferential rejection of Mg^{2+} over Li^+ due to its higher hydrated radius and differing diffusion coefficient, as detailed in Table 2.

The effectiveness of NF membranes in ion separation is significantly influenced by their charge [100]; positively charged membranes are particularly adept at differentiating between multivalent cations such as Mg^{2+} and Li^+ [5,101,102]. These membranes offer considerable advantages for Li^+ extraction from brine, highlighting their adaptability and effectiveness [103]. NF technology is characterized by its heightened selectivity among ion types, typically following the rejection sequence of $Mg^{2+} > Ca^{2+} > Li^+ > Na^+$. It benefits from higher hydraulic permeability in membranes, facilitating convective transfer and reducing energy consumption. The adoption of novel and existing materials further amplifies these benefits, promoting more efficient and energy-saving separation processes [104,105].

2.2. Analysis of performance metrics of NF membrane

The functionality of NF membranes is intricately linked to the dynamics of pore size and molecular interaction. These membranes are designed to allow the passage of ions and molecules based on their size, closely correlating to the MWCO of the membrane. This relationship is quantitatively assessed using the Stokes-Einstein equation, which calculates the radius (r_s) of organic molecules (m). The equation is given by:

$$r_s = \frac{kT}{6\pi\mu D_s} \tag{1}$$

Here, k is the Boltzmann constant (1.380649×10^{-23} J/K), μ is viscosity (Pa·s), T is the temperature (K), and D_s is the diffusion coefficient (m^2/s). This formula allows for a precise correlation between molecular weight and effective pore size, aiding in the accurate measurement of organic molecules' radii [40].

The efficiency of NF membranes in separating different solutes is measured by several key performance indicators including retention rate (R_{obs}, %), separation factor (SF), and membrane flux (J_w). The retention rate is defined as:

$$R_{obs} = \left(1 - \frac{C_P}{C_F}\right) \times 100\% \tag{2}$$

where C_P and C_F are the concentrations of the permeate and feed solutions (mol/L), respectively. This metric indicates the percentage of solute retained by the membrane. The separation factor for ions such as Li^+ and Mg^{2+}, crucial for applications in Li recovery, is evaluated using:

$$S_{Li,Mg} = \frac{C_{Li,p}/C_{Mg,p}}{C_{Li,f}/C_{Mg,f}} \tag{3}$$

Here, $C_{Mg,p}$ and $C_{Li,p}$ represent the permeate concentration (mol/L) of Mg^{2+} and Li^+, respectively, while $C_{Mg,f}$ and $C_{Li,f}$ are their concentrations (mol/L) in the feed [22]. A separation factor of 1 indicates no selective separation between Mg^{2+} and Li^+.

2.3. Operating conditions influencing NF process for Li recovery

Effective Li recovery via NF requires a strategic pre-treatment approach that capitalizes on the selectivity of NF membranes. This selectivity is influenced by factors such as pore size, membrane charge, ionic strength, solute properties, hydration, pH, operational pressure, and feed temperature. Each factor affects salt movement through the membrane, contingent on the membrane's specific properties and the operational conditions [83]. A comprehensive summary of the literature specifying the NF operating conditions for Li recovery from various brines is provided in Table 3.

2.3.1. Temperature

Temperature significantly impacts NF processes by influencing both the structural integrity of the membrane and the physical properties of the solution. Manufacturers specify optimal operating temperatures for each NF membrane type; for instance, the DK membrane operates effectively up to 323 K. Temperature exceeding this range can induce thermal expansion of the membrane, potentially causing pore enlargement and altered permeability. Yan et al. observed increased permeation and decreased retention of Mg and Li as temperatures rose from 293 to 313 K [81].

While higher temperatures can enhance flux rates, they may reduce separation efficiency, particularly when separating Mg from Li in brines with high Mg^{2+}/Li^+ ratios. At elevated temperatures, lower viscosity reduces concentration polarization, enhances solute diffusion, and intensifies turbulence within the flow. These conditions, though favorable for increasing flux, can compromise Mg/Li separation. Sun et al. [40] observed that temperature increases beyond 18–20 °C adversely affect membrane selectivity by elevating osmotic pressure, reducing solution viscosity, and altering pore sizes. Accurate temperature control is thus essential for optimizing Li recovery and maintaining consistent separation performance [40,81].

2.3.2. Pressure

Effective separation via NF membranes requires the externally applied pressure to surpass the osmotic pressure difference ($\Delta\pi$) across the membrane. Osmotic pressure, vital for separation, emerges from solute concentration disparities on either side of the membrane, driving solvent migration towards higher solute concentrations. This osmotic mechanism facilitates the selective passage and retention of specific ions and molecules during NF operations. Influenced by factors including temperature and feed concentration, osmotic pressure adheres to the principles of the solution-diffusion model. The membrane flux ($L/m^2 \cdot h$) equation [109] is expressed as:

$$J_w = L_p(\Delta P - \sigma\Delta\pi) \tag{4}$$

where L_p represents the water permeability coefficient ($L/m^2 \cdot h \cdot bar$), σ is the reflection coefficient, and ΔP (MPa) denotes the transmembrane pressure. The osmotic pressure difference is given by:

$$\Delta\pi = \Delta c_s RT \tag{5}$$

Here, R is the gas constant (83.1 $cm^3\ bar^{-1}\ mol^{-1}\ K^{-1}$), T (in K) represents the absolute temperature, and Δc_s is the difference in salt concentration.

In NF operations, particularly when targeting efficient Li recovery,

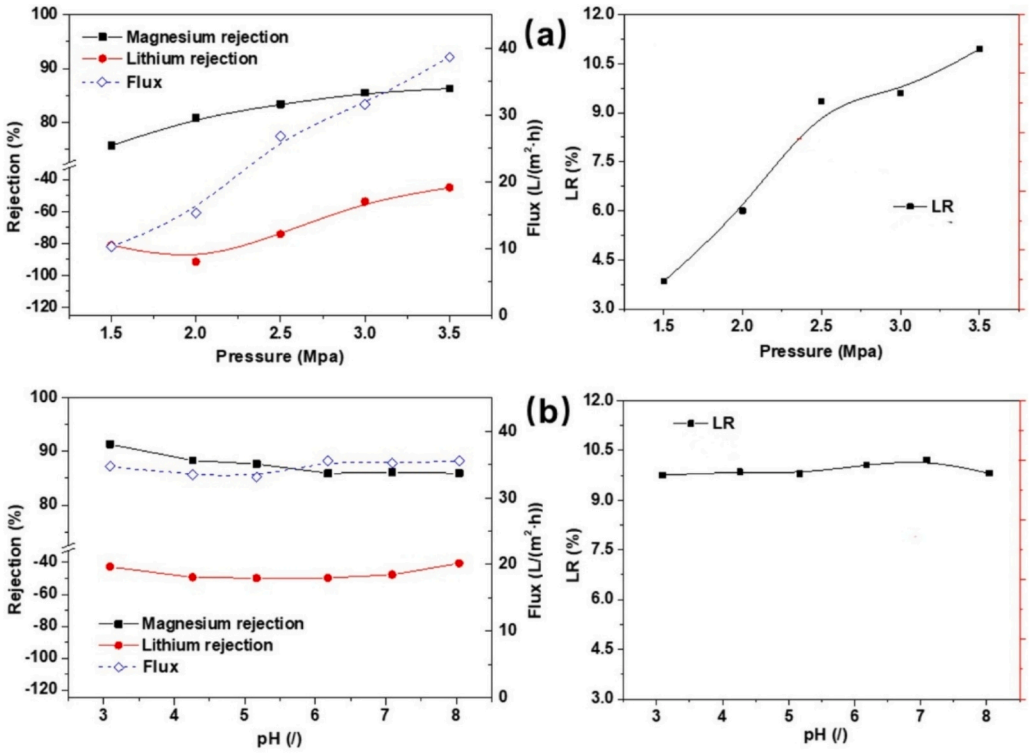

Fig. 5. Effects of operating parameters on ions rejections, permeate volumetric flow rate, and Li recovery in the NF process: (a) Operating pressure. (b) pH of feed solution. Experimental conditions: temperature of 25 ± 1 °C, operating pressure of 3.5 MPa, feed solution pH of 8.0 [110].

maintaining optimal transmembrane pressure is crucial. As a consistent feed concentration, membrane flux is predominantly influenced by pressure. Ion accumulation at the membrane surface can lead to concentration polarization, affecting both solute flux and ion rejection. Higher pressure conditions significantly enhance Li separation from Mg. For example, applying a pressure of 3.5 MPa achieved 92 % Mg rejection [81]. Further investigation by Sun et al. [40] using the Desal-2540 NF membrane showed that increased pressure leads to higher water flux and Mg rejection, thereby enhancing separation efficiency in brine wi0th high Mg^{2+}/Li^{+} ratios. Zhao et al. [110] explored the efficacy of integrating bipolar membrane ele00ctrodialysis (BMED) with NF, RO, and continuous electrodialysis (CED) processes to extract Li hydroxide from salt lake brine with a high Mg/Li ratio. This study examined how operating pressure within this integrated membrane framework (NF-RO-CED-BMED) influences Li recovery, maintaining operational conditions like a feed temperature of 25 ± 1 °C and a feed pH of 8.0. Results indicated that both Li^{+} and Mg^{2+} rejection rates improved as pressure increased from 1.5 to 3.5 MPa, significantly lowering Mg^{2+} concentration in the permeate at the elevated pressure. Conversely, Li rejection decreased within the same pressure range, suggesting a preferential passage of Li through the membrane. This investigation highlighted that Li recovery benefits from increased pressure, attributable to enhanced volumetric flux and improved Li retention, as shown in Fig. 5a.

2.3.3. pH effect

The operational efficacy of NF membranes is significantly influenced by the pH of the solution, affecting membrane pore size, surface charge, and hydrophilicity through electrical interactions with organic and inorganic substances. Sun et al. demonstrated that a lower pH favors Mg rejection while decreasing Li rejection [40]. Zhao et al. [110] further investigated pH effects within a multi-stage Li recovery system (NF-RO-CED-BMED) (Fig. 5b), finding that Mg rejection declines with increasing pH, whereas Li rejection dips at pH 5.17 before beginning to rise again. Notably, the membrane's volumetric flux remains relatively stable across different pH levels.

The isoelectric point (IEP) of the membrane, pivotal in determining its charge properties, shifts with the presence of divalent ions. Below the IEP, the membrane assumes a positive charge, reducing its rejection capabilities due to weakened electrostatic repulsions. Above the IEP, increased electrostatic repulsions and the influence of Donnan equilibrium enhance Li rejection. The identified IEP of the DK membrane at pH 5.17 represents a shift from previous reports, indicating how the presence of divalent ions can influence membrane behavior. Additionally, as the pH rises above the IEP, Mg retention decreases slightly before stabilizing, illustrating the subtle impact of pH on Li recovery in the NF system (Fig. 5b).

Li et al. examined the complex interplay between pH and salinity on the separation efficiency of Mg^{2+}/Li^{+}, revealing that heightened salinity leads to decreased flux primarily due to increased viscosity and concentration polarization [111]. While pH has a less pronounced impact on flux, a lower pH enhances the dielectric exclusion of multivalent ions, favoring Mg^{2+}/Li^{+} separation. Optimal pH management is especially critical in multi-stage NF processes. A notable study demonstrated that adjusting the pH to 3.5 in a dual-phase system significantly improved the Mg^{2+}/Li^{+} ratio, reducing it from 13.25 to 0.17 after separation [112]. This adjustment emphasizes the critical role of pH in optimizing the separation dynamics of NF systems and enhancing overall recovery efficiency.

3. Regulation of NF membrane for enhanced Li selective separation

Optimizing the selectivity of NF membranes is essential not only for improving the quality of permeate but also for enhancing the efficiency of resource recovery [113]. Developing innovative strategies to regulate NF membranes is crucial for achieving superior Li selectivity, which is fundamental for effective extraction from brine sources.

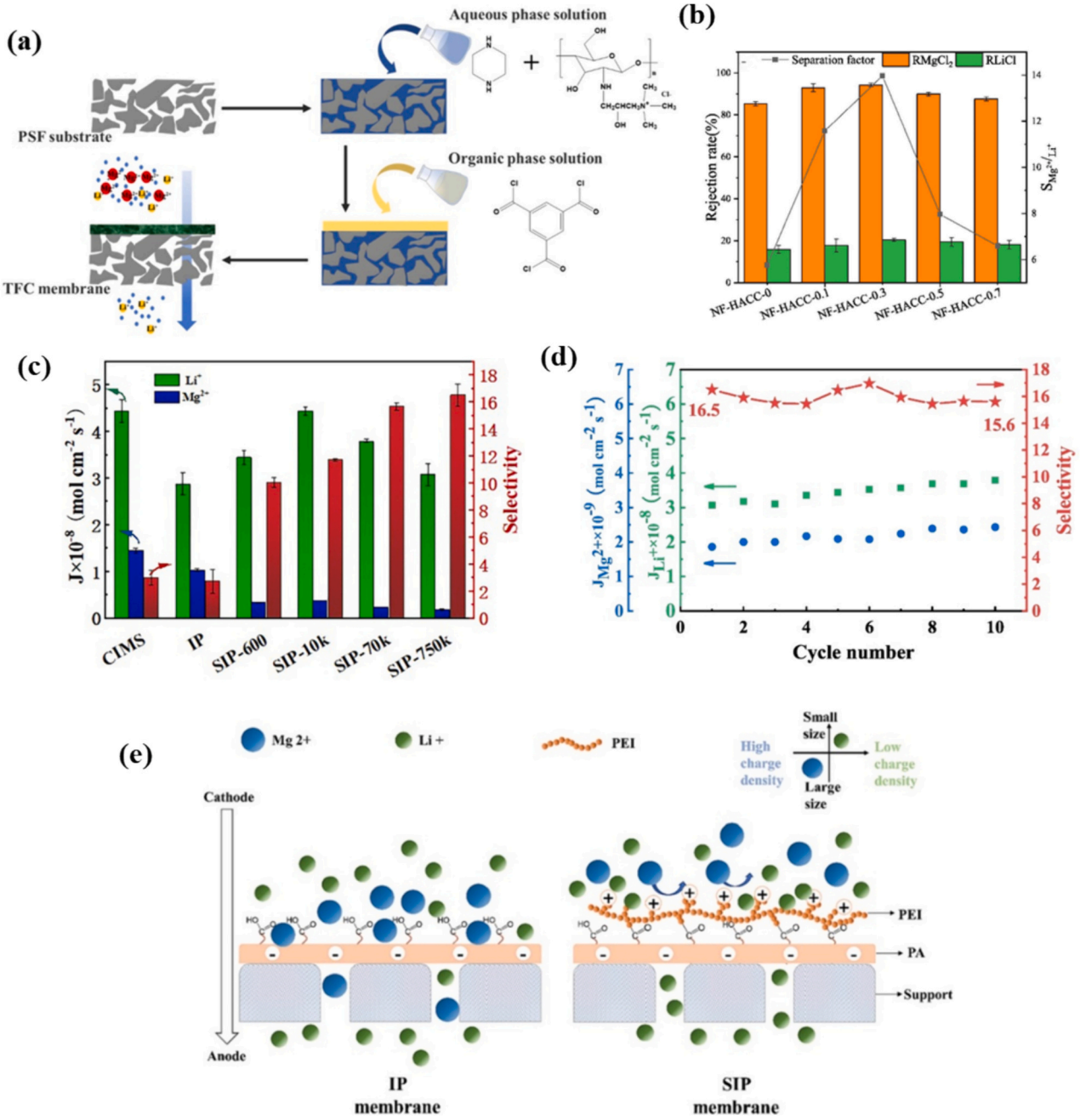

Fig. 6. Detailed representations of NF membrane processes and performance: (a) Schematic illustration of the TFC NF membrane manufacturing process. (b) Performance efficiency of NF membranes for individual $MgCl_2$ and LiCl separation [114]. (c) Ion flux and selectivity in engineered NF membranes (ENFMs). (d) Cyclic performance of the SIP-750 k membrane. (e) Diagram depicting the selective transmembrane movement of Li^+ and Mg^{2+} during electrodialysis [115].

3.1. Advanced interfacial polymerization (IP) processes

Refining the design of NF membrane through advanced interfacial polymerization (IP) processes represents a promising avenue for enhancing membrane structure and composition, which are critical for improving separation performance and Li selectivity. This approach involves incorporating innovative materials such as hydroxypropyltrimethyl ammonium chloride chitosan (HACC) [114] and developing electro-NF membranes [115] through layered interfacial polymerization (IP) techniques. Such advancements are pivotal in fabricating membranes that offer improved Mg^{2+}/Li^+ selectivity, navigating the typical trade-off between selectivity and permeability. Zhang et al. [114] advanced the field of IP for Li recovery from brine using NF by incorporating HACC, known for its hydrophilicity and strong positive charge. They developed a process for preparing thin-film composite (TFC) NF membranes, illustrated in Fig. 6a. In their methodology, HACC was blended with piperazine (PIP) and reacted with trimesoyl chloride (TMC) to fabricate positively charged NF membranes. This tailored IP process using HACC resulted in a thinner separation layer, improved hydrophilicity, and consistent pore size in the modified NF membrane, significantly enhancing Mg^{2+}/Li^+ separation efficiency and permeability. Furthermore, the incorporation of quaternary ammonium groups from HACC also enhanced the membrane's antibacterial properties.

Following optimization, the NF-HACC-0.3 membrane achieved a remarkable separation factor of 115 for a solution comprising 1866 ppm $MgCl_2$ and 134 ppm LiCl. The performance of NF membranes with various HACC concentrations in separating $MgCl_2$ or LiCl solutions is

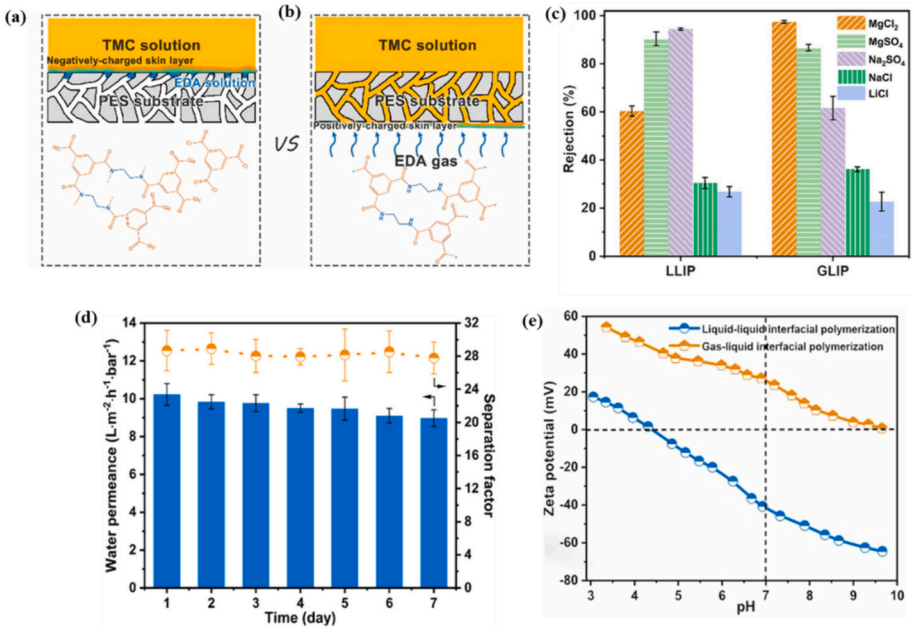

Fig. 7. Schematic and performance characteristics of NF membranes produced via IP: (a) At the liquid/liquid interface (LLIP). (b) At the gas/liquid interface (GLIP). (c) Salt rejection profiles for several inorganic salts using NF membranes fabricated by LLIP and GLIP. (d) Long-term stability of GLIP-manufactured NF membranes, tested over a 5-min reaction time, with feed solutions containing 100 mg/L LiCl and 2000 mg/L $MgCl_2$. (e) Zeta potential measurements demonstrating prolonged activity of NF membranes [116].

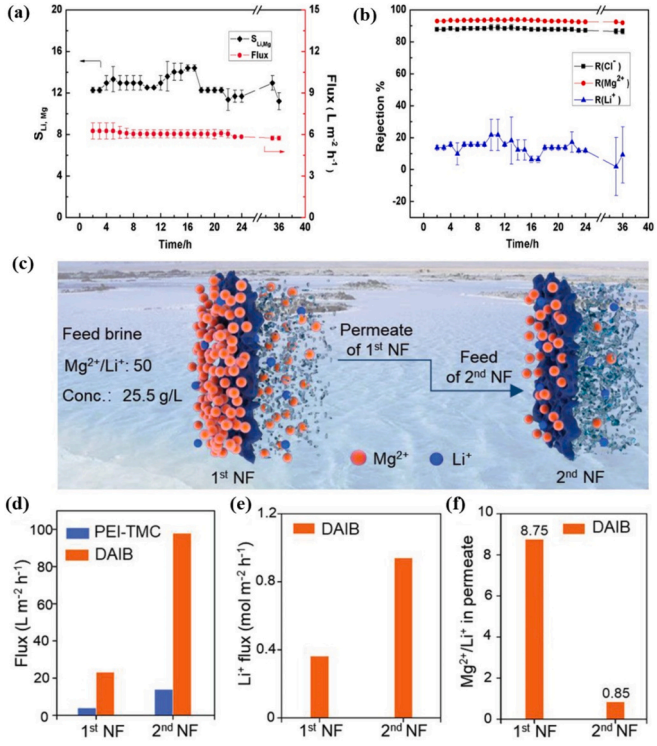

Fig. 8. Performance analysis of the ideal PA-B2-E3 membrane during a 36-h filtration cycle: (a) Separation factor for $S_{Li,Mg}$, and corresponding flux. (b) Removal efficiencies for Cl^-, Li^+, and Mg^{2+} under operational parameters of 1.0 MPa, pH 5.5, C_{Mg2+} = 2.4 g/L, and Mg^{2+}/Li^+ = 24 [82]. (c) Diagram of the two-step NF process for professing a concentrated salt blend (LiCl: 0.5 g/L, $MgCl_2$: 25 g/L) at 6 bar pressure, with the second stage feed being the permeate from the first stage. (d) Water flux measurements for the first and second stages using PEI-TMC and DAIB membranes. (e) Li^+ flux and (f) Mg^{2+}/Li^+ selectivity in the permeates of the first and second NF stages, respectively [118].

depicted in Fig. 6b. Additionally, this membrane exhibited a water permeance of 157 ± 7.5 L m^{-2} h^{-1} MPa^{-1}, more than doubled that of the pristine membrane. This method presents a promising approach for preparing and developing specialized NF membranes tailored for Mg^{2+}/Li^+ separation, offering significant potential for Li extraction from brine sources.

Chen et al. reported the fabrication of electro-NF membranes (ENFMs) via sequential interfacial polymerization (SIP). This technique involves embedding polyethyleneimine (PEI) on the surface of the membrane, significantly enhancing its selectivity and reducing the electrical resistance [115]. The chemical modification of the membrane surface creates robust chemical interactions with the membrane matrix, substantially improving stability. By varying PEI's molecular weight, adjustments were made to the membranes' pore size and surface charge, effectively enhancing Li^+/Mg^{2+} selectivity through electrostatic repulsion and pore size sieving. Incrementing PEI's molecular weight altered the membrane surface's zeta potential from negative to positive and constricted the pore size. Fig. 6c illustrates a direct correlation between Mg^{2+}/Li^+ selectivity and the Li^+ to Mg^{2+} flux ratio, showcasing the ENFMs' superior selectivity post-SIP process compared to traditional IP membranes. This enhancement demonstrated increased Li^+ flow and reduced Mg^{2+} flux, effectively challenging the conventional trade-off between selectivity and permeability. The cyclic performance of the SIP-750 k membrane, tested over 10 cycles, is depicted in Fig. 6d. This membrane exhibited excellent cyclic durability, maintaining consistent properties across multiple cycles, thereby indicating robust long-term stability for practical applications. Despite a slight increase in Mg ion flux over the extended operation, the selectivity remained impressively high at >15.6, confirming the ENFMs' robust performance. Fig. 6e presents the transmembrane movement pathway of Mg^{2+}/Li^+ under an electric field, guided by zeta potential, MWCO, and XPS results. At an optimal current density of 10 mA cm^{-2}, the ENFMs exhibited substantial Li^+ flux (3.08×10^{-8} mol cm^{-2} s^{-1}) and remarkable Li^+/Mg^{2+} selectivity (16.55), coupled with minimal membrane electrical resistance (2.42 Ω cm^2) and elevated limiting current density (50.6 mA cm^{-2}), underscoring their efficacy in Li extraction.

Further advancing this domain, Wu et al. developed a novel

positively-charged NF membrane using a gas/liquid interfacial polymerization (GLIP) technique, an alternative to the conventional liquid/liquid interfacial polymerization (LLIP) [116]. Unlike LLIP (illustrated in Fig. 7a), GLIP (Fig. 7b) substitutes the amine solution with amine gas, resulting in a surplus of amine monomers relative to acyl chloride monomers, thereby fostering a positively charged membrane surface. The GLIP process, by allowing slower reaction kinetics, offers greater control over the surface charges and average pore sizes of the PA layers. This adaptability is crucial for tailoring NF membrane structures to optimize Li^+/Mg^{2+} selectivity. The NF membrane fabricated via GLIP demonstrated a high $MgCl_2$ rejection rate of 98.5 % and a low LiCl rejection rate of 22.6 %, indicative of exceptional selectivity. Fig. 7c shows the rejection rates of different inorganic salts using NF membranes produced by both LLIP and GLIP, with reaction time of 2 min for LLIPs and 5 min for GLIP, at an inorganic salt concentration of 1000 mg/L. Over prolonged operations, these membranes maintained a high Li^+/Mg^{2+} separation factor of 28, as shown in Fig. 7d. Fig. 7e presents the zeta potential of NF membranes from both IP methods, demonstrating consistent performance over time, thereby affirming their structural stability and practical utility for Li recovery from brines.

3.2. Surface modification

Enhancing NF membrane performance for ion separation and permeability can be effectively achieved through strategic surface modifications using monomers or chelating agents. This method has garnered significant attention in research, with diverse techniques and materials being employed to enhance NF membranes' capabilities. A notable advancement in this area was demonstrated by Li et al. [82], who developed a composite NF membrane with a positively charged surface layer, designated as PA-B. This layer was synthesized using TMC and branched poly(ethylene imine) (BPEI) through IP on polyetherimide support. The performance of the PA-B NF membrane was evaluated using a simulated brine solution composed of LiCl/$MgCl_2$. The results validated the membrane's enhanced efficiency in Li recovery from brine.

To further augment Li^+ selectivity over Mg^{2+}, the PA-B NF membrane underwent additional treatment with the chelating agent EDTA. The optimized EDTA-modified NF membrane, referred to as PA-B2-E3, exhibited a separation factor of around 9.2 for the LiCl/$MgCl_2$ mixture with a Mg^{2+}/Li^+ mass ratio of 24. This membrane demonstrated commendable stability over a 36-h filtration period, detailed in Fig. 8a. During its operation, the membrane consistently rejected around 90 % of Mg^{2+} and Cl^-, while maintaining a Li rejection rate at around 10 %. These results highlighted the membrane's refined ability to selectively isolate Li from brines, making it a potent solution for Li recovery applications (Fig. 8b).

Recent advancements have leveraged layer-by-layer construction and embedding of positively charged compounds such as amine-functionalized ionic liquids to significantly improve Mg^{2+}/Li^+ separation [117–120]. Peng et al. developed a technique that considerably enhances the selectivity and permeability of NF membranes by modifying their surface with diaminoethimidazole bromide (DAIB) monomers [118]. This approach involves the creation of positively charged, ultra-permeable membranes that effectively separate Li ions from brines with high Mg^{2+}/Li^+ concentration ratios. The modified nano-heterogeneous membrane, based on PEI–TMC polyamide TFCM, incorporates DAIB which possesses bidentate amine groups. This configuration allows for the selective passage and swelling of hydrated Li^+ ions while effectively blocking larger Mg^{2+} ions, facilitated by nano-heterogeneity that improves surface hydrophilicity and reduces water transport resistance across the approximately 100 nm thick separation layer. In performance testing, the DAIB-modified membranes underwent two NF cycles with concentrated Mg^{2+}/Li^+ brine. The initial cycle used simulated salt lake brine with a 25.5 g/L concentration and a 50 Mg^{2+}/Li^+ ratio, reducing the Mg^{2+}/Li^+ ratio in the permeate to 8.75 (Fig. 8c). The subsequent cycle, using this permeate as feed, further decreased the Mg^{2+}/Li^+ ratio to 0.85, significantly simplifying subsequent Li purification steps (Fig. 8d-f) [95,121]. At an operating pressure of 6 bar, the membrane demonstrated substantial Li flux (0.7 mol m^{-2} h^{-1}) for brines with a 20 Mg^{2+}/Li^+ ratio, highlighting its enhanced water permeability - a fivefold increase compared to the pristine membrane - and excellent stability with 95.8 % $MgCl_2$ rejection over 200 h of continuous operation.

Further membrane innovation, Feng and team enhanced PA membranes, composed of interfacially polymerized PEI and TMC, by incorporating a novel monomer, quaternized bipyridine (QBPD) [120]. The QBPD-modified membrane exhibited a significant increase in pure water flux, approximately 96.6 L m^{-2} h^{-1} while maintaining an $MgCl_2$ rejection rate of around 92 % ± 3. This marked improvement in flow rate, 2.8 times higher than that of unmodified membranes, is attributed to the partial degradation and structural changes in the PA layer, resulting in a less dense selective layer. Its improved surface charge effectively reduced the Mg^{2+}/Li^+ ratio of the feed from 50 to around 8 by selectively filtering the ion mixture. The QBPD membrane sustained stable separation performance over 162 h at 0.6 MPa. Given its excellent performance, employing the QBPD membrane is a viable option for Li extraction from salt lakes with high Mg^{2+}/Li^+ ratios.

3.3. Surface charge regulation

Recent advancements in NF membrane technology have focused on manipulating surface charge to improve Li selectivity. Innovations such as interlayer charge compensation and the strategic blockage of nanolayers have significantly advanced Li selectivity [122,123]. The deliberate design of charge distributions within NF membranes plays a pivotal role in achieving a high degree of Li separation. Membranes engineered with a specific mix of charges, tailored to precise spatial distributions, have demonstrated enhanced Li selectivity, highlighting the critical role of surface charge patterns in ion separation [124].

At neutral pH, most commercial thin-film composite polyamide (TFC-PA) NF membranes exhibit a negative charge, predominantly due to the presence of carboxyl groups introduced during the IP process [125]. While negatively charged membranes are common, those with positive charges have proven especially effective in Li recovery from brine, particularly in differentiating Li from Mg ions [116,126]. Research indicates that size exclusion predominantly occurs in fully aromatic membranes, while Donnan exclusion is more significant in ion separation for semi-aromatic membranes [127]. Given the close hydrate ion radii of Li^+ (0.382 nm) and Mg^{2+} (0.428 nm), typical negatively charged commercial NF membranes often struggle with effectively separating these cations, as indicated in Table 2. This challenge has steered efforts towards the development of positively charged NF membranes tailored specifically for Mg^{2+}/Li^+ separation.

Extensive research efforts have been directed towards fabricating positively charged NF membranes with enhanced selectivity. During the IP process, replacing traditional amines like piperazine with alternatives such as nanocellulose, 1,4-bis(3-aminopropyl) piperazine, or polyethyleneimine (PEI) introduces more positively charged groups [128–131]. Tailoring the surface charge through electrostatic interactions can significantly refine a membrane's selectivity, improving the distinction between monovalent and multivalent ions. This shift from negative to positive surface charges on TFC-PA membranes favors monovalent ions, creating a stronger repulsion against divalent ions and enhancing Li extraction [22,132].

Recent studies have focused on the innovative use of the Layer-by-Layer (LbL) technique for NF membrane filtration to improve Li recovery efficiency. Moradi et al. [133] demonstrated that depositing alternating layers of positively and negatively charged polyelectrolytes, especially poly(diallyldimethylammonium chloride) (PDADMAC) and poly(sodium 4-styrenesulfonate)(PSS), enhances the membrane's selectivity. This modification strategy improves the rejection of divalent cations such as Mg^{2+} and Ca^{2+}, while facilitating the passage of

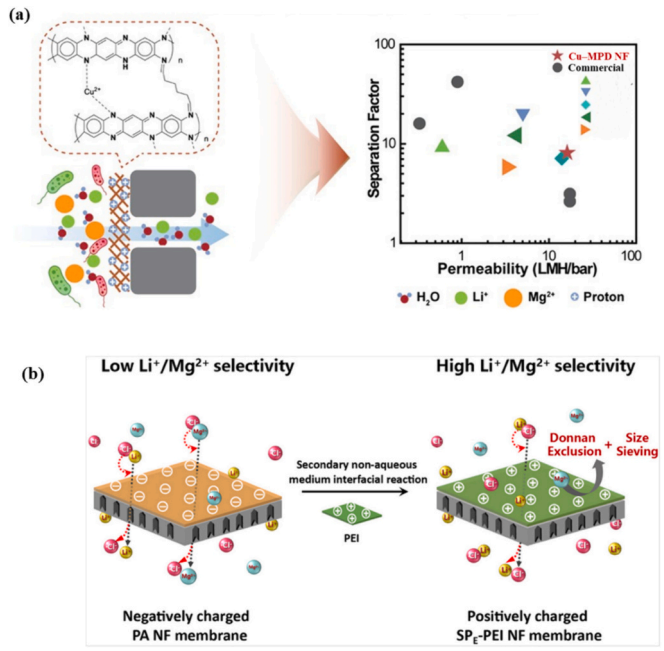

Fig. 9. Comprehensive performance and design characteristics of NF membranes: (a) Metal-coordinated NF membrane on the left; a juxtaposition of water permeance and Li^+/Mg^{2+} separation factors, including results from the literature, commercial membranes, and the membrane developed by Wang et al. [73]. (b) Illustration of surface-charge inversion in SP-PEI membranes, facilitating the synchronous reinforcement of Donnan exclusion and size sieving effects [134].

monovalent ions like Na^+ and Li^+, thereby optimizing the membrane for Li recovery. The performance of these modified membranes was tested with synthetic brine solutions designed to mimic real seawater conditions, assessing their capacity to selectively separate Li ions based on ion size and charge.

Furthermore, innovations in non-polyamide NF membranes have also been explored. A noteworthy approach includes the Cu^{2+}-assisted MPD self-polymerization process [73]. These membranes, enhanced with Cu^{2+}, exhibited superior water flow and Mg^{2+}/Li^+ selectivity compared to both commercial and laboratory-produced counterparts. The performance improvements, particularly under acidic conditions, were highlighted in Fig. 9a. Detailed structural and functional analyses were conducted using quartz crystal microbalance with dissipation (QCM-D) technology, which provided insights into how membrane structure and surface charge density vary with pH.

Dan et al. developed a novel approach by inverting the surface charge of the NF membrane to introduce a positively charged layer [134]. This modification, grounded in the DLVO theory of surface interactions, resulted in a membrane with high positive charge density capable of effectively separating Li from Mg^{2+} ions. These membranes demonstrated long-term stability, a high separation factor ($S_{Li/Mg}$) of 12.37, and notable resistance to fouling by Ca^{2+}, particularly in challenging conditions with high Mg^{2+}/Li^+ mass ratios of 150. The introduction of amine groups on the membrane surface not only enhanced its stability by providing high cationic selectivity but also prevented the accumulation of multivalent cations like Mg^{2+} and Ca^{2+}, which typically cause scaling and reduced performance. The use of low-molecular-weight PEI in the modification process contributed to a denser and more electropositive surface, thereby enhancing the membrane's overall durability in Li extraction applications. The fabrication of SP-PEI membranes involved a charge inversion through a secondary reaction in a non-aqueous medium, as depicted in Fig. 9b. This method proves both efficient and simple, offering significant potential for scaling up for industrial applications.

3.4. Surface functionalization

Surface functionalization of NF membrane involves the modification of membrane surfaces by attaching functional groups or molecules that impart desired properties such as hydrophilicity or specific surface charges via physical or chemical methods. This technique not only transforms membrane surface properties but also synergizes with standard membrane manufacturing processes, promoting easy integration into production lines to improve cost-effectiveness and scalability. However, the durability of these modified surfaces under prolonged operational conditions still requires through validation [135,136].

Soyekwo et al. reported innovative insights into how surface functionalization using multication side chains can remarkably improve ion separations by molecularly tuning ion-membrane electrostatic interactions in polymeric membranes [137]. Their study introduced a novel approach to surface functionalization through the incorporation of triquaternary ammonium-based ionic liquid (TQAIL), creating nanoscale structural heterogeneity. This heterogeneity not only enhances the surface hydrophilicity of the membrane but also reduces internal resistance, thereby improving Li/Mg selectivity and water permeability. By embedding TQAIL with multication side chains into the polyamide layer of NF, the study effectively regulates the surface charge, leading to the formation of highly positively charged nanochannels, which facilitate a much higher permeability and selectivity for Li over Mg.

Wu et al. established an effective Li extraction method using a positively charged NF membrane tailored for brines with high Mg^{2+}/Li^+ ratios by grafting an amine-functionalized ionic liquid, specifically 1-(3-aminopropyl)-3-methylimidazolium bis(trifluoromethanesulfonyl) imide ([MimAP][Tf_2N]), onto a polymeric PIP-TMC layer [119]. The fabrication and separation performance of this membrane for simulated brine is shown in Fig. 10a and b. Initially, the NF-IL-0 membrane exhibited negative zeta potentials at various pH levels, as presented in Fig. 10c. After modification, the membranes acquired a positive charge (at pH 6.4) due to the introduction of quaternary ammonium group in [MimAP][Tf_2N], significantly enhancing selectivity between mono- and divalent cations, particularly between Li^+ and Mg^{2+}. These membranes exhibited an increased water permeance rate of 37.8 L/(m^2·h), achieving 83.8 % rejection of $MgCl_2$ and 24.4 % rejection of LiCl. When tested with simulative brine (Mg^{2+}/Li^+ ratio = 20), the NF-IL-2.0 % membrane displayed rejection rates of about 81.9 % for Mg^{2+} and 45.2 % for Li^+. The stability and long-term performance of this modified PA membrane was evaluated in a 30-h experiment, demonstrating its durability without significant degradation, and achieving a high selectivity ($S_{Li/Mg}$) of 8.12, as shown in Fig. 10d.

Furthermore, Soyekwo et al. introduced a new ionic liquid monomer, N1-(6-aminohexyl)-N1,N1,N6,N6,N6-pentamethylhexane-1,6-diaminium bromide (DABIL), covalently attached to a pristine polyamide TFC membrane through a subsequent amidation reaction, as depicted in Fig. 10e [138]. This modification aimed to enhance the membrane's surface charge strength and stability, thereby improving its selective separation capability for Li from high Mg^{2+}/Li^+ mixtures. The incorporation of DABIL into the PA network resulted in increased hydrophilicity, larger pore sizes, and enhanced Donnan exclusion effects, significantly advancing the membrane's ion separation capabilities.

Molecular dynamics simulations have highlighted that the interaction energies between water molecules and the multi-cation groups are crucial in determining the membrane's surface properties. The DABIL-modified membranes demonstrated remarkable improvements in water permeability and ion selectivity. Specifically, a study incorporating DABIL-5 in the membrane's structure depicted in Fig. 10f shows that this modification results in water permeability six times greater than that of the unmodified membrane and achieves a Li^+/Mg^{2+} selectivity of 26.49. These capabilities surpass those of existing state-of-the-art positively charged membranes, making the DABIL-modified membrane a highly promising tool for Li extraction.

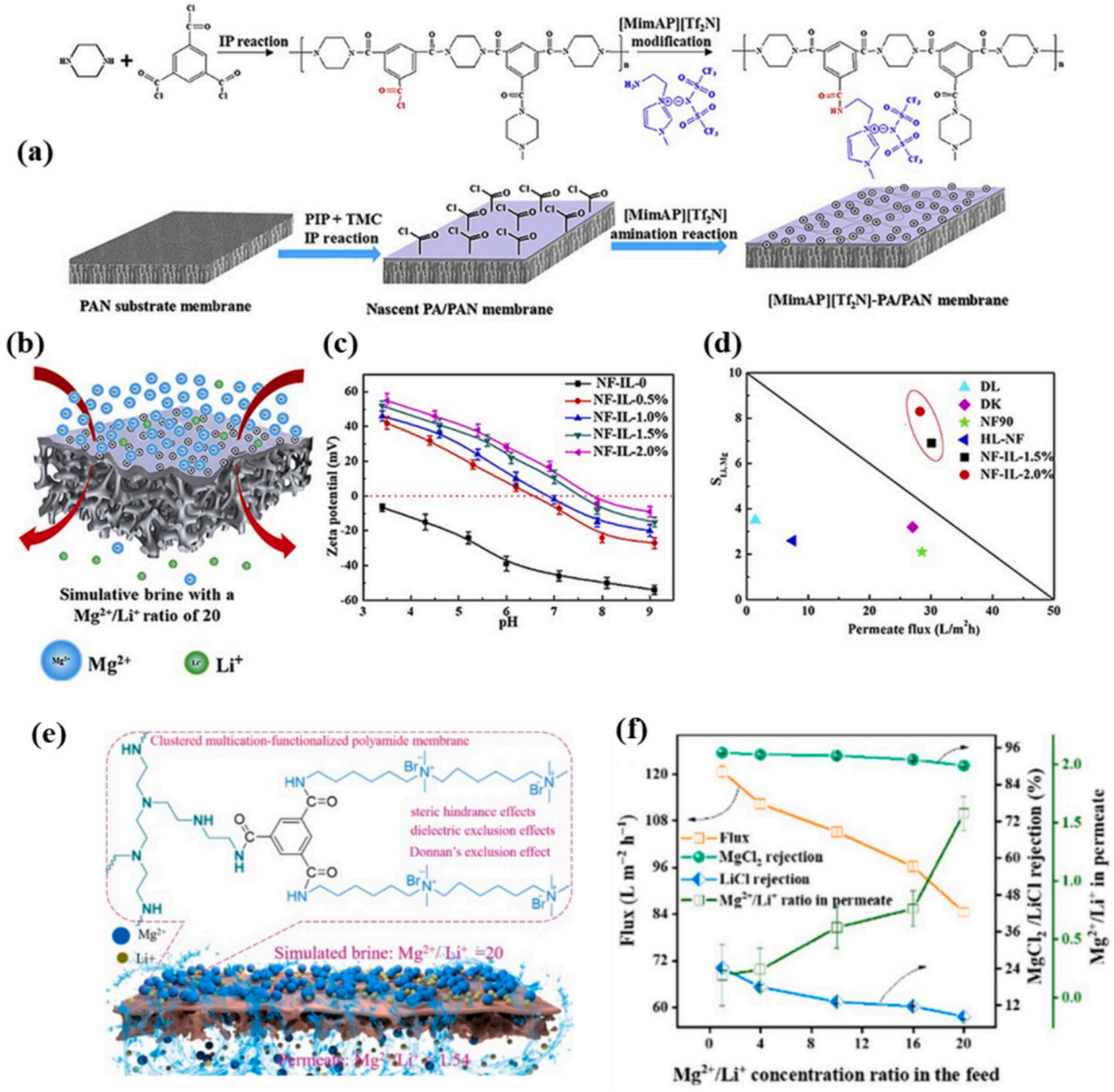

Fig. 10. (a) Advanced functionalities and comparative performance of NF membranes: (a) Illustration of the synthesis of a [MimAP][Tf2N]-PA/PAN NF membrane for Li^+ separation from simulative brine. (b) Separation functionality of the membrane using simulative brine. (c) The NF membranes' zeta potentials. (d) Performance evaluation of commercially available NF and NF-IL-c membranes, comparing $S_{Li,Mg}$ vs. permeate flux for simulated brine [119]. (e) Diagram showing the pristine polyamide (PEI − TMC TFC) NF membrane and its modification with DABIL molecules (DABIL TFC NF). (f) Effects of varying Mg^{2+}/Li^+ ratios in feed mixtures on the separation performance of the DABIL-5 membrane (conditions: 0.5 g/L LiCl, pH 6.6, 30 °C, and 5 bar) [138].

3.4.1. Incorporation of γ-cyclodextrins (γ-CDs) in membrane fabrication

Zhao et al. [139] utilizes γ-cyclodextrins (γ-CDs) and PEI in an advanced interfacial polymerization process with TMC to fabricate TFC NF membranes. This method results in an extra-thin active layer optimized for Li separation. The hydrophilic surface and hydrophobic cavity of γ-CDs improve the surface characteristics of the membrane, leading to improved water flux and selective separation of Li ions. The amphipathic cavities of γ-CDs play a crucial role in the functionalization of the membrane surface, facilitating separate sieving of Li and Mg ions and thereby enhancing Li recovery.

3.4.2. Development of Janus NF membrane

Guo et al. developed a novel three-layered Janus NF membrane, which includes a polyethersulfone (PES) substrate, a hydrophilic and negatively charged carboxylate cellulose (CNC–COOH) nanocrystal interlayer, and a top ultra-thin, positively charged PA layer [23]. The intermediate layer's negative potential, derived from its abundance of carboxyl groups, complements the hydrophobic PA layer's positive charge from unreacted amino groups. This double Janus NF membrane configuration enhances stability and results in exceptional water flux and effective separation capabilities for Mg^{2+} and Li^+ ions. The structural integrity during operation is underscored by high solute retention and permeance, with the CNC-COOH interlayer enhancing membrane stability by imparting a strong negative potential and improving hydrophilicity, essential for a stable PA layer formation. The original PES substrate membrane is inherently hydrophobic and lacks functional groups, rendering it electrically neutral as depicted in Fig. 11a. In contrast, the Janus membrane, enhanced with functional groups, exhibits distinct electrostatic properties, as illustrated in Fig. 11b. During brine treatment, the electrostatic repulsion in the PA layer creates a concentration gradient that selectively impedes Mg^{2+} ions while facilitating the passage of Li^+ ions due to electrostatic attraction. This dual

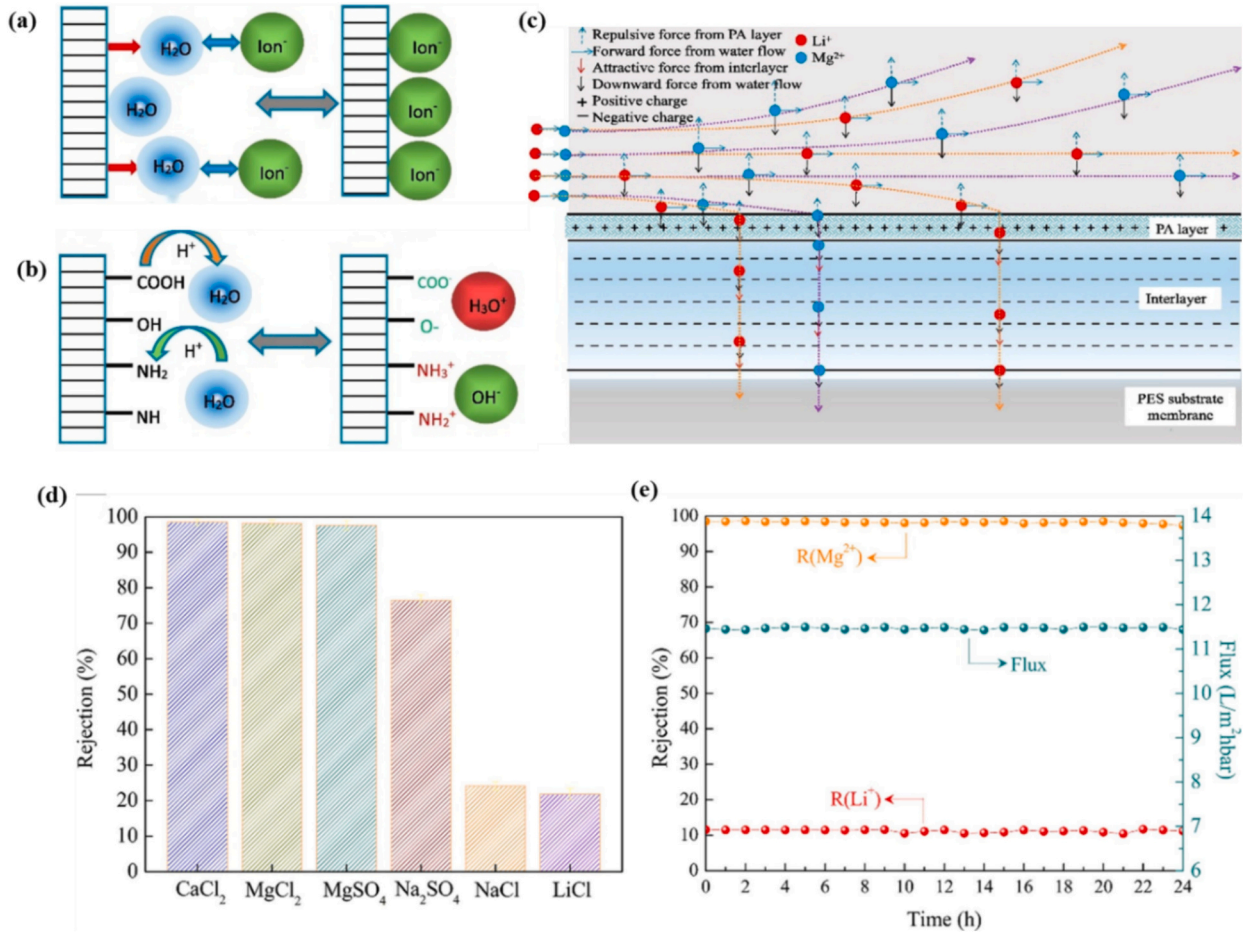

Fig. 11. Characterization and performance evaluation of NF membranes: (a) Illustration of charge generation in a PES substrate membrane without functional groups. (b) Formation of charges in the presence of various functional groups. (c) Diagrammatic representation of force analysis in the triple-layered Janus membrane, detailing the Mg^{2+} and Li^{+} ion transport pathways [23]. (c) Optimized NF Membrane rejections for selected inorganic salts and (d) extended performance assessment for Mg^{2+} separation from Li^{+} [72].

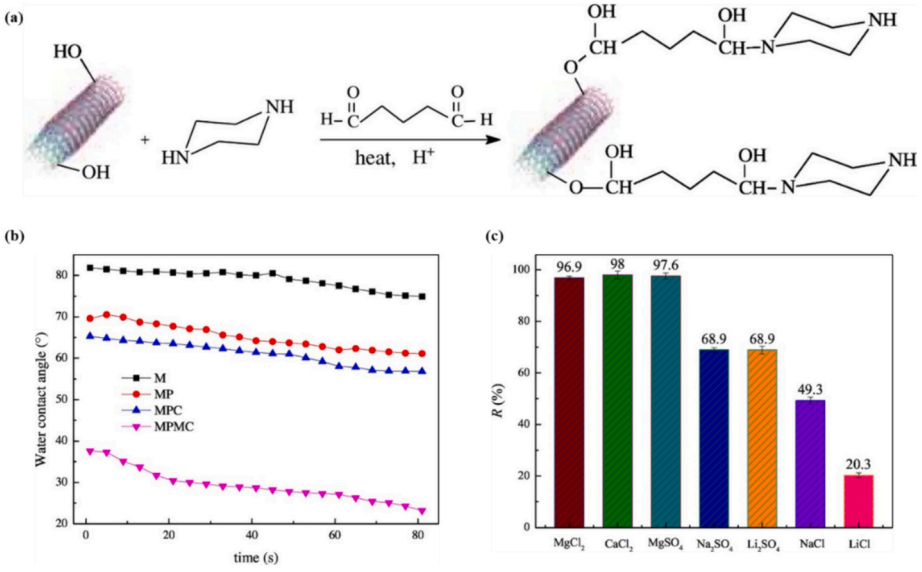

Fig. 12. Detailed analyses of NF membrane modifications and performance: (a) Grafting reaction on hydroxy contained MWCNTs. (b) Comparative hydrophilicity of the NF membranes and the substrate. (c) Rejection performance of the PEI/M-CNTs (MPMC) membrane for various salts at a concentration of 2000 ppm [20].

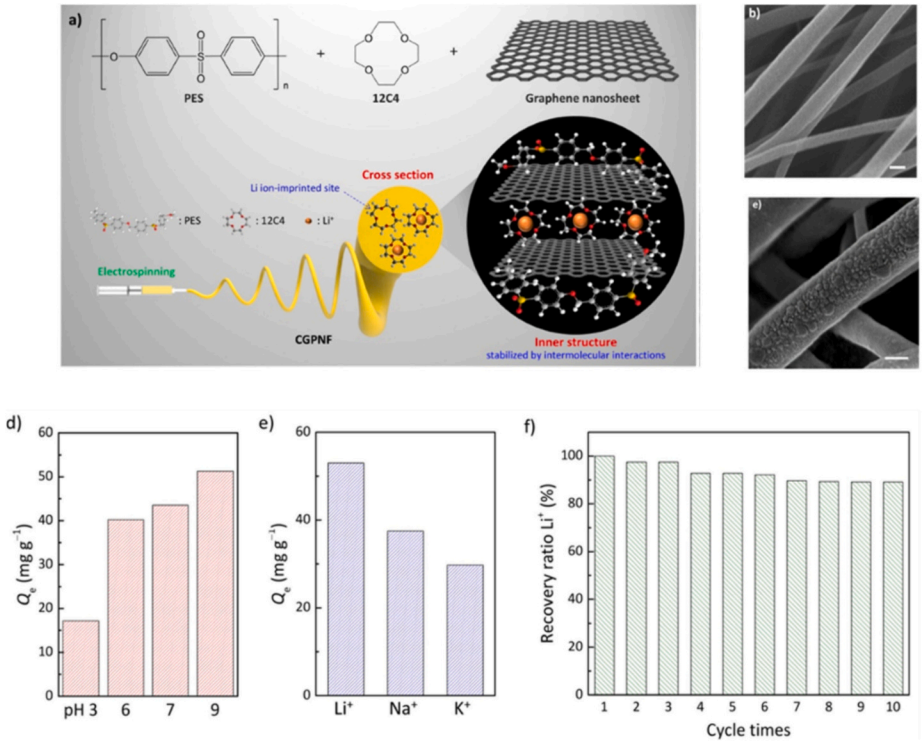

Fig. 13. Development and characterization of CGPNF membranes: (a) Diagram of the electrospinning process used to fabricate CGPNF membranes from 12C4/graphene/PES dispersions, combining two-dimensional graphene nanosheets with crown ether molecules. (b) SEM images of CGPNF membranes before and (c) after Li-ion adsorption, with (c) presenting a magnified view (Scale bar = 100 nm). (d) Influence of pH on the membrane's adsorption capabilities, and (d) impact of metal ions. (f) Regeneration capacity of the membrane for Li recovery [141].

mechanism is schematically represented in Fig. 11c. With this innovative Janus membrane, a Mg^{2+}/Li^{+} feed mass ratio of 30 results in a rejection disparity of approximately 74 % between Mg^{2+} and Li^{+}, achieving a separation factor of 12.2 for $S_{Li,Mg}$.

3.4.3. Enhancement of UF substrate membrane with MWCNTs-COOK

Xu et al. [72] further enhanced UF substrate membranes by incorporating potassium carboxylate functionalized multi-walled carbon nanotubes (MWCNTs-COOK). This modification not only improved the structural integrity and stability of the membranes but also facilitated the formation of a robust PA layer via IP. The eco-friendly oxidation process used to functionalize these MWCNTs-COOK ensured their high water solubility and effective dispersion in polar solvents, which was crucial for anchoring them in the PES UF substrates. This foundational stability was pivotal in maintaining the polyamide layer's integrity throughout the IP process. The Incorporation of MWCNTs-COOK significantly enhanced the bonding between the substrate and the PA layer, improving hydrophilicity, porosity, and the water permeability of the UF membrane. Performance analysis of the NF membrane with an optimum 0.012 wt% MWCNTs-COOK revealed a high separation factor ($S_{Li,Mg}$) of 58.66 and a notable difference in rejection between Li^{+} and Mg^{2+} of 86.9 %, substantially outperforming many previously established NF membranes. This membrane demonstrated a high flux of 11.46 L m^{-2} h^{-1} bar^{-1}, which is 2.28 times higher than that of its unmodified counterpart. Fig. 11d shows the rejection performance of this optimized NF membrane towards divalent cations and a stronger attraction towards divalent anions (SO_4^{2-}) compared to monovalent anions (Cl^{-}). The larger ions faced higher transmission resistance due to their hydrated radius, affecting the rejection ratio of inorganic salts through steric hindrance and electrostatic interactions. Long-term testing of the MWCNTs-COOK-modified NF membrane, as depicted in Fig. 11e, confirmed its consistent high permeable flux and stable Mg^{2+}/Li^{+} separation performance. This study exemplifies the feasibility and efficiency of integrating MWCNTs-COOK into UF substrate membranes to enhance Mg^{2+}/Li^{+} separation in NF applications, paving the way for accelerated Li enrichment processes.

3.5. Incorporating nanomaterials

The incorporation of functional nanomaterials such as graphene oxides (GOs), carbon nanotubes (CNTs), titanium dioxide (TiO_2), covalent organic frameworks (COFs), and metal-organic frameworks (MOFs) into NF membranes represents a promising approach to mitigate the trade-off between permeability and separation efficiency. These nanomaterials can modify the surface composition of membranes, enhancing interactions with Li ions and thereby improving selectivity and separation performance.

3.5.1. Enhanced NF membrane with MWCNTs

Xu et al. [20] developed a positively charged NF membrane using PEI and TMC, where permeability was further augmented by incorporating hydroxyl-rich, modified MWCNTs with piperazine (PIP). This modification not only increased the hydrophilicity of the NF membrane but also formed low-resistance water channels at the interface between the CNTs and the PA, as depicted in Fig. 12a and b. [140]. The resulting modified polymeric MWCNT (MPMC) membrane exhibited a marked increase in hydrophilicity after IP, leading to a remarkable enhancement in water flux, which reached 56.1 L m^{-2} h^{-1} at 4 bar. Salt rejection rates were elevated up to 96.9 %, attributed to the hydrophilic groups and PIP-grafted chains on the modified CNTs. This membrane also displayed excellent selective separation abilities, with high rejections for divalent salts like $MgCl_2$, $CaCl_2$, and $MgSO_4$ exceeding 97 %, while maintaining lower rejection rates for monovalent cations, below 70 % as shown in Fig. 12c. Furthermore, it demonstrated effective separation capabilities for Mg^{2+} and Li^{+}, coupled with durability, underscoring its utility for Li recovery from seawater brine with high Mg^{2+}/Li^{+} ratios.

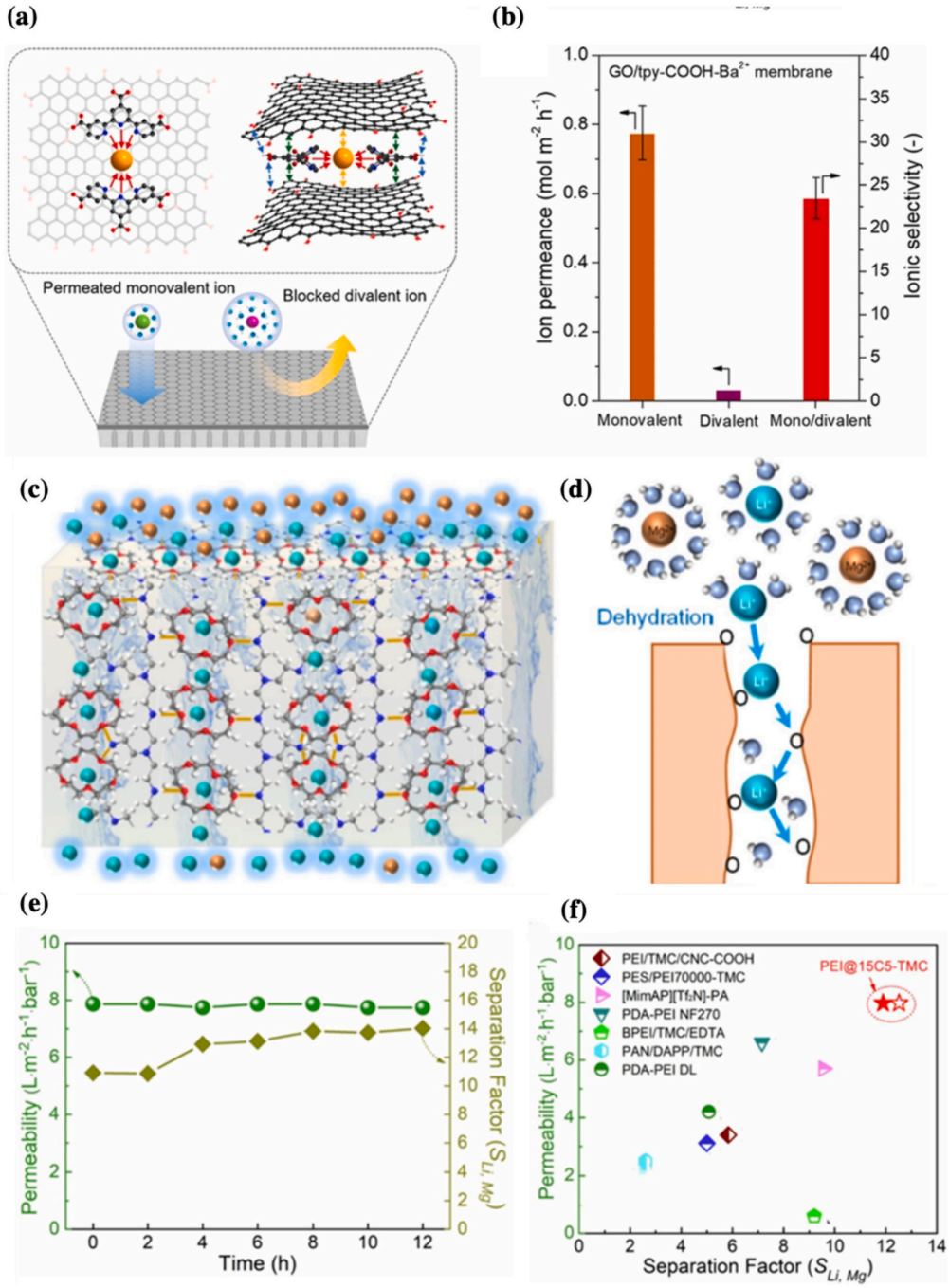

Fig. 14. Comprehensive illustration of ion separation mechanisms and membrane performance: (a) Schematic showing the chelation-based metal cation stabilization strategy in GO membranes from a top and side view, highlighting the selective permeation of monovalent ions over divalent ions. (b) Permeance rates for monovalent and divalent ions and the selectivity of these ions in GO/tpy–COOH–Ba^{2+} membranes [147]. (c) Schematic depicting the hydrated Li^{+} and Mg^{2+} transfer via the 15C5 channels. (d) Illustration of the hopping mechanism that facilitates fast and specific Li^{+} transport within the 15C5 channels. (e) Stability performance of the PEI@15C5-TMC membrane in Mg^{2+}/Li^{+} separation with a mass ratio of 20. (f) Comparative performance of the PEI@15C5-TMC membrane against other polymeric NF membranes previously reported [144].

3.5.2. Graphene-incorporated PES nanofiber membranes

Jo et al. [141] developed a graphene-in-polyethersulfone (PES) nanofiber membrane embedded with the macrocyclic chelating ligand (12C4) molecules, enhancing the membrane's durability and reusability for targeted Li recovery from aqueous solutions. The fabrication process of these composite graphene PES nanofiber (CGPNF) membranes is illustrated in Fig. 13a. These membranes consist of nanofibers initially measuring 100 nm in diameter, but this dimension and their surface roughness increase upon Li adsorption, as evidenced by SEM images in Fig. 13b and c, showing the CGPNF membranes before and after Li binding. The addition of graphene to the 12C4/graphene/PES mixture influences the electrospinning parameters such as viscosity and conductivity, which in turn affect the final diameter of the nanofibers. Post-adsorption, the CGPNF membranes demonstrate a 6 % to 7 % increase in fiber diameter and acquire a rougher surface, indicating successful Li capture.

Nitrogen sorption tests confirm that the inclusion of graphene sheets enhances the stability of the nanofibers, improving porosity and surface

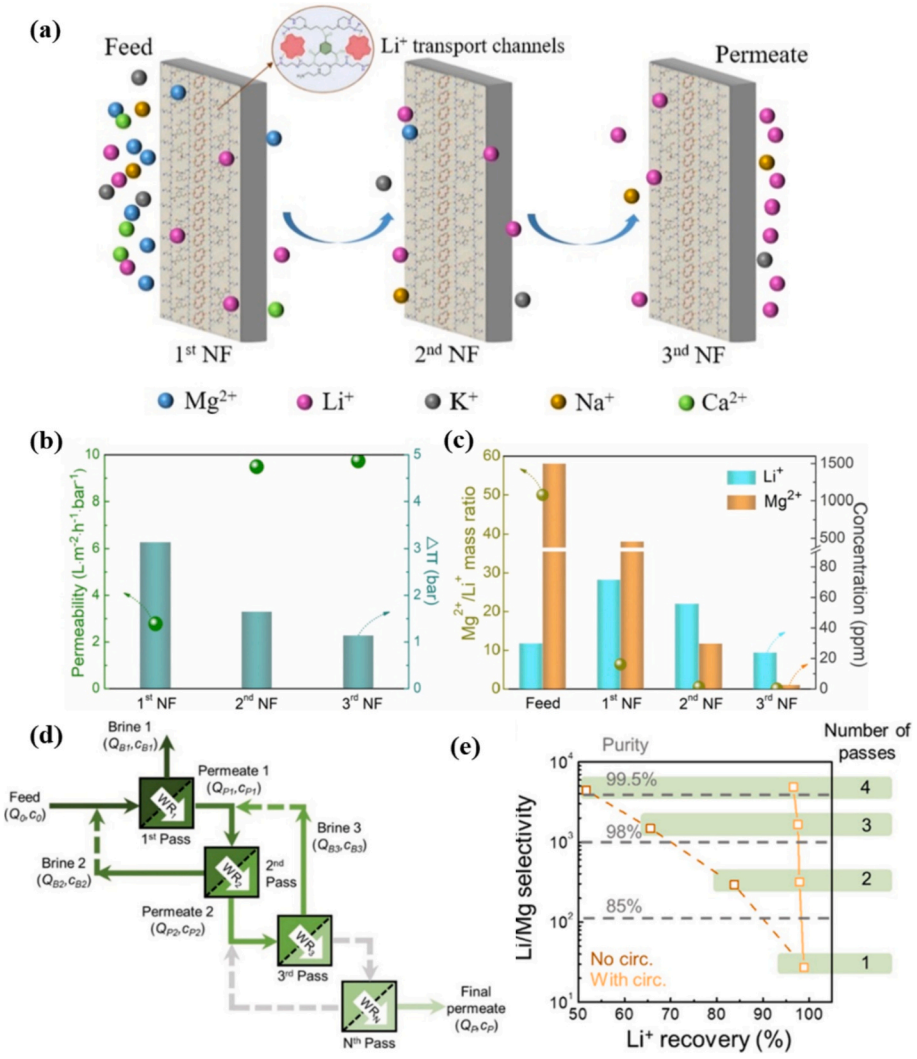

Fig. 15. Overview of NF process and performance using PEI@15C5-TMC membrane: (a) Depiction of the separation mechanism and technological process utilized by the PEI@15C5-TMC membrane [149]. (b) Analysis of permeability and osmotic pressure ($\Delta\pi$) difference across the PEI@15C5-TMC membrane at each stage of the NF process. (c) Concentrations of Li^+ and Mg^{2+} in both permeate and feed solutions of each stage, including the mass ratio of Mg^{2+}/Li^+ [144]. (d) Schematic representation of the multi-pass NF process for Li^+/Mg^{2+} separation. (e) Comparative analysis and recovery of Li^+/Mg^{2+} with and without recirculation, as a function of the number of passes, using a LiCl/$MgCl_2$ feed solution at a pressure of 6 bar [74].

area, in addition to increasing surface roughness, chemical heterogeneity, and hydrophilicity. The pH level of the solution impacts the CGPNF membrane's adsorption capacity, with higher pH levels proving more advantageous, as shown in Fig. 13d. Selectivity tests detailed in Fig. 13e reveal that the CGPNF-2 membrane possesses significantly lower adsorption capacities for sodium and potassium ions—by 29 % and 44 %, respectively—compared to Li ions. The membrane's regeneration involves repeated adsorption/desorption cycles using hydrochloric acid, where the CGPNF-2 membrane maintains over 97 % of its original adsorption capacity after 3 cycles, as indicated in Fig. 13f. In a dynamic flow system, the CGPNF membrane reached an adsorption peak of 86.3 mg g^{-1} for Li and preserved >93 % of its capacity after ten regeneration cycles, highlighting its efficacy and longevity for Li recovery applications.

3.6. Implementation of artificial nanochannels in NF membranes

The development of NF membranes equipped with artificial nanochannels represents a cutting-edge approach in NF technology, specially engineered to selectively transport Li ions. These channels are meticulously designed to allow pores just under the hydrated diameter of Li^+ ions (0.76 nm) to preferentially admit them. As Li^+ ions approach these pores, they undergo partial dehydration, effectively reducing their size to navigate through these precisely sized channels [142]. Zhang et al. [143] demonstrated the ultrafast and selective transport of alkali metal ions in ZIF-8 membrane, where Li^+ ions move faster than Na^+, K^+, and Rb^+ ions. This selective speed is due to the specific interactions within the tailored nanochannels that favor Li over other alkali metals.

Li et al. [144] successfully designed an NF membrane with artificial channels that not only enhance water flux but also improve Li^+ ion transference. This membrane was synthesized using an IP method combining TMC and PEI with 15-crown-5 ether (15C5), a molecular known for its specific ion affinity to Li^+. In tests with simulated brine demonstrating a high Mg to Li ratio (MLR) of 20, the PEI@15C5-TMC membrane effectively reduced the MLR to 1.7, achieving an $S_{Li,Mg}$ separation factor of 14. Despite its negative zeta potential, which indicates a separation mechanism beyond the Donnan effect, the membrane facilitates Li^+ ion transport primarily through dehydration processes occurring at and within the channels [145,146].

Graphene oxide (GO) membranes are distinguished by their two-dimensional nanochannels, which demonstrate exceptional selectivity for monovalent over divalent ions due to their unique pore architecture.

Table 4
Performance characteristics of NF membranes for enhanced Li selectivity.

Regulation of NF membrane for enhanced Li^+ selectivity	Membrane material/process	Brine type	Test condition/operating parameters	Li^+/Mg^{2+} separation ability	Flux (L/m^2h bar)	TRL	Ref
IP process	NF90 commercial membrane	Brine (contains Li^+ and Mg^{2+})	• $Mg^{2+}/Li^+ = 20$ • 2000 ppm • 3 bar	2.10	–		[19]
Advanced IP processes	HACC- PIP: TMC (comonomer addition)	Li brine	• 2000 ppm • 6 bar	115	1.57 ± 0.075	4–5	[114]
	SIP-750k membrane (electro-nanofiltration membranes via sequential interfacial polymerization)	Brines from seawater and salt lake	• Current density: 10 mA/cm^2 • Membrane area: 16 cm^2 • Feed solution: 0.1 M LiCl and 0.1 M $MgCl_2$ (120 mL) • 6 bar	16.55	3.08×10^{-8} $mol{\cdot}cm^{-2}{\cdot}s^{-1}$	4–5	[115]
	Positively charged NF (gas/liquid interfacial polymerization (GLIP))	Natural brine	• $Mg^{2+}/Li^+ = 20$	27.38	4.3	4	[116]
Surface modification	TMC/BPEI/EDTA	Simulative brine of mixed LiCl-$MgCl_2$	• $Mg^{2+}/Li^+ = 24$ • 2000 ppm • 4 bar	9.26	0.6	3–4	[82]
	NF-TC membranes	Salt lake brine	• $Mg^{2+}/Li^+ = 20$ • 2000 ppm • 5 bar	167	40	4–5	[151]
	Quaternized bipyridine-modified PEI (source: synthetic salt solution)	Salt lake brine	• $Mg^{2+}/Li^+ = 50$ • 2000 ppm • 6 bar	5.2	81.6	3–4	[120]
	PEI–TMC polyamide TFCM, modified with DAIB	Brine (high Mg^{2+}/Li^+ ratio)	• $Mg^{2+}/Li^+ = 20$ • 6 bar	–	0.7 mol m^{-2} h^{-1}	3–5	[118]
Surface charge regulation	DK commercial membrane	Salt lake brine	• $Mg^{2+}/Li^+ = 18$–24 • 16 bar	2.94	–	3	[152]
	[MimAP][Tf2N]-PA/PAN	Brine (high Mg^{2+}/Li^+ ratio)	• $Mg^{2+}/Li^+ = 20$ • 3 bar	8.12	9.43	4	[119]
	PEI grafted on PA	Simulated brine	• $Mg^{2+}/Li^+ = 20$ • 4 bar	33.4	12	1–3	[128]
	Cu − MPD NF membrane	Simulated brine	• $Mg^{2+}/Li^+ = 23$ • 2000 ppm • 5 bar	8	16.2	3–4	[73]
	SPE-PEI	Salt lake brine	• $Mg^{2+}/Li^+ = 150$ • 2000 ppm • 6 bar	12.37		3–4	[134]
Advanced IP processes & surface charge regulation	DL-2540 commercial membrane	Salt lake brine	• $Mg^{2+}/Li^+ = 60$ • 20 bar	2.86	–	4–6	[40]
	PES-PEI/TMC	Salt lake brine	• $Mg^{2+}/Li^+ = 20$ • 2000 ppm • 8 bar	20	5.02	4–5	[22]
	DAPP/TMC	Brine (high Mg^{2+}/Li^+ ratio)	• $Mg^{2+}/Li^+ = 20$ • 2000 ppm • 3 bar	2.60	–	4–6	[19]
Surface functionalization	Zwitterion-functionalized g-C_3N_4 (BHC-CN)	Salt lake brine	• $Mg^{2+}/Li^+ = 73$ • 0.4 MPa • 20 °C	16–23.9	5.6–2	4–6	[129]
Incorporating nanomaterials & surface functionalization	PEI/TMC/CNC-COOH/PES	Salt lake brine	• $Mg^{2+}/Li^+ = 30$ • 2000 ppm • 8 bar	12.2	4.17	1–3	[23]
	PEI/TMC/CNC-COOH/PES	Salt lake brine	• $Mg^{2+}/Li^+ = 60$ • 2000 ppm • 8 bar	5.85	3.4	1–3	[23]
	PES-MWCNTs-COOK/PEI-TMC	Salt-lake brine	• $Mg^{2+}/Li^+ = 20$ • 2000 ppm • 3 bar	58.66	11.46	4–5	[72]
Incorporating nanomaterials	PES/(PIP-PHF)/TMC	brine or seawater	• $Mg^{2+}/Li^+ = 21.4$ • 2000 ppm • 6 bar	13.16	6.7	3–4	[153]
	PES-GO/PEI/TMC	Brine (high Mg^{2+}/Li^+ ratio)	• $Mg^{2+}/Li^+ = 20$ • 2000 ppm • 3 bar	16.13	11.15	4–6	[154]
	PEI/GQDs-NH_2/TMC	Salt lake brine	• $Mg^{2+}/Li^+ = 20$ • 2000 ppm • 3 bar	27.86	11.94	3–4	[131]
Multi-pass filtration	PEI@15C5-TMC	Salt lake brine	• $Mg^{2+}/Li^+ = 50$ • $Mg^{2+}/Li^+ = 6.4$ • $Mg^{2+}/Li^+ = 0.1$	14	1st NF-2.8 2nd NF-9.5 3rd NF-9.7	4–5	[144]

Li et al. [147] advanced GO membranes' ion sieving capabilities through a stabilization method using polydentate ligands to bind metal cations (Fig. 14a). These modified GO membranes, integrated with ligand-M^{2+} coordination complexes, form stable nanochannels that impede divalent ions via steric hindrance while allowing monovalent ions to pass, compensating for their hydration and thus achieving high ion selectivity. The GO/tpy–COOH–Ba^{2+} membrane displayed a monovalent ion transmission rate of approximately 0.78 mol m^{-2} h^{-1} and a selectivity

Table 5
Characteristics of commercially available NF membranes for brine treatment, summarizing key features of various NF membranes from different manufacturers, including their polymer type, MWCO, specific applications in brine types, $MgSO_4$ rejection rates, optimal operating conditions, and significant outcomes such as ion rejection rates and membrane performance.

Membrane material/ manufacturer	Type of polymer	MWCO [Da]	Brine type	$MgSO_4$ rejection [%]	Optimum conditions	Outcome	Ref
NFX 2540 from Synder Filtration	PA TFC	150–300	SWRO desalination brine	99.0	• 10 bar • Permeate recovery = 80 %	• $Mg(OH)_2$(s) with the highest purities (97 %)	[155]
PRO-XS2 from Hydrnautics	PA TFC	–	Synthetic SWRO brines	87 %	20 bar	• Rejections of 71 % for Ca(II) and 89 % for Mg(II) with brine • SF = 9.6	[156]
DK from Veolia	PA TFC	150–300	SWRO desalination brine	96.0	8 to 30 bar	• Demonstrated negative surface membrane charge • Highest permeability (3.5 LMH bar^{-1}) and selectivity factor (>0.6) for multivalent elements relative to monovalent ones	[157]
NF2 membrane from Rising Sun Membrane Technology	PA		Synthetic geothermal brine		• 15 bar • pH 10	• Highest Li recovery reaching >75 %	[61]

ratio of around 23.5 for mono/divalent ions, as evidenced in Fig. 14b.

Theoretical and experimental findings confirm that water molecules significantly hinder ion permeation, where ions with lower hydration energies more easily shed their hydration layers for entry into the transport channels [148]. Li^+ ions, with a hydration energy of 515 kJ/mol, face a lower barrier to dehydration and channel entry compared to Mg^{2+} ions, which possess a higher hydration energy of 1828 kJ/mol, thus encountering greater difficulty in shedding their hydration shells (Fig. 14c). The incorporation of 15C5 in the membrane channels specifically enhances Li^+ complexation due to the size and shape alignment with Li^+ ions. This specialized interaction facilitates Li^+ transport through an electrostatic hopping mechanism along the channels' negatively charged walls [69,146], with oxygen atoms in the 15C5 providing a tailored route for Li transport (Fig. 14d). The durability of the PEI@15C5-TMC membrane was validated during a 12-h NF trial, maintaining high water permeability (8.0 L m^{-2} h^{-1} bar^{-1}) and an impressive Li^+/Mg^{2+} separation factor ($S_{Li,Mg}$) of about 12, as detailed in Fig. 14e and f. This showcases the membrane's capability for efficient Li recovery, offering a promising direction for future enhancements in NF membrane technology.

3.7. Multi-pass filtration

3.7.1. Three-stage NF process utilizing PEI@15C5-TMC membranes

Li et al. developed a three-stage NF process employing PEI@15C5-TMC membranes, tailored for the effective separation of Mg^{2+}/Li^+ in complex salt lake brines [144]. This innovative approach the selective permeability properties of the membranes, where changes in salinity adjust the osmotic pressure differences ($\Delta\pi$) across the membrane, influencing water flow. Initial tests immersed the membrane in a salt solution for 7 days, confirming the stability of the 15C5 component within the membrane structure. Further stability assessments included 10 rinses and ATR-FTIR analysis, which verified no leaching of the 15C5, demonstrating exceptional membrane stability. A continuous 12-h NF trial further validated the stable permeability and separation performance of the membrane under operational conditions, as illustrated in Fig. 15a.

The multi-stage process effectively reduced the Mg^{2+}/Li^+ mass ratio (MLR) from 50 in the feed to 6.4 after the first stage, achieving a 99.8 % Mg^{2+} rejection and a permeability of 2.8 L m^{-2} h^{-1} bar^{-1} (Fig. 15b). In subsequent stage, the permeability increased to 9.5 L m^{-2} h^{-1} bar^{-1} in the second stage and to 9.7 L m^{-2} h^{-1} bar^{-1} in the third, with the MLR further dropping to 0.1. These improvements were facilitated by decreasing $\Delta\pi$, which initially was 3.3 bar due to concentrated brine, reducing to 1.6 and then to 1.1 bar in later stages, as shown in Fig. 15c. The monitored concentrations of Li^+ and Mg^{2+} in the permeate at each stage confirmed efficient ion separation, culminating in approximately 95 % Li carbonate production by adding Na_2CO_3.

3.7.2. Multi-pass NF technologies with brine recirculation

Wang et al. introduced a novel multi-pass NF technique incorporating brine recirculation, designed to achieve high selectivity without compromising Li recovery [74]. In this process, the permeate from each pass is repressurized and fed into the subsequent pass, enriching Li/Mg selectivity by continually rejecting the less permeable ion, Mg^{2+}. Each pass's feed is the permeate from the prior pass, with brine from each pass

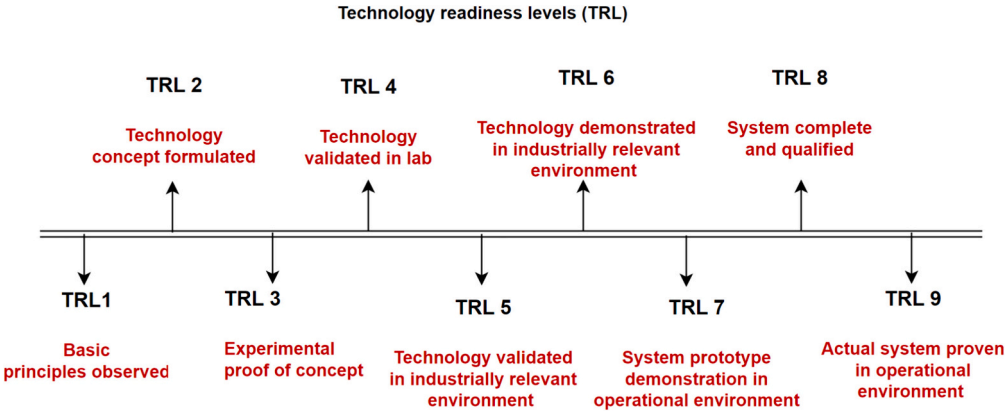

Fig. 16. Standard technology readiness scale.

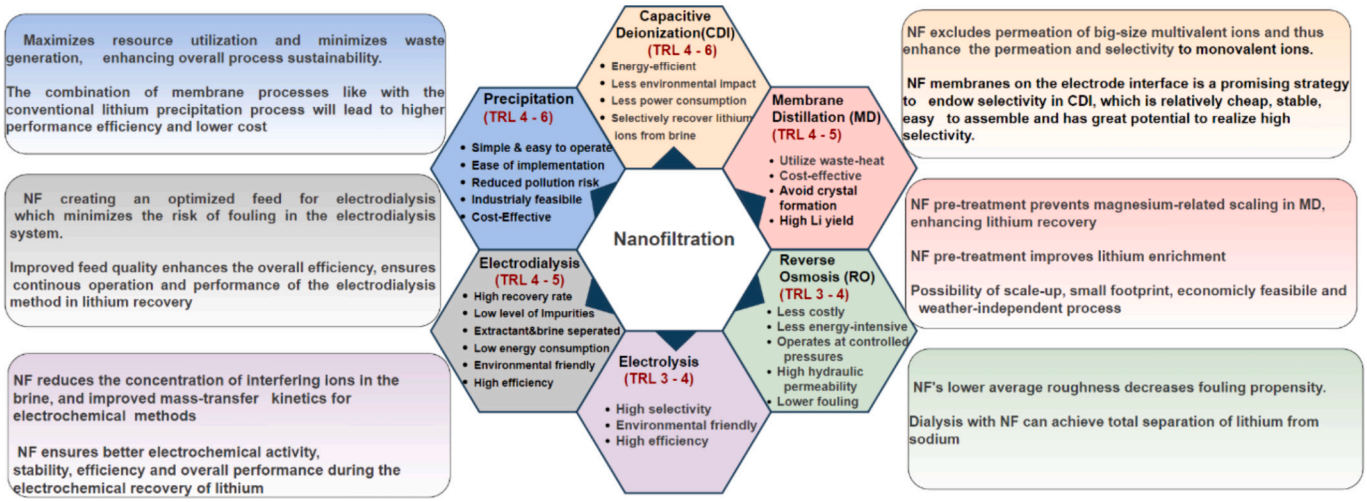

Fig. 17. Synergistic benefits of integrating NF with various Li recovery methods. This diagram outlines how NF enhances the efficiency, sustainability, and cost-effectiveness of processes such as capacitive deionization (CDI), membrane distillation (MD), reverse osmosis (RO), and electrodialysis (ED) in Li recovery. Key advantages include improved feed quality for electrolysis, reduced fouling, increased selectivity for monovalent ions, and better electrochemical activity, contributing to more effective and environmentally friendly Li extraction.

recirculated to feed the preceding pass, as depicted in Fig. 15d. This setup allows for varying water recovery rates and applying different pressures in each pass, optimizing the system's efficiency. Theoretical simulations suggest that a four-pass NF process without brine recirculation can achieve a Li^+/Mg^{2+} selectivity above 4000, corresponding to 99.5 % purity, but with a significant Li loss of 15–20 % in the second and fourth passes (dashed line in Fig. 15e). Conversely, with brine circulation, the process is theoretically predicted to reach an ultrahigh Li^+/Mg^{2+} selectivity over 4500 with a Li recovery exceeding 95 %, illustrated by the solid line in Fig. 15e. This indicates that brine recirculation effectively balances selectivity with recovery, making them invaluable strategy in the multi-pass design. The multi-pass NF technique, particularly with recirculation, demonstrates exceptional potential in achieving high Li^+/Mg^{2+} selectivity while maintaining robust Li recovery. The energy consumption of this process is notably reduced from 0.30 to 0.18 kWh mol^{-1} due to the efficient Li recovery enabled by brine recirculation, despite the increased capital costs and complexity. A comprehensive techno-economic analysis would be crucial to evaluate the economic viability of this advanced multi-pass NF process compared to other Li^+/Mg^{2+} separation technologies, considering all stages of Li extraction treatment. This technique not only showcases potential in Li^+/Mg^{2+} separation but could also advance other membrane-based separation technologies, enhancing NF-based solute-solute separations in resource extraction and recovery scenarios.

4. Technology readiness levels (TRLs) : NF processes for selective Li separation

The evaluation of NF processes for Li selectivity from brines integrates detailed performance analysis from Table 4 with the commercially available membranes in Table 5, offering a nuanced understanding of their respective their Technology Readiness Levels (TRL) and operational efficiencies. The TRL chart (Fig. 16), adapted from [150], offers a concise overview of the maturity and integration potential of these NF techniques into commercial Li recovery operations.

Table 4 highlights the diverse array of NF membranes, each tailored for specific brine types and characterized by unique separation capabilities and technological maturity. The NF90 commercial membrane, despite its moderate Li/Mg^{2+} separation ability and lower selectivity ratio, has an established presence in the field, reflecting a higher TRL indicative of commercial deployment readiness. Advanced membranes like HACC-PIP-TMC composites showcase a higher Li/Mg^{2+} separation ability of 115 and a flux of 1.57 L m^{-2} h^{-1} bar^{-1}, suggesting superior performance due to innovative material use and process refinement, with TRLs around 4–5, indicating they are close to commercial application. Surface-modified membranes, such as those utilizing TMC/BPEI/EDTA, offer enhanced Li/Mg^{2+} separation abilities and high flux rates, reflecting their effectiveness and the potential for scale-up, pending further long-term operational validation.

Commercially available membranes such as NFX 2540, PRO-XS2, DK, and NF2 are also evaluated for their performance in Li recovery, as detailed in Table 5. NFX 2540 demonstrates exceptionally high $MgSO_4$ rejection at 99 %, operating optimally at 10 bar with an 80 % permeate recovery, making it suitable for immediate commercial application. Its high TRL is indicative of readiness for large-scale operations. PRO-XS2 and DK membranes, while showing robust performance with $MgSO_4$ rejection rates of 87 % and 96 % respectively, vary in operational pressures and outcomes, suggesting that while they are commercially available, optimization may still be required to maximize their efficiency in Li recovery processes. The NF2 membrane, noted for achieving the highest Li recovery of >75 % from synthetic geothermal brine, showcases significant potential for Li extraction applications, with a TRL indicating it is ready for broader commercial use.

The integration of NF membranes for specific applications, such as those optimized for high Mg^{2+}/Li^+ ratios in salt lake brine, achieves very high selectivity factors. The commercial viability of these membranes hinges on their ability to maintain high performance over extended operational periods, as indicated by long-term stability tests. Membranes such as the SPE-PEI, which demonstrates a significant selectivity factor and operational flux, are particularly promising for commercial deployment.

Combining the analytical perspectives from Tables 4 and 5 provides a comprehensive overview of the readiness of various NF technologies for commercial deployment in Li recovery from brines. While many membranes show high Li selectivity and operational efficiency, their long-term stability and adaptability to different brine compositions remain critical areas for ongoing development. Continuous material innovation and process optimization will be essential as these technologies advance through higher TRL stages. Comprehensive techno-economic analyses will also be crucial to assess their commercial potential and strategize their integration into existing Li recovery infrastructures, ensuring they meet the stringent requirements of industrial applications.

Table 6
Characteristics of reported integrated systems for Li recovery from brine.

Technology	Brine	NF material & Operating conditions	Final recovery of Li (%)	TRL	Key outcomes & remarks	Limiting factor/barrier	Ref
RO-NF-MDC	RO brine	• 39 °C • Initial volume of 1 L for simulations	73.8	3–4	• Li recovery using membrane crystallization (MCr) from RO brine • Use of vacuum membrane distillation (VMD) instead of direct contact membrane distillation (DCMD) • Li-contained precipitates as LiCl at a water recovery rate of 97 %	• Ore grade degradation increases production costs, including water and energy • Induction time caused a delay in the start of precipitation in experiments	[159]
MD-NF	Simulated salt lake brine	• NF270 at 20 °C • pH 5 • 8 bar • Constant cross-flow velocity of 40 cm/s • MD operated with feed at 40 °C and distillate at 20 °C	80	4–5	• Achieved 23 % and 44 % Li separation through NF90 and NF270 membranes, respectively. • Li concentration enriched by up to 80 % after MD treatment	• MD influenced by temperature and salt concentration	[93]
NF-MD-precipitation	Salt-lake brine	• TFC PA NF membrane • 20 °C • 8 bar • NF membrane compacted with ultrapure water for stability	42	4–5	• Improved Li enrichment by MD from 2.5 to 5 through NF pre-treatment • Li concentration by MD increased from 82 to 410 mg/L	• Reduced permeate flux by membrane scaling during long-term operation. • Li recovery affected by competitive other cations like Mg	[160]
NF-MD	Li-containing artificial brine	• NE 70 • water flux (25.1 L m^{-2} h^{-1}) • Rejection (>30 %) of divalent ions (Ca^{2+} and Mg^{2+}), • Low rejection (<10 %) of monovalent ions (Na^{+} and Li^{+}).	91.6, 12-fold increased	4–5	• NF pre-treatment required for removal of divalent ions (Ca^{2+} and Mg^{2+}) that are prone to form crystals. • Increased Li concentration from 100 to 1200 ppm. • Helps avoid crystal formation and process failure.	• MD alone ineffective at removing divalent ions, potentially leading to crystal formation and system clogging. • Risk of halite crystal formation without NF, impacting process efficiency.	[70]
Low pressure reverse osmosis (LPRO)	Salt-lake brine	• PA UF membrane • 0–41 bar • 21 °C	85	3–4	• Decreased fouling propensity by NF's lower average roughness • NF fouling by Salt Lake brines diluted 10 times. • Total separation of Li from sodium through dialysis with NF.	• LPRO alone failed to achieve total separation between Li and Na.	[83]
MD-thermoelectric generation		• PA UF membrane	–	3–4	• Effective removal of Ca^{2+} and Mg^{2+} via NF, preventing equipment fouling. • Generating electricity for making the process self-sustaining. • Rendering Li to pass through, improving Li recovery	• High costs of installation and operation. • Low efficiency of thermoelectric generators.	[161]
CDI-NF	–	–	–	1–3	• Enhanced removal of small ions and organic molecules. • Improved water quality due to dual filtration and ion capture processes. • Potential for lower energy consumption compared to traditional desalination methods.	• Electrode selectivity & capacity.	[162]
NF-solvent extraction-selective precipitation	Simulated NF-treated seawater desalination brine	–	74	4–6	• Enhanced the practicability of recovery by higher Li concentration in desalination brine • NF membranes concentrating Li by about 3 times from seawater desalination brine • Effective in blocking larger, highly charged particles from passing through	• Requirement of expensive chemicals specified for solvent extraction • Careful control required for selective precipitation to avoid impurities • Energy-intensive solvent extraction and selective precipitation processes	[68]

(*continued on next page*)

Table 6 (*continued*)

Technology	Brine	NF material & Operating conditions	Final recovery of Li (%)	TRL	Key outcomes & remarks	Limiting factor/barrier	Ref
Electrochemical intercalation-deintercalation (EID)-NF-RO- evaporation, and precipitation,	Salt Lake brine with the Mg^{2+}/Li^{+} ratio of 58.8	• Disc tube NF membrane based on PA material. • pH 3–11 • 2.0 MPa • 25 °C	86.1	4	• Successful demonstration on a mini-pilot scale • Divalent ion removal from Li-rich solution via NF. • Reduction in alkali usage and minimized Li loss with Mg^{2+} removal during Mg $(OH)_2$ production. • Effective Li^{+} and Mg^{2+} separation. • Efficient rejection of multivalent ions, including Mg^{2+} and SO_4^{2-}.	• NF technology limited to brine with very low sodium and potassium content. • Dilution necessary after high salinity brine potassium removal, consuming large water volumes.	[163]
BMED-NF-RO-CED	High Mg^{2+}/Li^{+} ratio Salt Lake brine	• DK NF membrane with PA active layer. • 0–3.5 MPa • 25 °C. • pH: 3.0–8.0 • BMED stack: CMB/AHA/BP	92	4–6	• Effective Mg^{2+} removal, achieving Mg^{2+}/Li^{+} ratio below 0.5. • Concentrates Li to above 14 g/L. • RO-CED integrated process applied for NF permeate enrichment. • High purity Li hydroxide produced via BMED.	• High energy consumption at 6.20 kWh/kg. • Current efficiency limited to 36.05 %.	[110]

5. Prospects NF integration with various Li recovery techniques

Several modern technologies have advanced to pilot and commercial stages for Li recovery from various brines, highlighting the need for an approach that is energy efficient, has a low carbon footprint and is scalable, modular, and cost-effective in terms of both capital and operational expenditures (CAPEX and OPEX). A promising strategy to enhance Li recovery involves combining NF pre-treatment with different recovery techniques [93,158]. The integration offers benefits such as selective separation of Li from impurities, reduced fouling, and improved energy efficiency. The integration offers benefits such as selective separation of Li from impurities, reduced fouling, and improved energy efficiency, as shown in Fig. 17, based on systems described in Table 6 and other hybrid systems for brine treatment. Traditional direct Li extraction methods like adsorption, ion exchange, and solvent extraction benefit significantly from NF pre-treatment. Adsorption, which is at TRL of 9, ion exchange at TRL 8, and solvent extraction at TRL 7, all show improved efficiency and efficacy when preceded by NF filtration that removes major impurities and concentrates Li ions. Furthermore, emerging membrane-based techniques, which are currently at TRL 4 and selectively transport Li^{+} ions through nanochannels, represent significant advancements in direct Li extraction (DLE) processes.

Producing Li hydroxide (LiOH) from salt lake brine with a high Mg^{2+}/Li^{+} ratio presents several challenges, including effective separation of Li and Mg, enrichment of Li, and achieving high purity in the final Li hydroxide product. Zhao et al. [110] addressed these issues by integrating the BMED process with NF, RO, and CED techniques (Fig. 18a) to process brines with a Mg^{2+}/Li^{+} mass ratio exceeding 30. The dual-stage NF and RO-CED processes significantly reduced Mg and enriched Li, achieving a Mg^{2+}/Li^{+} ratio below 0.5 and a Li content in the NF permeate over 14 g/L. The Li-rich solution was then processed through BMED to produce LiOH, yielding a Li concentration in the alkali solution of over 1.0 M, with a current efficiency of 36.1 % and energy consumption of 6.2 kWh/kg, surpassing previous studies. This integrated membrane process effectively separates Li and Mg from high Mg^{2+}/Li^{+} ratio brines, continuously producing 99.6 % pure LiOH.

Park et al. introduced a novel Li recovery method that utilizes a combination of membrane distillation (MD) and NF [70]. Initially, the process employs NF pre-treatment to enrich the Li in the brine while filtering out unwanted ions such as calcium and magnesium. Three commercial NF membranes (NE 40, NE 70, and NE 90) were tested, with the NE 70 membrane chosen due to its optimal water flux (25.1 L m^{-2} h^{-1}), significant rejection of divalent ions (Ca^{2+} and Mg^{2+}, >30 %), and minimal rejection of monovalent ions (Na^{+} and L^{+}, <10 %) (Fig. 18b and c). The pre-treatment altered the artificial brine's composition, reducing Ca^{+} and Mg^{2+} concentrations by 40 % while keeping Li^{+} and Na^{+} levels stable. The MD stage, utilizing the NF-treated brine, effectively enriched Li in the brine. However, crystal formation on the membrane surface necessitated periodic MD cleaning, as water flux was immediately restored with a minor ion concentration dilution (Fig. 18d and e). After 140 h, the process increased the brine's Li concentration from 100 ppm to 1200 ppm, making it suitable for integration with other technologies for high-quality Li production. This membrane-based method demonstrates the potential to utilize low-concentration Li brine with only a fraction of one-tenth of the capital cost, processing time, and physical footprint associated with conventional techniques. By reducing reliance on chemicals heavily used in traditional processes and inhibiting crystal formation, this approach averts process disruptions and promotes a more sustainable and economical Li recovery process.

Italian company Tenova Advanced Technologies (TAT) developed the LipTM process, utilizing NF technology to selectively extract alkaline earth elements from brines. This process can efficiently extract Li from brines with concentrations as low as 20×10^{-6}, reducing Li levels in the raffinate to as low as 1×10^{-6}. The Clayton Valley salt marsh brine Li extraction project in the United States, conducted by Canadian company Pure Energy, employs the LipTM process in conjunction with extraction, ion exchange, and precipitation processes. In May 2018, Pure Energy completed a pilot plant design for this approach, with pilot trials set to assess its commercial feasibility [164], underscoring the practical application of NF in enhancing Li recovery while minimizing environmental disruptions.

Eramet, in collaboration with IFPEN (the French Institute of Petroleum and New Energies) and Seprosys, is developing the Centenario Ratones Li salt lake project in Salta, Argentina. This project employs a series of advanced techniques to produce Li carbonate suitable for battery applications with a very high yield of direct extraction (Fig. 19a) [149] [165]. Key stages include NF and RO to further separate and concentrate Li. The final step in this innovative process involves converting Li into battery-grade Li_2CO_3 using a single filtration and washing step with sodium carbonate. The process boasts an extraction yield of ~90 %, and requires only half the brine typically needed by

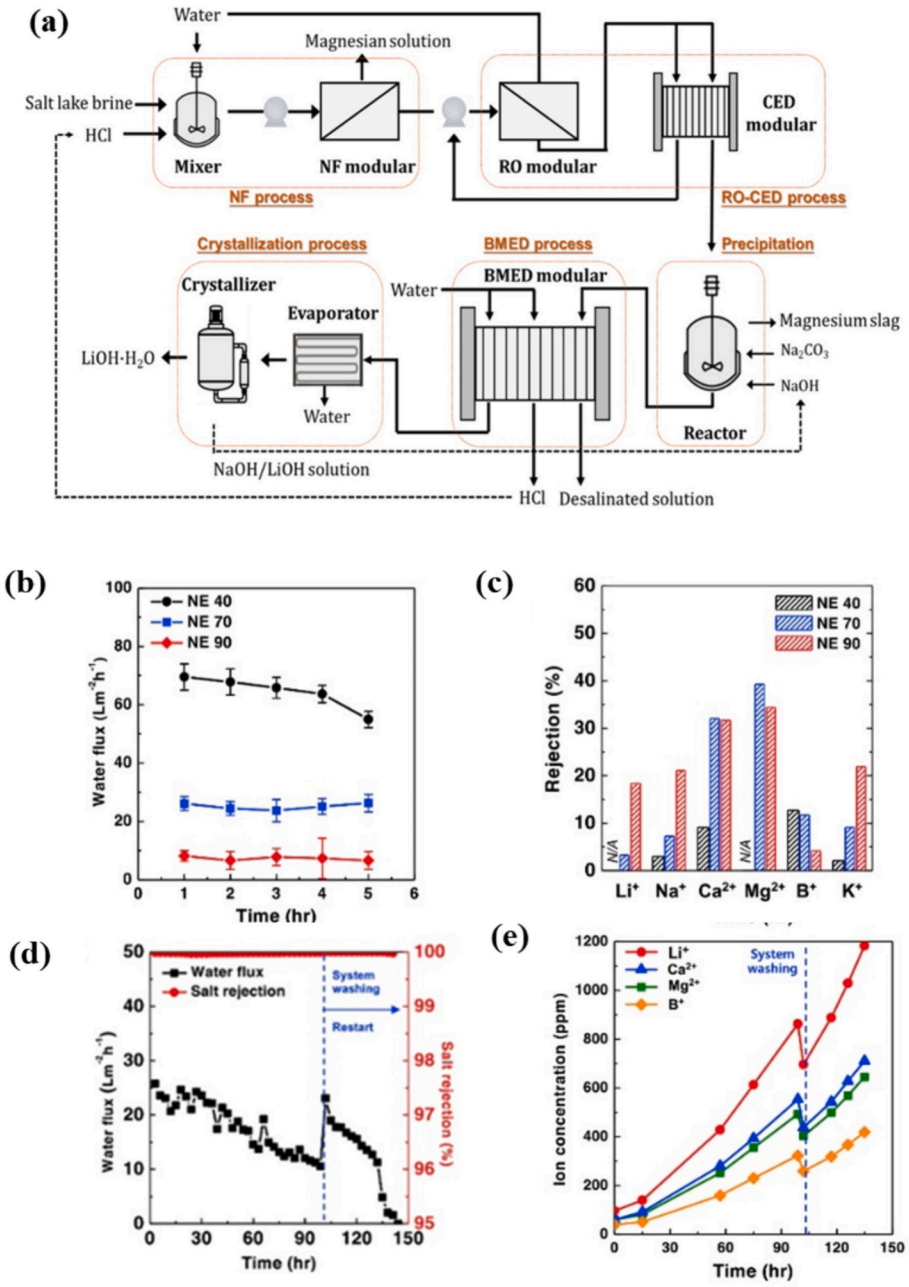

Fig. 18. Overview of integrated Li recovery technologies and NF membrane performance: (a) Schematic illustration of emerging Li recovery technique incorporating NF, RO, ED, and BMED [110]. (b) Water flux and (c) salt rejection profiles for NF tests conducted with three commercial membranes (NE 40, 70, and 90). (d) Performance evaluation of the membrane-based Li recovery method using NF, detailing salt rejection and water flux. (e) Ion concentration profiles in the brine during operation [70].

conventional extraction process, showcasing the efficiency and sustainability of integrating NF in Li recovery operations.

Chinese companies have made significant advancements in extracting Li from salt-lake brines with high mineral-to-Li ratios (MLR), notably boosting Li production capabilities. Golmud Zangge Lithium Industry Co., Ltd. has developed a unique technology combining simulated continuous adsorption with NF/RO for impurity removal and a one-step synthesis method [149] to produce battery-grade Li carbonate. This method successfully produced battery-grade Li_2CO_3 from previously discharged brine at the Qarham salt lake (Fig. 19b), demonstrating the scalability and efficacy of combining adsorption techniques with NF and RO for enhanced Li recovery.

DuPont has introduced the FilmTec™ LiNE-XD NF membrane elements, specially designed for purifying Li brine [166]. These advanced membranes, featuring specialized chemistry, support Direct Lithium Extraction (DLE) operations, facilitating sustainable Li production from various sources like salt lake brine, geothermal brine, and clay deposits. The LiNE-XD and LiNE-XD HP series are tailored to Li brine purification, achieving high Li passage from chloride-rich brine streams while offering exceptional selectivity over divalent metals such as magnesium. The efficiency of these FilmTec™ LiNE-XD membranes contributes to enhanced water and Li recovery rates and lowers energy consumption. Their distinctive membrane chemistry ensures consistent performance and longevity, addressing the growing demand for effective and eco-friendly Li brine processing solutions.

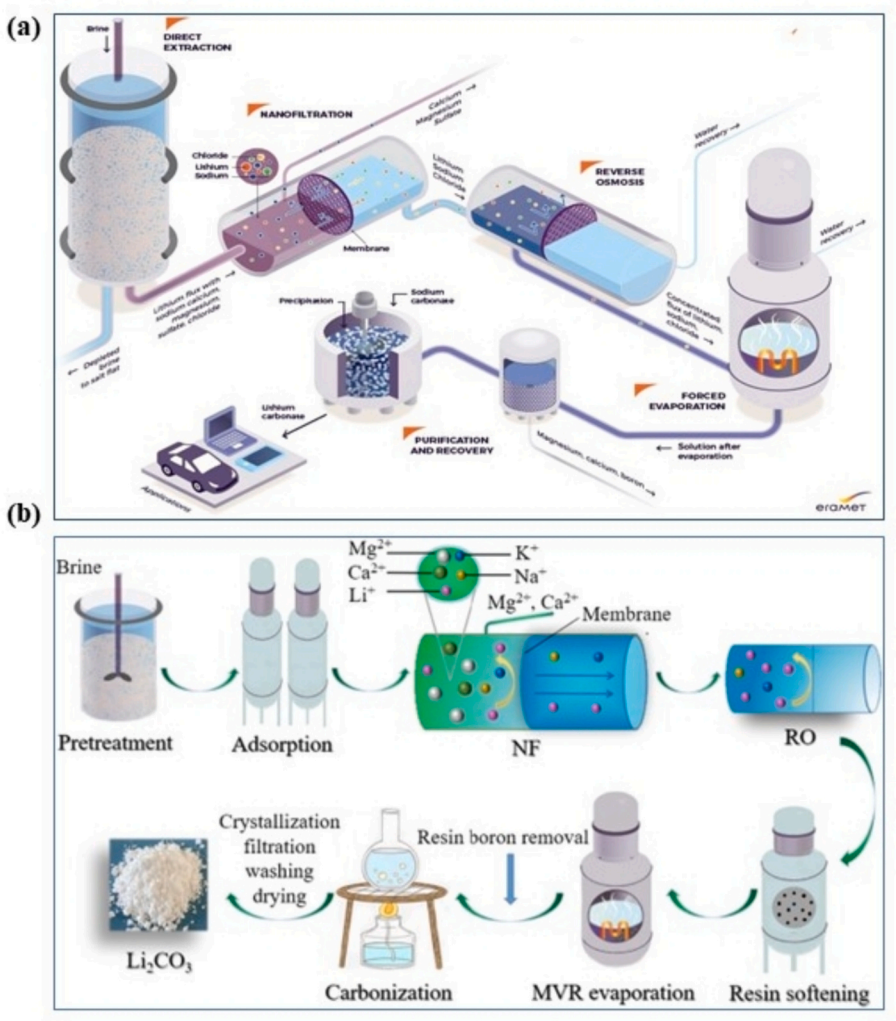

Fig. 19. Comparative Li extraction processes: (a) A detailed flowchart depicting the Li extraction process by Eramet [165], showcasing stages from direct extraction to forced evaporation involving NF and RO. (b) The Golmud Zangge Li extraction sequence illustrates steps from pretreatment through NF and RO to resin softening and carbonization, culminating in the production of Li carbonate [149].

6. Potential challenges in the NF process for Li recovery

Li extraction from brine using NF has emerged as a leading commercial method, prized for its straightforward operation and low energy demands. Despite these advantages, several challenges inhibit its broader industrial application, particularly the physicochemical properties of the membranes and the operational complexities of large-scale systems.

Traditional NF membranes often exhibit limited monovalent selectivity, complicating the efficient separation of Li from other similarly charged ions such as sodium and potassium, which possess comparable valances and ionic sizes. The significant presence of Mg, often with Mg^{2+}/Li^{+} ratios exceeding 20 and potentially reaching 200, underscores the necessity for membranes with enhanced selectivity [167]. Current commercial membranes, which are typically negatively charged, struggle to distinguish between the similar hydration radii of Mg^{2+} (0.428 nm) and Li^{+} (0.382 nm), making it difficult to meet industrial standards for Li purity and recovery efficiency [168,169]. Additionally, differentiating Li^{+} from other monovalent ions like Na^{+} and K^{+}, which share comparable valences and ionic sizes, poses another significant hurdle [5]. Scaling-prone ions like Ca^{2+} and SO_4^{2-} in brines further challenge the separation performance of NF membranes, leading to fouling that reduces their operational longevity. Moreover, the high salinity of certain feed sources necessitates dilution to manage the operational pressures and maintain membrane permeability, adding to the process's complexity and cost.

The structural integrity of NF membranes is at risk under the continuous high-pressure gradients required to process highly saline brines, such as those from desalinated seawater. This mechanical stress can induce microcracks in the membranes, significantly curtailing their operational lifespan and solute separation capabilities. Consequently, the energy consumption associated with NF increases with higher salinity levels, reducing its economic attractiveness [5]. Although positively charged NF surfaces have shown higher performance in Mg^{2+}/Li^{+} separation, the fabrication of such membranes presents considerable challenges. Negatively charged traditional PA-based NF membranes, while common, show suboptimal selectivity due to Donnan and electrostatic effects [116]. Furthermore, positively charged membranes are susceptible to microbial contamination, which can compromise their effectiveness and durability unless equipped with strong antibacterial properties [22].

The commercial viability of NF membranes requires enhancements to extract Li^{+} efficiently from salt lake brines. Many NF membranes currently demonstrate low permeability and insufficient separation factors, limiting their practical applications. Membrane fouling remains a significant obstacle, reducing permeability and selectivity, which is particularly problematic in systems like NF90, where permeability was observed to halve and selectivity decreased after just 6 hrs of operation

[83]. To address these challenges, further advancements in membrane materials are essential. While improvements might enable more efficient separation in single-pass NF processes, achieving industrially relevant Li purity remains challenging. Polymer NF membranes typically exhibit low Li permeability, whereas high-permeability nanofluidic devices face scale-up and fabrication challenges [118].

Sophisticated Li recovery systems using NF are generally more expensive than traditional evaporative methods due to the higher capital investments required for the advanced materials [170]. Proper assessment and management of operational conditions are crucial to enhance the effectiveness of membrane processes for various brines or wastewaters, making NF more economically viable for high ion recovery. This analysis underscores the critical need for continued research and development in NF technology to overcome these barriers, potentially revolutionizing Li recovery processes to meet the escalating demands of the battery and renewable energy sectors.

7. Future directions and conclusion

The increasing demand and price of Li, propelled by the growing sectors of portable electronics and electric vehicles, highlight the need for sustainable Li extraction from diverse sources. Recent strides in membrane technology, particularly in the realm of NF, have been poised as a pivotal method for Li extraction from brines and seawater, capable of refining Li concentration and adjusting the Mg^{2+}/Li^{+} ratio effectively. Innovative developments in membrane fabrication and modification have culminated in high-performance membranes designed for efficient Li extraction. The focus for future advancements in NF technology centers on membranes that not only offer exceptional selectivity and reduced energy consumption but also demonstrate robust cycling performance essential for prolonged industrial applications. However, achieving this necessitates overcoming substantial challenges inherent to membrane operations, such as optimizing functionality and enhancing operational efficiency.

Future research endeavors will likely concentrate on designing selectively permeable membranes specifically for Li separation in NF processes. It is crucial to manage operational conditions meticulously - such as adjusting pressure, pH levels, and temperature - to maintain membrane integrity and avoid premature degradation. Enhanced substrate materials may significantly improve the efficacy of NF membranes, propelling Li recovery processes towards higher efficiency and reliability.

Explorations into multi-pass NF filtration systems should prioritize the optimization of operating pressure and water recovery rates at each stage, employing advanced NF membranes that outperform conventional commercial options. Research should extend into systems handling highly concentrated feed solutions, focusing on the optimal dilution factor that balances separation performance with economic feasibility. Understanding and managing the trade-offs between membrane permeability and Li selectivity are crucial for selecting suitable membranes for specific applications. Hence, ongoing research should aim to refine NF processes for Li recovery, emphasizing the reduction of energy demands and minimizing fouling tendencies.

Given the proven capability of NF in Li extraction, there is a compelling need to reduce operational costs through system optimization and membrane improvements. These should particularly aim at advancing antifouling properties and augmenting Li selectivity. Thorough optimization of either individual or hybrid NF methods in Li extraction must also consider factors like energy efficiency, system stability, and product quality. Combining NF with other separation methods could further improve the extraction of Li ions from brine solutions.

Seawater desalination brine presents a viable alternative Li source for regions devoid of traditional mining resources. This approach not only promises a reduced environmental footprint but also aligns with sustainable mining practices. However, the existing NF configurations employed in Li extraction from seawater require further refinement to achieve the efficiency levels of conventional mining processes. Therefore, enhancing NF technology and its integration with other recovery methods is crucial. Focused research and development are needed to improve productivity and performance in the Li recovery process, paving the way for its industrial-scale application.

Declaration of competing interest

The authors declare that they have no known competing financial interests or personal relationships that could have appeared to influence the work reported in this paper.

Data availability

Data will be made available on request.

Acknowledgement

This publication was made possible by a UREP grant (#UREP30-115-2-040) from the Qatar National Research Fund (QNRF)-Qatar Research Development and Innovation (QRDI) and from the Australian Research Council (ARC) Discovery Projects (DP230100238). H.P is grateful to the National Research Foundation of Korea (2018R1A6A1A03024962 and RS-2023-00254645).

References

[1] T. Le, X. Chen, H. Dong, W. Tarpeh, A. Perea-Cachero, J. Coronas, S.M. Martin, M. Mohammad, A. Razmjou, A.R. Esfahani, N. Koutahzadeh, P. Cheng, P. R. Kidambi, M.R. Esfahani, An evolving insight into metal organic framework-functionalized membranes for water and wastewater treatment and resource recovery, Ind. Eng. Chem. Res. 60 (2021) 6869–6907, https://doi.org/10.1021/acs.iecr.1c00543.

[2] P. Greim, A.A. Solomon, C. Breyer, Assessment of lithium criticality in the global energy transition and addressing policy gaps in transportation, Nat. Commun. 11 (2020) 4570, https://doi.org/10.1038/s41467-020-18402-y.

[3] M.B. Marcelo Azevedo, Ken Hoffman, Aleksandra Krauze, Lithium mining: how new production technologies could fuel the global EV revolution. https://www.mckinsey.com/industries/metals-and-mining/our-insights/lithium-mining-how-new-production-technologies-could-fuel-the-global-ev-revolution#/, 2022. (Accessed 27 March 2024).

[4] J. Wood, Batteries are a key part of the energy transition. Here's why. https://www.weforum.org/agenda/2021/09/batteries-lithium-ion-energy-storage-circular-economy/, 2021. (Accessed 27 March 2024).

[5] X. Li, Y. Mo, W. Qing, S. Shao, C.Y. Tang, J. Li, Membrane-based technologies for lithium recovery from water lithium resources: a review, J. Membr. Sci. 591 (2019) 117317, https://doi.org/10.1016/j.memsci.2019.117317.

[6] H. Ambrose, A. Kendall, Understanding the future of lithium: part 1, resource model, J. Ind. Ecol. 24 (2020) 80–89, https://doi.org/10.1111/jiec.12949.

[7] J. Szlugaj, B. Radwanek-Bąk, Lithium sources and their current use, Gospod. Surowcami Miner./Miner. Resour. Manag. 38 (2022) 61–88, https://doi.org/10.24425/gsm.2022.140613.

[8] C.P. Grey, D.S. Hall, Prospects for lithium-ion batteries and beyond—a 2030 vision, Nat. Commun. 11 (2020) 6279, https://doi.org/10.1038/s41467-020-19991-4.

[9] S. Yang, F. Zhang, H. Ding, P. He, H. Zhou, Lithium metal extraction from seawater, Joule 2 (2018) 1648–1651, https://doi.org/10.1016/j.joule.2018.07.006.

[10] Mineral commodity summaries, in: Mineral Commodity SummariesReston, VA, 2023, 2023, p. 210, https://doi.org/10.3133/mcs2023.

[11] X. Sun, H. Hao, F. Zhao, Z. Liu, Global lithium flow 1994–2015: implications for improving resource efficiency and security, Environ. Sci. Technol. 52 (2018) 2827–2834, https://doi.org/10.1021/acs.est.7b06092.

[12] I. Castano, Scramble for Riches: Can South America's Lithium Triangle Mint New Millionaires?. https://www.nasdaq.com/articles/scramble-for-riches-can-south-americas-lithium-triangle-mint-new-millionaires, 2023. (Accessed 27 March 2024).

[13] E.W. Kathryn Ledebur, Can South American Lithium Power Biden's Battery Plans?. https://foreignpolicy.com/2023/04/12/us-energy-transition-lithium-triangle-evs-batteries-latin-america-policy/, 2023. (Accessed 27 March 2024).

[14] L. Sigal, Focus: Argentina's lithium pipeline promises 'white gold' boom as Chile tightens control. https://www.reuters.com/markets/commodities/argentinas-lithium-pipeline-promises-white-gold-boom-chile-tightens-control-2023-04-24/, 2023. (Accessed 27 March 2024).

[15] S.B. MacDonald, Chile's New Lithium Policy, White Gold, and Geopolitics. https://globalamericans.org/chiles-new-lithium-policy-white-gold-and-geopolitics/, 2023. (Accessed 27 March 2024).

[16] T.A.S.-K. Ryan, C. Berg, South America's Lithium Triangle: Opportunities for the Biden Administration. https://www.csis.org/analysis/south-americas-lithium-triangle-opportunities-biden-administration, 2021. (Accessed 27 March 2024).

[17] M.S. Sajna, T. Elmakki, K. Schipper, S. Ihm, Y. Yoo, B. Park, H. Park, H.K. Shon, D. S. Han, Integrated seawater hub: a nexus of sustainable water, energy, and resource generation, Desalination 571 (2024) 117065, https://doi.org/10.1016/j.desal.2023.117065.

[18] J. Zhai, A. Balogun, S. Bhattacharjee, R.J. Vogler, R. Khare, M. Malmali, A. Deonarine, Y.-x. Shen, Nanofiltration as pretreatment for lithium recovery from salt lake brine, J. Membr. Sci. 710 (2024) 123150, https://doi.org/10.1016/j.memsci.2024.123150.

[19] X. Li, C. Zhang, S. Zhang, J. Li, B. He, Z. Cui, Preparation and characterization of positively charged polyamide composite nanofiltration hollow fiber membrane for lithium and magnesium separation, Desalination 369 (2015) 26–36, https://doi.org/10.1016/j.desal.2015.04.027.

[20] H.-Z. Zhang, Z.-L. Xu, H. Ding, Y.-J. Tang, Positively charged capillary nanofiltration membrane with high rejection for Mg2+ and Ca2+ and good separation for Mg2+ and Li+, Desalination 420 (2017) 158–166, https://doi.org/10.1016/j.desal.2017.07.011.

[21] X. Zhao, H. Yang, Y. Wang, Z. Sha, Review on the electrochemical extraction of lithium from seawater/brine, J. Electroanal. Chem. 850 (2019) 113389, https://doi.org/10.1016/j.jelechem.2019.113389.

[22] P. Xu, W. Wang, X. Qian, H. Wang, C. Guo, N. Li, Z. Xu, K. Teng, Z. Wang, Positive charged PEI-TMC composite nanofiltration membrane for separation of Li+ and Mg2+ from brine with high Mg2+/Li+ ratio, Desalination 449 (2019) 57–68, https://doi.org/10.1016/j.desal.2018.10.019.

[23] C. Guo, N. Li, X. Qian, J. Shi, M. Jing, K. Teng, Z. Xu, Ultra-thin double Janus nanofiltration membrane for separation of Li+ and Mg2+: "drag" effect from carboxyl-containing negative interlayer, Sep. Purif. Technol. 230 (2020) 115567, https://doi.org/10.1016/j.seppur.2019.05.009.

[24] S.M. Hossain, H. Yu, Y. Choo, G. Naidu, D.S. Han, H.K. Shon, ZiF-8 induced carbon electrodes for selective lithium recovery from aqueous feed water by employing capacitive deionization system, Desalination 546 (2023) 116201, https://doi.org/10.1016/j.desal.2022.116201.

[25] S. Zavahir, T. Elmakki, M. Gulied, Z. Ahmad, L. Al-Sulaiti, H.K. Shon, Y. Chen, H. Park, B. Batchelor, D.S. Han, A review on lithium recovery using electrochemical capturing systems, Desalination 500 (2021) 114883, https://doi.org/10.1016/j.desal.2020.114883.

[26] D.H. Daniel Ernesto Galli, Maria de las Mercedes Otaiza, Claudia del Rosario Cachagua, Rene Enrique Santillan, PROCESS FOR RECOVERING LITHIUM FROM A BRINE, in: U.S. Patent (Ed.), 2014, https://patents.google.com/patent/US8641992B2/en)❱ .

[27] Lithium recovery from brines, Lenntech, in: https://www.lenntech.com/processes/lithium-recovery.htm.

[28] D. Fuentealba, C. Flores-Fernández, E. Troncoso, H. Estay, Technological tendencies for lithium production from salt lake brines: progress and research gaps to move towards more sustainable processes, Resour. Policy 83 (2023) 103572, https://doi.org/10.1016/j.resourpol.2023.103572.

[29] M.L. Vera, W.R. Torres, C.I. Galli, A. Chagnes, V. Flexer, Environmental impact of direct lithium extraction from brines, Nat. Rev. Earth Environ. 4 (2023) 149–165, https://doi.org/10.1038/s43017-022-00387-5.

[30] E. Knapik, G. Rotko, M. Marszałek, Recovery of lithium from oilfield brines—current achievements and future perspectives: a mini review, Energies 16 (2023) 6628, https://doi.org/10.3390/en16186628.

[31] How Is Brine Mining Used for Lithium Recovery?, SAMCO. https://samcotech.com/how-is-brine-mining-used-for-lithium-recovery/.

[32] Lithium Processing - Brine, in: https://www.pall.com/content/dam/pall/chemicals-polymers/literature-library/non-gated/application-notes/lithium-processing-brine.pdf, 2024.

[33] J. Farahbakhsh, F. Arshadi, Z. Mofidi, M. Mohseni-Dargah, C. Kök, M. Assefi, A. Soozanipour, M. Zargar, M. Asadnia, Y. Boroumand, V. Presser, A. Razmjou, Direct lithium extraction: a new paradigm for lithium production and resource utilization, Desalination 575 (2024) 117249, https://doi.org/10.1016/j.desal.2023.117249.

[34] S.B.a.M.H. Susanna Ventura, Selective Recovery of Lithium From Brines, PROCEEDINGS, 43rd Workshop on Geothermal Reservoir Engineering, Stanford University, Stanford, California, February .

[35] T.P. Mernagh, E.N. Bastrakov, S. Jaireth, P. de Caritat, P.M. English, J.D. A. Clarke, A review of Australian salt lakes and associated mineral systems, Aust. J. Earth Sci. 63 (2016) 131–157, https://doi.org/10.1080/08120099.2016.1149517.

[36] Z.H. Foo, D. Rehman, A.T. Bouma, S. Monsalvo, J.H. Lienhard, Lithium concentration from salt-lake brine by Donnan-enhanced nanofiltration, Environ. Sci. Technol. 57 (2023) 6320–6330, https://doi.org/10.1021/acs.est.2c08584.

[37] S. Xu, J. Song, Q. Bi, Q. Chen, W.-M. Zhang, Z. Qian, L. Zhang, S. Xu, N. Tang, T. He, Extraction of lithium from Chinese salt-lake brines by membranes: design and practice, J. Membr. Sci. 635 (2021) 119441, https://doi.org/10.1016/j.memsci.2021.119441.

[38] A. Grant, From Catamarca to Qinghai: The Commercial Scale Direct Lithium Extraction Operations. https://www.jadecove.com/research/fromcatamarcatoqinghai, 2020. (Accessed 26 April 2024).

[39] S.E. Kesler, P.W. Gruber, P.A. Medina, G.A. Keoleian, M.P. Everson, T. J. Wallington, Global lithium resources: relative importance of pegmatite, brine and other deposits, Ore Geol. Rev. 48 (2012) 55–69, https://doi.org/10.1016/j.oregeorev.2012.05.006.

[40] S.-Y. Sun, L.-J. Cai, X.-Y. Nie, X. Song, J.-G. Yu, Separation of magnesium and lithium from brine using a Desal nanofiltration membrane, J. Water Process Eng. 7 (2015) 210–217, https://doi.org/10.1016/j.jwpe.2015.06.012.

[41] X.-S. Liu, X.-D. Wang, M. Yao, W. Cui, H. Yan, Effects of Fe doping on oxygen vacancy formation and CO adsorption and oxidation at the ceria(111) surface, Catal. Commun. 63 (2015) 35–40, https://doi.org/10.1016/j.catcom.2014.09.032.

[42] X. Liu, Y. Ma, G. Liu, S. Xiang, Z. Cui, Magnesium ion effect in the process of lithium migration in salt lake, Desalin. Water Treat. 250 (2022) 148–158, https://doi.org/10.5004/dwt.2022.28121.

[43] Y. Zeng, B. Jiang, Q.R. Yang, G.F. Quan, J.J. He, Z.T. Jiang, F.S. Pan, Effect of Li content on microstructure, texture and mechanical behaviors of the as-extruded Mg-Li sheets, Mater. Sci. Eng. A 700 (2017) 59–65, https://doi.org/10.1016/j.msea.2017.05.110.

[44] Y. Zhao, H. Xing, M. Rong, Z. Li, X. Wei, C. Chen, H. Liu, L. Yang, Quantum chemical calculation assisted efficient lithium extraction from unconventional oil and gas field brine by β-diketone synergic system, Desalination 565 (2023) 116890, https://doi.org/10.1016/j.desal.2023.116890.

[45] A. Kumar, H. Fukuda, T.A. Hatton, J.H.V. Lienhard, Lithium recovery from oil and gas produced water: a need for a growing energy industry, ACS Energy Lett. 4 (2019) 1471–1474, https://doi.org/10.1021/acsenergylett.9b00779.

[46] P.J. Daitch, Lithium Extraction From Oilfield Brine, The University of Texas at Austin, 2018. http://hdl.handle.net/2152/65645.

[47] S. Bogner, MGX minerals lithium technology wins independent verification. https://stockhouse.com/news/newswire/2017/04/20/mgx-minerals-lithium-technology-wins-independent-verification, 2017. (Accessed 27 March 2024).

[48] J. Neff, K. Lee, E.M. DeBlois, Produced water: overview of composition, fates, and effects, in: K. Lee, J. Neff (Eds.), Produced Water: Environmental Risks and Advances in Mitigation Technologies, Springer, New York, 2011, pp. 3–54, https://doi.org/10.1007/978-1-4614-0046-2_1.

[49] S.E. Can Sener, V.M. Thomas, D.E. Hogan, R.M. Maier, M. Carbajales-Dale, M. D. Barton, T. Karanfil, J.C. Crittenden, G.L. Amy, Recovery of critical metals from aqueous sources, ACS Sustain. Chem. Eng. 9 (2021) 11616–11634, https://doi.org/10.1021/acssuschemeng.1c03005.

[50] W.T. Stringfellow, M.K. Camarillo, Flowback verses first-flush: new information on the geochemistry of produced water from mandatory reporting, Environ Sci Process Impacts 21 (2019) 370–383, https://doi.org/10.1039/C8EM00351C.

[51] W.T. Stringfellow, P.F. Dobson, Technology for the recovery of lithium from geothermal brines, Energies 14 (2021) 6805, https://doi.org/10.3390/en14206805.

[52] M.P. Paranthaman, L. Li, J. Luo, T. Hoke, H. Ucar, B.A. Moyer, S. Harrison, Recovery of lithium from geothermal brine with lithium–aluminum layered double hydroxide chloride sorbents, Environ. Sci. Technol. 51 (2017) 13481–13486, https://doi.org/10.1021/acs.est.7b03464.

[53] EuGeLi: lithium extraction from geothermal brines in Europe. https://www.brgm.fr/en/current-project/eugeli-lithium-extraction-geothermal-brines-europe, 2022. (Accessed 27 March 2024).

[54] I. Ihsanullah, J. Mustafa, A.M. Zafar, M. Obaid, M.A. Atieh, N. Ghaffour, Waste to wealth: a critical analysis of resource recovery from desalination brine, Desalination 543 (2022) 116093, https://doi.org/10.1016/j.desal.2022.116093.

[55] B.A. Sharkh, A.A. Al-Amoudi, M. Farooque, C.M. Fellows, S. Ihm, S. Lee, S. Li, N. Voutchkov, Seawater desalination concentrate—a new frontier for sustainable mining of valuable minerals, npj Clean Water 5 (2022) 9, https://doi.org/10.1038/s41545-022-00153-6.

[56] H. Yu, S.M. Hossain, C. Wang, Y. Choo, G. Naidu, D.S. Han, H.K. Shon, Selective lithium extraction from diluted binary solutions using metal-organic frameworks (MOF)-based membrane capacitive deionization (MCDI), Desalination 556 (2023) 116569, https://doi.org/10.1016/j.desal.2023.116569.

[57] M.S. Diallo, M.R. Kotte, M. Cho, Mining critical metals and elements from seawater: opportunities and challenges, Environ. Sci. Technol. 49 (2015) 9390–9399, https://doi.org/10.1021/acs.est.5b00463.

[58] Q.-B. Chen, H. Ren, Z. Tian, L. Sun, J. Wang, Conversion and pre-concentration of SWRO reject brine into high solubility liquid salts (HSLS) by using electrodialysis metathesis, Sep. Purif. Technol. 213 (2019) 587–598, https://doi.org/10.1016/j.seppur.2018.12.018.

[59] L.S. Ribeiro, T.N.C. Dantas, A.A. Dantas Neto, K.C. Melo, M.C.P.A. Moura, P.T. P. Aum, The use of produced water in water-based drilling fluids: influence of calcium and magnesium concentrations, Braz. J. Pet. Gas 10 (2016) 233–245, https://doi.org/10.5419/bjpg2016-0019.

[60] V.G. Le, T.A. Luu, H.T. Tran, N.T. Bui, M. Mofijur, M.K. Nguyen, X.T. Bui, M. B. Bahari, H.N. Vo, C.T. Vu, G.-P.C. Chien, Y.-H. Huang, Recovery of lithium from industrial Li-containing wastewater using fluidized-bed homogeneous granulation technology, Minerals 14 (2024) 603, https://doi.org/10.3390/min14060603.

[61] S. Sutijan, S.A. Darma, C.M. Hananto, V.S. Sujoto, F. Anggara, S.N. Jenie, W. Astuti, F.R. Mufakhir, S. Virdian, A.P. Utama, H.T. Petrus, Lithium separation from geothermal brine to develop critical energy resources using high-pressure nanofiltration technology: characterization and optimization, Membranes (2023), https://doi.org/10.3390/membranes13010086.

[62] J. Gilron, Chapter 12 - brine treatment and high recovery desalination, in: N. P. Hankins, R. Singh (Eds.), Emerging Membrane Technology for Sustainable

Water Treatment, Elsevier, Boston, 2016, pp. 297–324, https://doi.org/10.1016/B978-0-444-63312-5.00012-7.
[63] I. Littlehales, S. Simões Neto, J.M. Dias Neto, J.-y. Lee, S. Ko, M. Mendes, G. Graham, S. Dyer, S. Peat, Systematic Modelling and Laboratory Testing to Allow the Potential for Economic Inorganic Scale Control in the Brazilian Pre-Salt Fields, Offshore Technology Conference BrasilRio de Janeiro, Brazil, 2023, https://doi.org/10.4043/32968-MS pp. D011S014R001.
[64] Y. Li, M. Wang, X. Xiang, Y.J. Zhao, Z.J. Peng, Separation performance and fouling analyses of nanofiltration membrane for lithium extraction from salt lake brine, J. Water Process Eng. 54 (2023) 104009, https://doi.org/10.1016/j.jwpe.2023.104009.
[65] S. Paudyal, X. Wang, S. Ko, W. Li, X. Yao, C. Leschied, R. Shen, D. Pimentel, A. T. Kan, M.B. Tomson, New Halite Testing Methods for High Temperature and From Low to Very High Calcium Content Brine, SPE International Oilfield Scale Conference and Exhibition, Scotland, UK, 2022, https://doi.org/10.2118/209509-MS.
[66] Y. L. Bronicki, A system for processing brines. https://patents.google.com/patent/WO2014140756A2/en, 2014.
[67] X. Dominguez-Benetton, (Invited) Lithium Recovery From Geothermal Brines, ECS Meeting Abstracts MA2022-02 1040, 2022, https://doi.org/10.1149/MA2022-02271040mtgabs.
[68] S. Raiguel, V.T. Nguyen, I. Reis Rodrigues, C. Deferm, S. Riaño, K. Binnemans, Recovery of lithium from simulated nanofiltration-treated seawater desalination brine using solvent extraction and selective precipitation, Solvent Extr. Ion Exch. 41 (2023) 425–448, https://doi.org/10.1080/07366299.2023.2206440.
[69] A. Razmjou, M. Asadnia, E. Hosseini, A. Habibnejad Korayem, V. Chen, Design principles of ion selective nanostructured membranes for the extraction of lithium ions, Nat. Commun. 10 (2019) 5793, https://doi.org/10.1038/s41467-019-13648-7.
[70] S.H. Park, J.H. Kim, S.J. Moon, J.T. Jung, H.H. Wang, A. Ali, C.A. Quist-Jensen, F. Macedonio, E. Drioli, Y.M. Lee, Lithium recovery from artificial brine using energy-efficient membrane distillation and nanofiltration, J. Membr. Sci. 598 (2020) 117683, https://doi.org/10.1016/j.memsci.2019.117683.
[71] W. Wang, Y. Zhang, X. Yang, H. Sun, Y. Wu, L. Shao, Monovalent cation exchange membranes with janus charged structure for ion separation, Engineering 25 (2023) 204–213, https://doi.org/10.1016/j.eng.2021.09.020.
[72] P. Xu, J. Hong, Z. Xu, H. Xia, Q.-Q. Ni, Positively charged nanofiltration membrane based on (MWCNTs-COOK)-engineered substrate for fast and efficient lithium extraction, Sep. Purif. Technol. 270 (2021) 118796, https://doi.org/10.1016/j.seppur.2021.118796.
[73] L. Wang, D. Rehman, P.-F. Sun, A. Deshmukh, L. Zhang, Q. Han, Z. Yang, Z. Wang, H.-D. Park, J.H. Lienhard, C.Y. Tang, Novel positively charged metal-coordinated nanofiltration membrane for lithium recovery, ACS Appl. Mater. Interfaces 13 (2021) 16906–16915, https://doi.org/10.1021/acsami.1c02252.
[74] R. Wang, R. Alghanayem, S. Lin, Multipass nanofiltration for lithium separation with high selectivity and recovery, Environ. Sci. Technol. 57 (2023) 14464–14471, https://doi.org/10.1021/acs.est.3c04220.
[75] T. Hubach, M. Pillath, C. Knaup, S. Schlüter, C. Held, Li+ separation from multi-ionic mixtures by nanofiltration membranes: experiments and modeling, Modelling (2023) 408–425, https://doi.org/10.3390/modelling4030024.
[76] Q. Chen, Z. Chen, H. Li, B.-J. Ni, Advanced lithium ion-sieves for sustainable lithium recovery from brines, Sustain. Horiz. 9 (2024) 100093, https://doi.org/10.1016/j.horiz.2024.100093.
[77] D. Kalmykov, S. Makaev, G. Golubev, I. Eremeev, V. Vasilevsky, J. Song, T. He, A. Volkov, Operation of three-stage process of lithium recovery from geothermal brine: simulation, Membranes (2021), https://doi.org/10.3390/membranes11030175.
[78] M. Gulied, S. Zavahir, T. Elmakki, H. Park, G.H. Gago, H.K. Shon, D.S. Han, Efficient lithium recovery from simulated brine using a hybrid system: direct contact membrane distillation (DCMD) and electrically switched ion exchange (ESIX), Desalination 572 (2024) 117127, https://doi.org/10.1016/j.desal.2023.117127.
[79] C.A. Quist-Jensen, A. Ali, S. Mondal, F. Macedonio, E. Drioli, A study of membrane distillation and crystallization for lithium recovery from high-concentrated aqueous solutions, J. Membr. Sci. 505 (2016) 167–173, https://doi.org/10.1016/j.memsci.2016.01.033.
[80] S. Zavahir, N.S. Riyaz, T. Elmakki, H. Tariq, Z. Ahmad, Y. Chen, H. Park, Y.-C. Ho, H.K. Shon, D.S. Han, Ion-imprinted membranes for lithium recovery: a review, Chemosphere 354 (2024) 141674, https://doi.org/10.1016/j.chemosphere.2024.141674.
[81] Y. Li, Y. Zhao, H. Wang, M. Wang, The application of nanofiltration membrane for recovering lithium from salt lake brine, Desalination 468 (2019) 114081, https://doi.org/10.1016/j.desal.2019.114081.
[82] W. Li, C. Shi, A. Zhou, X. He, Y. Sun, J. Zhang, A positively charged composite nanofiltration membrane modified by EDTA for LiCl/MgCl2 separation, Sep. Purif. Technol. 186 (2017) 233–242, https://doi.org/10.1016/j.seppur.2017.05.044.
[83] A. Somrani, A.H. Hamzaoui, M. Pontie, Study on lithium separation from salt lake brines by nanofiltration (NF) and low pressure reverse osmosis (LPRO), Desalination 317 (2013) 184–192, https://doi.org/10.1016/j.desal.2013.03.009.
[84] X. Zhang, W. Zhao, Y. Zhang, V. Jegatheesan, A review of resource recovery from seawater desalination brine, Rev. Environ. Sci. Biotechnol. 20 (2021) 333–361, https://doi.org/10.1007/s11157-021-09570-4.
[85] Q. Li, H. Liu, B. He, W. Shi, Y. Ji, Z. Cui, F. Yan, Y. Mohammad, J. Li, Ultrahigh-efficient separation of Mg2+/Li+ using an in-situ reconstructed positively charged nanofiltration membrane under an electric field, J. Membr. Sci. 641 (2022) 119880, https://doi.org/10.1016/j.memsci.2021.119880.
[86] M.E.A. Ali, Nanofiltration process for enhanced treatment of RO brine discharge, Membranes 11 (2021) 212, https://doi.org/10.3390/membranes11030212.
[87] H. B., H. R., A.-Z. H., O. W., Brackish water treatment by ceramic TiO2 low-pressure nanofiltration membranes, Global NEST J. 25 (4) (2023) 138–147, https://doi.org/10.30955/gnj.004513.
[88] Q. Peng, R. Wang, Z. Zhao, S. Lin, Y. Liu, D. Dong, Z. Wang, Y. He, Y. Zhu, J. Jin, L. Jiang, Extreme Li-Mg selectivity via precise ion size differentiation of polyamide membrane, Nat. Commun. 15 (2024) 2505, https://doi.org/10.1038/s41467-024-46887-4.
[89] J.G.C.H.M. Saif, S. Pawlowski, Lithium Recovery From Brines by Lithium Membrane Flow Capacitive Deionization (Li-MFCDI) – A Proof of Concept, 2023, https://doi.org/10.5281/zenodo.8298881.
[90] A.M. Fathi, A.S. Al-Hussaini, M.A.-E. Swidan, A.K. Daif, Appraising influences of temperature and concentration on high rejection nanofiltration and their application in saline water, AJBAS 2 (2021) 168–180, https://doi.org/10.21608/ajbas.2021.75579.1053.
[91] A.H. Avci, D.A. Messana, S. Santoro, R.A. Tufa, E. Curcio, G. Di Profio, E. Fontananova, Energy harvesting from brines by reverse electrodialysis using nafion membranes, Membranes 10 (2020) 168, https://doi.org/10.3390/membranes10080168.
[92] D. Yadav, S. Hazarika, P.G. Ingole, Recent development in nanofiltration (NF) membranes and their diversified applications, Emerg. Mater. 5 (2022) 1311–1328, https://doi.org/10.1007/s42247-021-00302-6.
[93] B.K. Pramanik, M.B. Asif, S. Kentish, L.D. Nghiem, F.I. Hai, Lithium enrichment from a simulated salt lake brine using an integrated nanofiltration-membrane distillation process, J. Environ. Chem. Eng. 7 (2019) 103395, https://doi.org/10.1016/j.jece.2019.103395.
[94] B. Van der Bruggen, Nanofiltration, in: E.M.V. Hoek, V.V. Tarabara (Eds.), Encyclopedia of Membrane Science and Technology, John Wiley & Sons, Inc., New Jersey, 2013, pp. 1–22, https://doi.org/10.1002/9781118522318.emst077.
[95] G. Liu, Z. Zhao, A. Ghahreman, Novel approaches for lithium extraction from salt-lake brines: a review, Hydrometallurgy 187 (2019) 81–100, https://doi.org/10.1016/j.hydromet.2019.05.005.
[96] B. Van der Bruggen, C. Vandecasteele, Modelling of the retention of uncharged molecules with nanofiltration, Water Res. 36 (2002) 1360–1368, https://doi.org/10.1016/S0043-1354(01)00318-9.
[97] A.E. Childress, M. Elimelech, Relating nanofiltration membrane performance to membrane charge (electrokinetic) characteristics, Environ. Sci. Technol. 34 (2000) 3710–3716, https://doi.org/10.1021/es0008620.
[98] N.S. Suhalim, N. Kasim, E. Mahmoudi, I.J. Shamsudin, A.W. Mohammad, F. Mohamed Zuki, N.L. Jamari, Rejection mechanism of ionic solute removal by nanofiltration membranes: an overview, Nanomaterials 12 (2022) 437, https://doi.org/10.3390/nano12030437.
[99] A. Priyadarshini, R. Jain, S.W. Tay, L. Hong, Nanofiltration of aqueous dye solution through the diffused rough pores of a carbonaceous–kaolinite amalgamation membrane, ACS ES&T Water 2 (2022) 414–424, https://doi.org/10.1021/acsestwater.1c00312.
[100] L. Giorno, E. Drioli, H. Strathmann, The principle of nanofiltration (NF), in: E. Drioli, L. Giorno (Eds.), Encyclopedia of Membranes, Springer, Berlin, Heidelberg, 2015, pp. 1–5, https://doi.org/10.1007/978-3-642-40872-4_2234-1.
[101] P. Li, H. Lan, K. Chen, X. Ma, B. Wei, M. Wang, P. Li, Y. Hou, Q. Jason Niu, Novel high-flux positively charged aliphatic polyamide nanofiltration membrane for selective removal of heavy metals, Sep. Purif. Technol. 280 (2022) 119949, https://doi.org/10.1016/j.seppur.2021.119949.
[102] S. Sarkar, A.K. SenGupta, P. Prakash, The Donnan membrane principle: opportunities for sustainable engineered processes and materials, Environ. Sci. Technol. 44 (2010) 1161–1166, https://doi.org/10.1021/es9024029.
[103] L. Ma, Q. Bi, Y. Tang, C. Zhang, F. Qi, H. Zhang, Y. Gao, S. Xu, Fabrication of high-performance nanofiltration membrane using polydopamine and carbon nitride as the interlayer, Separations 9 (2022) 180, https://doi.org/10.3390/separations9070180.
[104] H.H.K. Minyaoui, M. Pontie, A. Hannachi, Integrated approach for brackish water desalination and distribution: which desalination technology to choose? Desalin. Water Treat. 73 (2017) 121–126, https://doi.org/10.5004/dwt.2017.20861.
[105] D. Menne, J. Kamp, J. Erik Wong, M. Wessling, Precise tuning of salt retention of backwashable polyelectrolyte multilayer hollow fiber nanofiltration membranes, J. Membr. Sci. 499 (2016) 396–405, https://doi.org/10.1016/j.memsci.2015.10.058.
[106] Y. Roy, D.M. Warsinger, J.H. Lienhard, Effect of temperature on ion transport in nanofiltration membranes: diffusion, convection and electromigration, Desalination 420 (2017) 241–257, https://doi.org/10.1016/j.desal.2017.07.020.
[107] Q.-B. Chen, Z.-Y. Ji, J. Liu, Y.-Y. Zhao, S.-Z. Wang, J.-S. Yuan, Development of recovering lithium from brines by selective-electrodialysis: effect of coexisting cations on the migration of lithium, J. Membr. Sci. 548 (2018) 408–420, https://doi.org/10.1016/j.memsci.2017.11.040.
[108] Q. Bi, Z. Zhang, C. Zhao, Z. Tao, Study on the recovery of lithium from high Mg2+/Li+ ratio brine by nanofiltration, Water Sci. Technol. 70 (2014) 1690–1694, https://doi.org/10.2166/wst.2014.426.
[109] I. Dammak, M.A. Neves, H. Nabetani, H. Isoda, S. Sayadi, M. Nakajima, Transport properties of oleuropein through nanofiltration membranes, Food Bioprod. Process. 94 (2015) 342–353, https://doi.org/10.1016/j.fbp.2014.04.002.
[110] Y. Zhao, H. Wang, Y. Li, M. Wang, X. Xiang, An integrated membrane process for preparation of lithium hydroxide from high Mg/Li ratio salt lake brine, Desalination 493 (2020) 114620, https://doi.org/10.1016/j.desal.2020.114620.

[111] Y.Z. Yan Li, Min Wang, Effects of pH and salinity on the separation of magnesium and lithium from brine by nanofiltration, Desalin. Water Treat. 97 (2017) 141–150, https://doi.org/10.5004/dwt.2017.21606.
[112] S.X. Qiuyan Bi, Separation of magnesium and lithium from brine with high Mg2+/Li+ ratio by a two-stage nanofiltration process, Desalin. Water Treat. 129 (2018) 94–100, https://doi.org/10.5004/dwt.2018.23062.
[113] K. Wang, X. Wang, B. Januszewski, Y. Liu, D. Li, R. Fu, M. Elimelech, X. Huang, Tailored design of nanofiltration membranes for water treatment based on synthesis–property–performance relationships, Chem. Soc. Rev. 51 (2022) 672–719, https://doi.org/10.1039/D0CS01599G.
[114] T. Zhang, Y. Chen, Q. Yu, H. Sun, K. Chen, H. Ye, S. Tang, H. Zhang, P. Li, Q. Jason Niu, Advanced Mg2+/Li+ separation nanofiltration membranes by introducing hydroxypropyltrimethyl ammonium chloride chitosan as a co-monomer, Appl. Surf. Sci. 616 (2023) 156434, https://doi.org/10.1016/j.apsusc.2023.156434.
[115] J. Chen, J. Wang, Z.-Y. Ji, Z. Guo, P. Zhang, Z. Huang, Electro-nanofiltration membranes with high Li+/Mg2+ selectivity prepared via sequential interfacial polymerization, Desalination 549 (2023) 116312, https://doi.org/10.1016/j.desal.2022.116312.
[116] M.-B. Wu, H. Ye, Z.-Y. Zhu, G.-T. Chen, L.-L. Ma, S.-C. Liu, L. Liu, J. Yao, Z.-K. Xu, Positively-charged nanofiltration membranes constructed via gas/liquid interfacial polymerization for Mg2+/Li+ separation, J. Membr. Sci. 644 (2022) 119942, https://doi.org/10.1016/j.memsci.2021.119942.
[117] R. He, C. Dong, S. Xu, C. Liu, S. Zhao, T. He, Unprecedented Mg2+/Li+ separation using layer-by-layer based nanofiltration hollow fiber membranes, Desalination 525 (2022) 115492, https://doi.org/10.1016/j.desal.2021.115492.
[118] H. Peng, Q. Zhao, A Nano-heterogeneous membrane for efficient separation of lithium from high magnesium/lithium ratio brine, Adv. Funct. Mater. 31 (2021) 2009430, https://doi.org/10.1002/adfm.202009430.
[119] H. Wu, Y. Lin, W. Feng, T. Liu, L. Wang, H. Yao, X. Wang, A novel nanofiltration membrane with [MimAP][Tf2N] ionic liquid for utilization of lithium from brines with high Mg2+/Li+ ratio, J. Membr. Sci. 603 (2020) 117997, https://doi.org/10.1016/j.memsci.2020.117997.
[120] Y. Feng, H. Peng, Q. Zhao, Fabrication of high performance Mg2+/Li+ nanofiltration membranes by surface grafting of quaternized bipyridine, Sep. Purif. Technol. 280 (2022) 119848, https://doi.org/10.1016/j.seppur.2021.119848.
[121] B. Swain, Recovery and recycling of lithium: a review, Sep. Purif. Technol. 172 (2017) 388–403, https://doi.org/10.1016/j.seppur.2016.08.031.
[122] K. Chen, F. Li, T. Wei, H. Zhou, T. Zhang, S. Zhao, T. Xie, H. Sun, P. Li, Q.J. Niu, An interlayer-based positive charge compensation strategy for the preparation of highly selective Mg2+/Li+ separation nanofiltration membranes, J. Membr. Sci. 684 (2023) 121882, https://doi.org/10.1016/j.memsci.2023.121882.
[123] T. Li, Y. Liu, C. Srinivasakannan, X. Jiang, N. Zhang, G. Zhou, S. Yin, S. Li, L. Zhang, Comparison of the Mg2+-Li+ separation of different nanofiltration membranes, Membranes 13 (2023) 753, https://doi.org/10.3390/membranes13090753.
[124] J. Luo, Y. Wan, Mix-charged nanofiltration membrane: engineering charge spatial distribution for highly selective separation, Chem. Eng. J. 464 (2023) 142689, https://doi.org/10.1016/j.cej.2023.142689.
[125] C.Y. Tang, Y.-N. Kwon, J.O. Leckie, Effect of membrane chemistry and coating layer on physiochemical properties of thin film composite polyamide RO and NF membranes: II. Membrane physiochemical properties and their dependence on polyamide and coating layers, Desalination 242 (2009) 168–182, https://doi.org/10.1016/j.desal.2008.04.004.
[126] F.S. Butt, A. Lewis, T. Chen, N.A. Mazlan, X. Wei, J. Hayer, S. Chen, J. Han, Y. Yang, S. Yang, Y. Huang, Lithium harvesting from the most abundant primary and secondary sources: a comparative study on conventional and membrane technologies, Membranes 12 (2022) 373, https://doi.org/10.3390/membranes12040373.
[127] S.S. Wadekar, R.D. Vidic, Influence of active layer on separation potentials of nanofiltration membranes for inorganic ions, Environ. Sci. Technol. 51 (2017) 5658–5665, https://doi.org/10.1021/acs.est.6b05973.
[128] Z. Yang, W. Fang, Z. Wang, R. Zhang, Y. Zhu, J. Jin, Dual-skin layer nanofiltration membranes for highly selective Li+/Mg2+ separation, J. Membr. Sci. 620 (2021) 118862, https://doi.org/10.1016/j.memsci.2020.118862.
[129] Q. Bi, C. Zhang, J. Liu, X. Liu, S. Xu, Positively charged zwitterion-carbon nitride functionalized nanofiltration membranes with excellent separation performance of Mg2+/Li+ and good antifouling properties, Sep. Purif. Technol. 257 (2021) 117959, https://doi.org/10.1016/j.seppur.2020.117959.
[130] Z. Wang, D. Xia, B. Wang, H. Liu, L. Zhu, Highly permeable polyamide nanofiltration membrane incorporated with phosphorylated nanocellulose for enhanced desalination, J. Membr. Sci. 647 (2022) 120339, https://doi.org/10.1016/j.memsci.2022.120339.
[131] P. Xu, J. Hong, Z. Xu, H. Xia, Q.-Q. Ni, Novel aminated graphene quantum dots (GQDs-NH2)-engineered nanofiltration membrane with high Mg2+/Li+ separation efficiency, Sep. Purif. Technol. 258 (2021) 118042, https://doi.org/10.1016/j.seppur.2020.118042.
[132] W. Cheng, C. Liu, T. Tong, R. Epsztein, M. Sun, R. Verduzco, J. Ma, M. Elimelech, Selective removal of divalent cations by polyelectrolyte multilayer nanofiltration membrane: role of polyelectrolyte charge, ion size, and ionic strength, J. Membr. Sci. 559 (2018) 98–106, https://doi.org/10.1016/j.memsci.2018.04.052.
[133] M.R. Moradi, A. Pihlajamäki, M. Hesampour, M. Figueira, M. Reig, J.L. Cortina, C. Valderrama, M. Mänttäri, Polyelectrolyte multilayers modification of nanofiltration membranes to improve selective separation of mono- and multivalent cations in seawater brine, J. Membr. Sci. 691 (2024) 122224, https://doi.org/10.1016/j.memsci.2023.122224.
[134] D. Lu, T. Ma, S. Lin, Z. Zhou, G. Li, Q. An, Z. Yao, Q. Sun, Z. Sun, L. Zhang, Constructing a selective blocked-nanolayer on nanofiltration membrane via surface-charge inversion for promoting Li+ permselectivity over Mg2+, J. Membr. Sci. 635 (2021) 119504 https://doi.org/10.1016/j.memsci.2021.119504.
[135] W.J. Koros, C. Zhang, Materials for next-generation molecularly selective synthetic membranes, Nat. Mater. 16 (2017) 289–297, https://doi.org/10.1038/nmat4805.
[136] J. Wang, J. Zhu, Y. Zhang, J. Liu, B. Van der Bruggen, Nanoscale tailor-made membranes for precise and rapid molecular sieve separation, Nanoscale 9 (2017) 2942–2957, https://doi.org/10.1039/C6NR08417F.
[137] F. Soyekwo, H. Wen, D. Liao, C. Liu, Fouling-resistant ionic graft-polyamide nanofiltration membrane with improved permeance for lithium separation from MgCl2/LiCl mixtures, J. Membr. Sci. 659 (2022) 120773, https://doi.org/10.1016/j.memsci.2022.120773.
[138] F. Soyekwo, H. Wen, D. Liao, C. Liu, Nanofiltration membranes modified with a clustered multiquaternary ammonium-based ionic liquid for improved magnesium/lithium separation, ACS Appl. Mater. Interfaces 14 (2022) 32420–32432, https://doi.org/10.1021/acsami.2c03650.
[139] Y. Zhao, N. Li, J. Shi, Y. Xia, B. Zhu, R. Shao, C. Min, Z. Xu, H. Deng, Extra-thin composite nanofiltration membranes tuned by γ-cyclodextrins containing amphipathic cavities for efficient separation of magnesium/lithium ions, Sep. Purif. Technol. 286 (2022) 120419, https://doi.org/10.1016/j.seppur.2021.120419.
[140] F.-Y. Zhao, Y.-L. Ji, X.-D. Weng, Y.-F. Mi, C.-C. Ye, Q.-F. An, C.-J. Gao, High-flux positively charged nanocomposite nanofiltration membranes filled with poly (dopamine) modified multiwall carbon nanotubes, ACS Appl. Mater. Interfaces 8 (2016) 6693–6700, https://doi.org/10.1021/acsami.6b00394.
[141] H. Jo, T.-H. Le, H. Lee, J. Lee, M. Kim, S. Lee, M. Chang, H. Yoon, Macrocyclic ligand-embedded graphene-in-polymer nanofiber membranes for lithium ion recovery, Chem. Eng. J. 452 (2023) 139274, https://doi.org/10.1016/j.cej.2022.139274.
[142] S. Sahu, M. Di Ventra, M. Zwolak, Dehydration as a universal mechanism for ion selectivity in graphene and other atomically thin pores, Nano Lett. 17 (2017) 4719–4724, https://doi.org/10.1021/acs.nanolett.7b01399.
[143] H. Zhang, J. Hou, Y. Hu, P. Wang, R. Ou, L. Jiang, J.Z. Liu, B.D. Freeman, A.J. Hill, H. Wang, Ultrafast selective transport of alkali metal ions in metal organic frameworks with subnanometer pores, Sci. Adv. 4 eaaq0066. doi:https://doi.org/10.1126/sciadv.aaq0066.
[144] H. Li, Y. Wang, T. Li, X.-K. Ren, J. Wang, Z. Wang, S. Zhao, Nanofiltration membrane with crown ether as exclusive Li+ transport channels achieving efficient extraction of lithium from salt lake brine, Chem. Eng. J. 438 (2022) 135658, https://doi.org/10.1016/j.cej.2022.135658.
[145] S.B. Sigurdardottir, R.M. DuChanois, R. Epsztein, M. Pinelo, M. Elimelech, Energy barriers to anion transport in polyelectrolyte multilayer nanofiltration membranes: role of intra-pore diffusion, J. Membr. Sci. 603 (2020) 117921, https://doi.org/10.1016/j.memsci.2020.117921.
[146] X. Zhou, Z. Wang, R. Epsztein, C. Zhan, W. Li, J.D. Fortner, T.A. Pham, J.-H. Kim, M. Elimelech, Intrapore energy barriers govern ion transport and selectivity of desalination membranes, Sci. Adv. 6 eabd9045. doi:https://doi.org/10.1126/sciadv.abd9045.
[147] P. Li, L. Jiang, L. Liu, P. Zhao, G. Xie, X. Xu, C. Liu, J. Jia, M. Liu, M. Zhang, Chelation-based metal cation stabilization of graphene oxide membranes towards efficient sieving of mono/divalent ions, J. Membr. Sci. 655 (2022) 120604, https://doi.org/10.1016/j.memsci.2022.120604.
[148] S. Munsif, N. Kosar, M.A. Hashmi, T. Mahmood, M.A. Gilani, K. Ayub, Synergic effect of pore size engineering and an applied electric field on the controlled permeation of alkali metal atoms and ions across pristine and defect-containing h-BN sheets, New J. Chem. 44 (2020) 7891–7901, https://doi.org/10.1039/C9NJ03962G.
[149] T. Zhang, W. Zheng, Q. Wang, Z. Wu, Z. Wang, Designed strategies of nanofiltration technology for Mg2+/Li+ separation from salt-lake brine: a comprehensive review, Desalination 546 (2023) 116205, https://doi.org/10.1016/j.desal.2022.116205.
[150] European Commission, G. Technology Readiness Levels (TRL). Horizon 2020; Brussels, Belgium. https://ec.europa.eu/research/participants/data/ref/h2020/wp/2014_2015/annexes/h2020-wp1415-annex-g-trl_en.pdf, 2015.
[151] G. Zhao, Y. Zhang, Y. Li, G. Pan, Y. Liu, Positively charged nanofiltration membranes for efficient Mg2+/Li+ separation from high Mg2+/Li+ ratio brine, Adv. Membr. 3 (2023) 100065, https://doi.org/10.1016/j.advmem.2023.100065.
[152] G. Yang, H. Shi, W. Liu, W. Xing, N. Xu, Investigation of Mg2+/Li+ separation by nanofiltration, Chin. J. Chem. Eng. 19 (2011) 586–591, https://doi.org/10.1016/S1004-9541(11)60026-8.
[153] Q. Shen, S.-J. Xu, Z.-L. Xu, H.-Z. Zhang, Z.-Q. Dong, Novel thin-film nanocomposite membrane with water-soluble polyhydroxylated fullerene for the separation of Mg2+/Li+ aqueous solution, J. Appl. Polym. Sci. 136 (2019) 48029, https://doi.org/10.1002/app.48029.
[154] P. Xu, J. Hong, X. Qian, Z. Xu, H. Xia, Q.-Q. Ni, "Bridge" graphene oxide modified positive charged nanofiltration thin membrane with high efficiency for Mg2+/Li+ separation, Desalination 488 (2020) 114522, https://doi.org/10.1016/j.desal.2020.114522.
[155] C. Morgante, T. Moghadamfar, J. Lopez, J.L. Cortina, A. Tamburini, Evaluation of enhanced nanofiltration membranes for improving magnesium recovery schemes

from seawater/brine: integrating experimental performing data with a techno-economic assessment, J. Environ. Manag. 360 (2024) 121192, https://doi.org/10.1016/j.jenvman.2024.121192.
[156] M. Figueira, D. Rodríguez-Jiménez, J. López, M. Reig, J. Luis Cortina, C. Valderrama, Evaluation of the nanofiltration of brines from seawater desalination plants as pre-treatment in a multimineral brine extraction process, Sep. Purif. Technol. 322 (2023) 124232, https://doi.org/10.1016/j.seppur.2023.124232.
[157] C. Morgante, J. Lopez, J.L. Cortina, A. Tamburini, New generation of commercial nanofiltration membranes for seawater/brine mining: experimental evaluation and modelling of membrane selectivity for major and trace elements, Sep. Purif. Technol. 340 (2024) 126758, https://doi.org/10.1016/j.seppur.2024.126758.
[158] S. Choi, B. Chang, J.H. Kang, M.S. Diallo, J.W. Choi, Energy-efficient hybrid FCDI-NF desalination process with tunable salt rejection and high water recovery, J. Membr. Sci. 541 (2017) 580–586, https://doi.org/10.1016/j.memsci.2017.07.043.
[159] C.A. Quist-Jensen, F. Macedonio, E. Drioli, Integrated membrane desalination systems with membrane crystallization units for resource recovery: a new approach for mining from the sea, Crystals 6 (2016) 36, https://doi.org/10.3390/cryst6040036.
[160] B.K. Pramanik, M.B. Asif, R. Roychand, L. Shu, V. Jegatheesan, M. Bhuiyan, F. I. Hai, Lithium recovery from salt-lake brine: impact of competing cations, pretreatment and preconcentration, Chemosphere 260 (2020) 127623, https://doi.org/10.1016/j.chemosphere.2020.127623.
[161] J. Renew, T. Hansen, Geothermal Thermoelectric Generation (G-TEG) With Integrated Temperature Driven Membrane Distillation and Novel Manganese Oxide for Lithium Extraction, United States, 2017, https://doi.org/10.2172/1360976.
[162] X. Zhang, K. Zuo, X. Zhang, C. Zhang, P. Liang, Selective ion separation by capacitive deionization (CDI) based technologies: a state-of-the-art review, Environ. Sci. Water Res. Technol. 6 (2020) 243–257, https://doi.org/10.1039/C9EW00835G.
[163] W. Xu, D. Liu, L. He, Z. Zhao, A comprehensive membrane process for preparing lithium carbonate from high Mg/Li brine, Membranes 10 (2020) 371, https://doi.org/10.3390/membranes10120371.
[164] Z. Liang, Y. Huipeng, L. Lin, D. Guofeng, Global technology trends of lithium extraction, Conserv. Util. Miner. Resour. 40 (2020) 24–31, https://doi.org/10.13779/j.cnki.issn1001-0076.2020.05.004.
[165] Our lithium extraction process, in: https://www.eramet.com/en/activities/lithium/our-lithium-extraction-process/ (accessed 27 March 2024).
[166] A. Cianek, DuPont Launches First Nanofiltration Membrane Elements for High Productivity Lithium-Brine Purification. https://www.dupont.com/news/dupont-launches-first-nanofiltration-membrane-elements-for-high-productivity-lithium-brine-purification.html, 2023. (Accessed 27 March 2024).
[167] J.F. Song, L.D. Nghiem, X.-M. Li, T. He, Lithium extraction from Chinese salt-lake brines: opportunities, challenges, and future outlook, Environ. Sci.: Water Res. Technol. 3 (2017) 593–597, https://doi.org/10.1039/C7EW00020K.
[168] H. Zhang, Q. He, J. Luo, Y. Wan, S.B. Darling, Sharpening nanofiltration: strategies for enhanced membrane selectivity, ACS Appl. Mater. Interfaces 12 (2020) 39948–39966, https://doi.org/10.1021/acsami.0c11136.
[169] Y. Zhang, L. Wang, W. Sun, Y. Hu, H. Tang, Membrane technologies for Li+/Mg2 + separation from salt-lake brines and seawater: a comprehensive review, J. Ind. Eng. Chem. 81 (2020) 7–23, https://doi.org/10.1016/j.jiec.2019.09.002.
[170] A. Khalil, S. Mohammed, R. Hashaikeh, N. Hilal, Lithium recovery from brine: recent developments and challenges, Desalination 528 (2022) 115611, https://doi.org/10.1016/j.desal.2022.115611.